P2Y Receptor Trafficking in Polarized Epithelial Cells

Darrell Ross DuBose Jr.

A dissertation submitted to the faculty of the University of North Carolina at Chapel Hill in partial fulfillment of the requirements for the degree of Doctor of Philosophy in the Department of Pharmacology.

Chapel Hill
2013

Approved by,

Robert Nicholas

Kendall Harden

Martina Gentzsch

Klaus Hahn

Eduardo Lazarowski

Abstract

DARRELL ROSS DUBOSE JR: P2Y Receptor Trafficking in Polarized Epithelial Cells
(Under the direction of Dr. Robert Nicholas)

A layer of interconnected epithelial cells line the organs of the human body. These cells have three functions: absorption of nutrients, secretion of wastes, and protection from pathogens. Chemically, epithelial cells are the mediators of nearly all interactions between the body and the world around us. In order to function properly, epithelial cells must maintain two distinct membrane regions with unique protein and lipid compositions. Disruption of these compositions results in diseases like cystic fibrosis, retinitis pigmentosa, nephrogenic diabetes insipidus, Dubin-Johnson syndrome, and polycystic kidney disease. To this day, many of the mechanisms underlying apical versus basolateral protein sorting remain unknown. The work presented here is focused on the sorting of the P2Y family of G protein coupled receptors and the transport of receptors between the apical and basolateral membrane regions of epithelial cells. Two separate but linked projects are detailed in this thesis. The first project details the delimitation and determination of key amino acids in the apical targeting sequence of the $P2Y_4$ receptor. The second project describes the development of a novel technique for determining the trafficking itineraries of proteins in polarized epithelial cells that is then applied to understand the trafficking mechanisms for the $P2Y_1$, $P2Y_2$, and $P2Y_4$ receptors. Together, these studies highlight the complexity and diversity of sorting and trafficking mechanisms at work in epithelial cells and suggest methods by which they may be better understood.

Table of Contents

List of Figures

List of Abbreviations

5’UTR – Five prime untranslated region

AC – Adenylate cyclase

ADP – Adenosine diphosphate

AMP – Adenosine monophosphate

AP - Apical

ATP – Adenosine triphosphate

BK2 – Bradykinin 2

BL – Basolateral

BSA – Bovine serum Albumin

cAMP – Cyclic adenosine monophosphate

CFTR – Cystic fibrosis transmembrane conductance regulator

CHO – Chinese hamster ovary

CNG – Cyclic nucleotide gated

DAG – Diacylglycerol

DMEM/F12 - Dulbecco's modified eagle medium/nutrient mixture F-12

DMSO - Dimethylsulfoxide

DNA – Deoxyribonucleic acid

DTT – Dithiothreitol

EGF – Epithelial growth factor

ENaC – Epithelial sodium channel

eNOS – Epithelial nitric oxide synthase

FLIPR – Fluorometric imaging plate reader

G protein - Guanosine nucleotide-binding proteins

GAP – GTPase activating protein

GDP – Guanosine diphosphate

GEF – Guanine nucleotide exchange factor

GFP – Green fluorescent protein

GMP – Guanosine monophosphate

GPCR – G protein-coupled receptor

GPI – Glycophosphatidylinositol

GST – Glutathione S-transferase

GTP – Guanosine triphosphate

IP_3 – Inositol 1,4,5-trisphosphate

IP_3R – IP_3 receptor

IPTG - Isopropylthio-β-galactoside

LDL – Low density lipoprotein

MAPK – Mitogen-activated protein kinase

MDCK – Madin-Darby canine kidney

NFDM – Non-fat dry milk

PBS – Phosphate buffered saline

PDZ – Post synaptic density protein/drosophila disc large tumor suppressor/zonula occludens-1

pen/strep – Penicillin/streptomycin

PFA – Paraformaldehyde

PI3K – Phosphatidylinositide 3-kinases

pIgR – Polymeric immunoglobulin receptor

PIP_2 - Phosphatidylinositol 4,5-bisphosphate

PKA – Protein kinase A

PKC – Protein kinase C

PKD – Polycystic kidney disease

PLC – Phospholipase C

PVDF – Polyvinylidene difluoride

RGS – Regulator of G protein signaling

RIA – Radio-immunosorbant assay

RIPA – Radio-immunoprecipitation assay

RNA – Ribonucleic acid

SDS-PAGE – Sodium dodecyl sulfate polyacrylamide gel electrophoresis

TM7 – Transmembrane region 7

TNFα – Tumor necrosis factor alpha

UDP – Uridine diphosphate

UTP – Uridine triphosphate

WT – Wild type

YFP – Yellow fluorescent protein

Chapter 1: Introduction

G protein coupled receptors and G protein signaling

G protein coupled receptors (GPCRs) are metabotropic transmembrane receptors – they mediate slow (second to minute responses) changes in cell physiology in response to extracellular ligands. GPCRs comprise about 750 proteins (in humans) that share a common seven-transmembrane structure. Of those, about half are olfactory or chemosensory receptors, 180 have known endogenous ligands, and 187 are known as orphan receptors (Vassilatis et al., 2003). An orphan receptor is a GPCR that is expected to be a receptor with an endogenous cognate ligand based on sequence homology with known receptors, but that ligand has not yet been discovered. GPCRs are of particular interest because they affect nearly every aspect of cell biology and are often expressed in a restricted, tissue-dependent manner. This, combined with extracellular binding sites, makes GPCRs highly attractive as potential drug targets. Indeed, almost half of the drugs on the market today target GPCRs (Drews, 2000).

All GPCRs have an extracellular N-terminus, thread through the plasma membrane seven times, and have an intracellular C-terminus. The basic structure of GPCRs forms an extracellular binding site to a wide range of external ligands and binding of these ligands causes a conformational change that activates intracellular effectors. The normal effector of a GPCR is a heterotrimeric G protein, though more recent evidence indicates GPCRs also have G protein-independent activity (McGarrigle and Huang, 2007).

G proteins act as molecular switches that regulate intracellular signaling. There are two types of G proteins: small (or Ras-like) G proteins and heterotrimeric G proteins. Small G proteins consist of a single catalytic subunit and are not directly associated with GPCRs. Heterotrimeric G proteins have three subunits: the catalytic alpha subunit (G_α), as well as beta and gamma subunits that form obligate heterodimers and are referred to simply as $G_{\beta\gamma}$ or βγ. At rest, G_α is bound to GDP and exists as a heterotrimer with $G_{\beta\gamma}$ and cannot interact with downstream effectors. When stimulated by an agonist-bound GPCR, GDP is released from G_α and GTP, which is present at high concentrations in the cell, binds to the G protein and causes a conformational change that releases G_α•GTP from $G_{\beta\gamma}$ and allows it to bind effectors. $G_{\beta\gamma}$ can also interact with effectors and trigger downstream signaling events. GTP is hydrolyzed to GDP by the inherent GTPase activity of G_α, which promotes rebinding to $G_{\beta\gamma,}$ and signaling ceases.

The nucleotide cycling of G proteins is a tightly controlled process; the two slowest steps, GDP release and GTP hydrolysis, are regulated by other proteins. The first step, release of GDP, is catalyzed by guanine nucleotide exchange factors (GEFs). There is a large class of specific GEFs for small G proteins, but for heterotrimeric G proteins the GEF is normally a GPCR. The second step of the cycle is the hydrolysis of GTP. Although G proteins have the inherent ability to hydrolyze GTP, it is rather slow; the reaction proceeds much faster with the association of a second class of enzymes – GTPase-activating proteins (GAPs). There are a variety of GAPs for both small and heterotrimeric G proteins, but some of the most common are known as regulators of G protein signaling (RGS) proteins.

There are at least 27 G_α, 5 G_β, and 14 G_γ subunits (Albert and Robillard, 2002;Hildebrandt, 1997), but downstream signaling is mainly dependent on the G_α subtype of the trimer. There are four classes of G_α proteins: Gq, Gs, Gi, and G12/13.

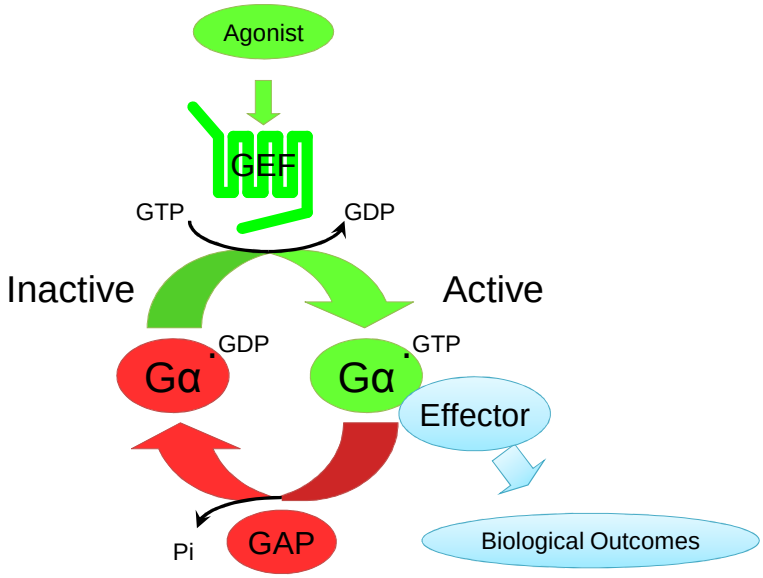

Figure 1.1. G proteins are tightly regulated molecular switches. G proteins cycle between inactive, GDP-bound, and active, GTP-bound states. Activation, the exchange of GDP for GTP is catalyzed by Guanine Nucleotide Exchange Factors (GEFs). Deactivation, the hydrolysis of GTP to GDP is catalyzed by GTPase Activating Proteins (GAPs).

These subunits have variable affinities for different GPCRs, and often a GPCR will signal through only one of the four classes.

GTP-bound Gq adopts a conformation that allows it to interact with its primary effector, phospholipase C. While bound to Gq-GTP, phospholipase C catalyzes the hydrolysis of phosphatidylinositol 4,5-bisphosphate (PIP_2) into diacylglycerol (DAG) and inositol 1,4,5-trisphosphate (IP_3). PIP_2 in the cell membrane normally stabilizes the opening of ion channels, including the epithelial sodium channel, ENaC. The reduction in PIP_2 concentration by PLC is sufficient to reduce ion flux through these channels. Upon cleavage, IP_3 is released into the cytoplasm, where it is free to bind its cognate receptor on the surface of the endoplasmic reticulum, releasing stored calcium ions. This spike in calcium activates a variety of effectors, including cell surface chloride and potassium channels, calmodulin, and protein kinase C. The DAG fragment remains membrane bound, where it recruits and activates protein kinase C. In addition to PLC, Gq can bind RhoGEFs (similar to G12/13, described below), beginning signaling cascades that affect the cytoskeleton.

Adenylate cyclase (AC) is the primary effector of both Gs and Gi. GTP-bound Gs binds AC to stimulate the production of cAMP. GTP-bound Gi binds AC at an allosteric site, blocking cAMP production. As a potent second messenger, cAMP activates many effectors, including cyclic-nucleotide gated ion channels and protein kinase A(which phosphorylates and activates CFTR as well as many other targets). Note that some of these ion channels are Ca^{2+} permeable, and as such can replicate some aspects of Gq signaling.

The final subtype, G12/13, couples receptors to Rho-family small G proteins through activation of RhoGEFs. Rho G proteins can then activate several signaling cascades, including those beginning with PI3K, PAK, FAK, and ROCK. Generally, these result in cytoskeletal rearrangement, often affecting cell motility, shape, or contractility.

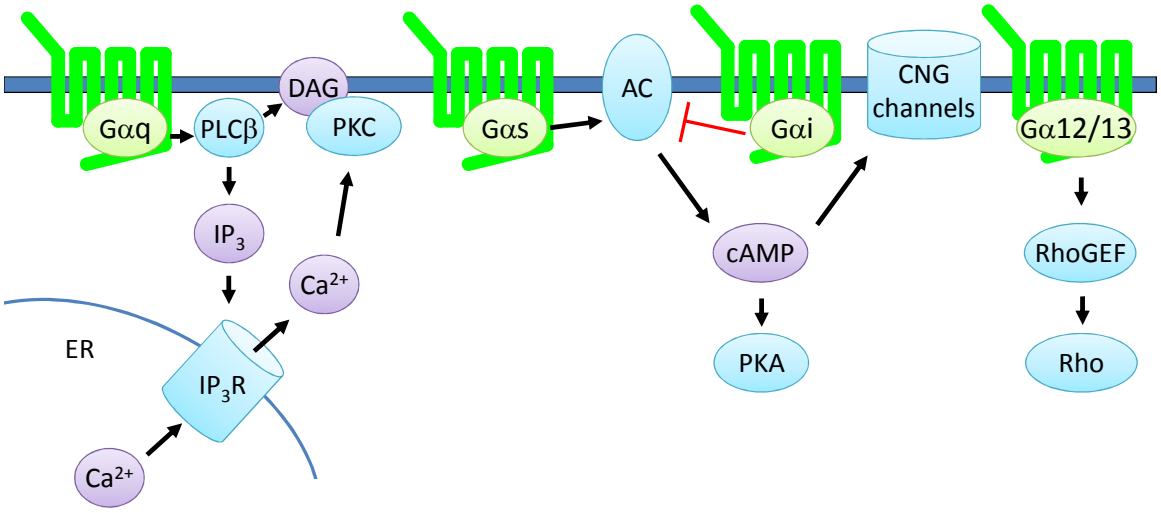

Figure 1.2. GPCR signaling is dependent on the Gα subtype. GPCRs signal through heterotrimeric G proteins. Gq activates PLC, resulting in increased intracellular Ca^{2+} and activation of PKC. Gs stimulates production of cAMP by adenylate cyclase, resulting in activation of PKA and a variety of ion channels; Gi inhibits these same effects. G12/13 binds rhoGEFs, activating Rho small G proteins, which act primarily to remodel the cytoskeleton.

Additionally, the $G_{\beta\gamma}$ dimer can also trigger signaling events when dissociated from G_{α}. $G_{\beta\gamma}$ directly binds inwardly rectifying K^{+} channels and voltage-gated Ca^{2+} channels, activating the former and inhibiting the latter. The dimer interacts with both AC and PLC and plays a role in their activation. $G_{\beta\gamma}$ also plays a role in the scaffolding and activation of kinase cascades, including PI3Ks and MAPKs. There may be variable effects from the various β and γ isoforms, but if they exist are poorly understood.

Nucleotide Signaling

Nucleotides are ubiquitous small molecules in nature involved in a wide variety of biological processes. They are the building blocks of DNA, RNA, and many enzymatic co-factors. They are also energy “currency”, used to drive forward reactions that would otherwise be unfavorable. They are cycled into potent second-messengers that transduce intracellular signals (e.g. cyclic AMP and cyclic GMP). Lastly, they are extracellular signaling molecules that bind transmembrane receptors, often in an autocrine/paracrine manner, to convey a signal across the plasma membrane. It is this receptor signaling role that is pertinent to this work.

Nucleotide receptors have been found in all cell types, where they mediate a plurality of cell activities. There are two distinct families of nucleotide receptors: P2X and P2Y. P2X receptors are transmembrane channels that open in response to binding extracellular ATP. Once open, Ca^{2+} and Na^{+} ions pass through the pore and depolarize the cell membrane. P2X receptors are primarily involved in synaptic and neuromuscular signaling. A functional P2X receptor is composed of three P2X subunits. There are seven known P2X subunits which can combine to form a variety of homo- and heteromeric receptors. The P2X subunits are designated $P2X_1$ through $P2X_7$.

The second family of nucleotide receptors, P2Y receptors, is part of the G protein coupled receptor superfamily.

P2Y Receptors

P2Y receptors are a family of GPCRs that respond to extracellular nucleotides. There have been eight P2Y receptors identified to date—$P2Y_1$, $P2Y_2$, $P2Y_4$, $P2Y_6$, $P2Y_{11}$, $P2Y_{12}$, $P2Y_{13}$, and $P2Y_{14}$. The numbering is not sequential because several receptors have been named as a P2Y receptor, only to be determined later either to not to be activated by nucleotides at all, or to be homologues of a mammalian P2Y receptor. For example, the p2y3 receptor was later determined to be the avian homologue of the human $P2Y_6$ receptor (Li et al., 1998). P2Y receptors can be divided into two subclasses based on their downstream signaling properties. The $P2Y_1$–like receptors ($P2Y_1$, $P2Y_2$, $P2Y_4$, $P2Y_6$, and $P2Y_{11}$) signal primarily through Gq, while the $P2Y_{12}$-like receptors ($P2Y_{12}$, $P2Y_{13}$, and $P2Y_{14}$) signal primarily through Gi. The $P2Y_{11}$ receptor, while most efficiently coupling to Gq, also signals through Gs to stimulate AC. The receptors can also be characterized by their activating ligands, as shown in Figure 1.3.

P2Y receptors are expressed in a wide variety of tissue types, but the subtype and density of the receptors varies significantly. For example, the $P2Y_1$ receptor is most highly expressed in brain, prostate, and placental tissues while $P2Y_2$ receptors are expressed at the highest levels in muscle, lung, and immune cells (Moore et al., 2001). The physiological output of P2Y receptor signaling also varies. A single receptor often has different signaling outcomes when expressed in different cell types. For example, in epithelial cells, activation of the $P2Y_1$ receptor leads to chloride secretion, while in platelets it induces shape change.

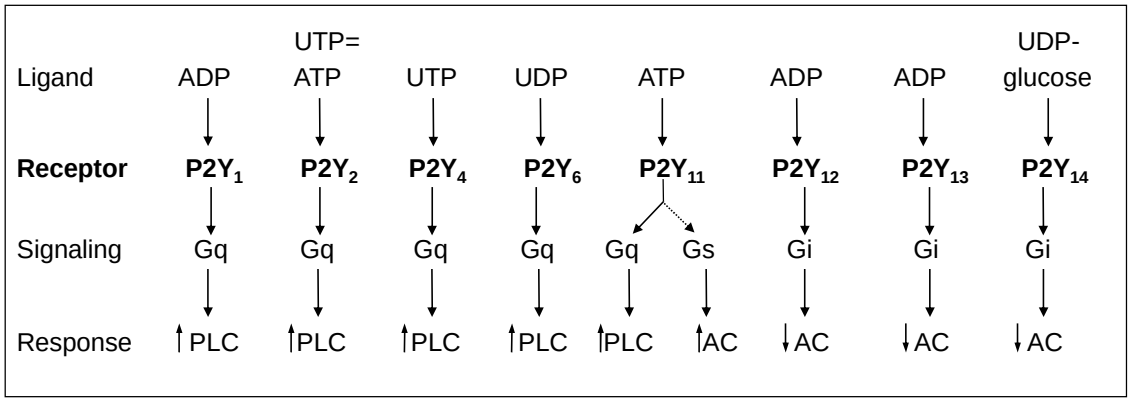

Figure 1.3. Endogenous agonists and signaling pathways of the eight cloned P2Y receptors.

$P2Y_1$ Receptor

The $P2Y_1$ receptor is a 373-amino acid protein encoded by a single exon on the forward strand of chromosome 3 (Genbank Accession Number S81950). For endogenous nucleotides, the $P2Y_1$ receptor responds primarily to ADP (K_i = 0.92 µM), but also to ATP (K_i = 17.7 µM), albeit with lesser efficacy (Palmer et al., 1998;Waldo and Harden, 2004). Synthetic agonists include 2-MeSADP (K_i = 0.0099 µM), ATPγS (K_i = 1.33 µM), 2-MeSATP (K_i = 1.87 µM), ADPβS (K_i = 2.42 µM), and (N)-methanocarba-2MeSADP (MRS2365, EC50 = 34 nM) (Bourdon et al., 2006;Waldo and Harden, 2004). Of these, only MRS2365 is highly selective for the $P2Y_1$ receptor. Selective antagonists (a rarity for P2Y receptors) have also been developed for the $P2Y_1$ receptor: MRS2179 (pKB = 6.75 (Moro et al., 1998), MRS2279 (pKB = 8.10) (Boyer et al., 2002), and MRS2500 (K_i = 0.79 nM and K_B = 1.74 nM) (Kim et al., 2003). These compounds have been instrumental in the study of $P2Y_1$ receptor physiology.

As mentioned above, the $P2Y_1$ receptor is involved in a wide variety of physiological processes depending on the tissue in which it is expressed. Of specific interest to this work, the G_q coupled P2Y receptors (including $P2Y_1$) induce luminal ion flux in epithelial cells, thus modulating osmotic balance between the body and external fluids (Christofi et al., 2004;Fang et al., 2006;Lee et al., 2007;Matos et al., 2005;Rajagopal et al., 2011). Interestingly, the $P2Y_1$ receptor is expressed only on the basolateral surface of all the epithelial cells in which its location has been investigated, meaning that it only responds to ADP released within the organ (i.e. those tissues with access to the basolateral membrane) and not from the lumen (Wolff et al., 2005). In contrast, $P2Y_2$, $P2Y_4$, and $P2Y_6$ receptors are primarily expressed at the apical membrane and therefore respond to nucleotides released at the luminal compartment.

In the circulatory system, the $P2Y_1$ receptor is involved in both endothelial-dependent and eNOS-stimulated smooth muscle relaxation (da Silva et al., 2009;Ralevic

and Burnstock, 1998). In platelets, the $P2Y_1$ receptor induces shape change that, along with $P2Y_{12}$ receptor activation, leads to aggregation (Hechler et al., 1998). $P2Y_1$ receptor antagonists are currently being investigated as potential antithrombotic agents (Bird et al., 2012). In bone, the $P2Y_1$ receptor functions in osteoclastic bone resorption (Hoebertz et al., 2001). The $P2Y_1$ receptor regulates a variety of functions in the nervous system as well. It inhibits N-type calcium channels (Filippov et al., 2000), modulates synaptic transmission (von Kugelgen and Wetter, 2000), and has a role in astrocyte calcium signaling (Fumagalli et al., 2003).

$P2Y_2$ Receptor

The $P2Y_2$ receptor is a 377-amino acid protein encoded by a single exon on the forward strand of chromosome 11. There are three known splice variants, but they differ only in the 5'UTR; hence, the encoded proteins are identical (Genbank Accession Numbers NM_176072, NM_002564, and NM_176071). The $P2Y_2$ receptor responds equally well to UTP (EC_{50} = 0.14 µM) and ATP (EC_{50} = 0.23 µM) (Lazarowski et al., 1995), but does not respond to the diphosphate forms of either nucleotide (Nicholas et al., 1996). Very recently, several potent, selective $P2Y_2$ receptor agonists were synthesized. Among these, 4-thio-β,γ-difluoromethylene-UTP (EC_{50} = 0.134 µM) showed >50-fold selectivity over the $P2Y_4$ and $P2Y_6$ receptors and is metabolically stable (El-Tayeb et al., 2011). This reagent should greatly aid future studies of the receptor. Nonselective agonists include Ap_4A (EC_{50} = 0.72 µM), ATPγS (EC_{50} = 1.72 µM), 5BrUTP (EC_{50} = 2.06 µM), dCp4U (INS37217) (EC_{50} = 0.22 µM), and Up4U (INS365) (EC_{50} = 0.1 µM) (Pendergast et al., 2001;Yerxa et al., 2002). Some progress has been made (Weyler et al., 2008), but thus far no selective antagonists of the $P2Y_2$ receptor have been developed.

Like the $P2Y_1$ receptor, the $P2Y_2$ receptor stimulates ion flux in epithelial cells via G_q activation (Ghanem et al., 2005;Hosoya et al., 1999;Hwang et al., 1996;Parr et al., 1994;Rajagopal et al., 2011). In contrast to the $P2Y_1$ receptor, the $P2Y_2$ receptor is expressed primarily at the apical surface and thus responds to luminal signals (Wolff et al., 2005). This physiological activity is pronounced in epithelium of both the lung and the lacrimal duct. As such, agonists of the $P2Y_2$ receptor are under investigation as potential therapeutic agents for cystic fibrosis and dry eye disease (Hosoya et al., 1999;Pintor et al., 2002;Yerxa et al., 2002).

Additionally, the $P2Y_2$ receptor has been linked with a long list of physiological activities, including both vasodilatation and vasoconstriction (da Silva et al., 2009;Ralevic and Burnstock, 1998), apoptosis in colorectal carcinoma cells (Burnstock and Knight, 2004), bone remodeling (Hoebertz et al., 2002), monocyte recruitment (Seye et al., 2003), cell proliferation (Burrell et al., 2003;Greig et al., 2003;Muscella et al., 2003;Schafer et al., 2003); neutrophil degranulation and infiltration (Ayata et al., 2012;Meshki et al., 2004), inflammation (Kruse et al., 2012;Schuchardt et al., 2011), HIV-1 infection (Seror et al., 2011), amyloid precursor processing (Leon-Otegui et al., 2011), wound healing (Boucher et al., 2011), metastasis (Schumacher et al., 2013), and neuroprotection (Chorna et al., 2004;Weisman et al., 2012).

$P2Y_4$ Receptor

The $P2Y_4$ receptor is a 365-amino acid protein encoded by a single exon on the reverse strand of the X chromosome (Genbank Accession Number X91852). The only endogenous full agonist of the human $P2Y_4$ receptor is UTP. Measured EC_{50} values have varied slightly, from 2.5 µM (Communi et al., 1995) to 0.55 µM (Kennedy et al., 2000). UDP is a partial agonist if it has any activity at all (Nguyen et al., 1995;Nicholas et al., 1996), and ATP is a relatively potent competitive antagonist (Kennedy et al., 2000).

Interestingly, the rat $P2Y_4$ receptor responds to a wider variety of ligands. Both UTP (EC_{50} = 0.20 μM) and ATP (EC_{50} = 0. 51 μM) are agonists, as well as Ap_4A (EC_{50} = 1.24 μM), ITP (EC_{50} = 1.82 μM), GTP (EC_{50} = 2. 28 μM), CTP (EC_{50} = 7.24 μM), and XTP (EC_{50} = 22.9 μM) (Kennedy et al., 2000). These differences in agonist activation have been traced to three amino acids (Asn-177, Ile-183, and Leu-190) in the second extracellular loop of the rat receptor (Herold et al., 2004). Until recently, no selective ligands of any type were known for the $P2Y_4$ receptor, making pharmacological differentiation between the $P2Y_2$ receptor and $P2Y_4$ receptor difficult. Recently, a few moderately selective $P2Y_4$ receptor agonists have been synthesized. First, iso-CMP (EC_{50} = 4.98 μM) is >20-fold selective for the $P2Y_4$ receptor versus $P2Y_2$ and $P2Y_6$ receptors (El-Tayeb et al., 2011). A second group synthesized N^4-(phenylpropoxy)-CTP (MRS4062, EC_{50} = 23 nM), Up_4-[1]3'-deoxy-3'-fluoroglucose (MRS2927, EC_{50} = 62 nM), and N^4-(phenylethoxy)-CTP (EC_{50} = 73 nM), each of which has 10-fold or greater selectivity for the $P2Y_4$ receptor versus $P2Y_2$ and $P2Y_6$ receptors (Maruoka et al., 2011).

High expression levels of the $P2Y_4$ receptor have been detected in the placenta, intestine, pituitary, and brain, with lower levels in liver, bone marrow, monocytes and lymphocytes (Communi et al., 1995;Jin et al., 1998;Moore et al., 2001), but relatively few physiological functions are known.

Like the $P2Y_1$ and $P2Y_2$ receptors, the $P2Y_4$ receptor functions to control ion flux and water homeostasis across epithelial cells via $G_{\alpha q}$ activation (Ghanem et al., 2005;Robaye et al., 2003). This function of the $P2Y_4$ receptor is most apparent in the intestine, where it is highly expressed (Moore et al., 2001). The jejunum of $P2Y_4$ receptor-knockout mice has been shown to lack a chloride secretion response to nucleotides, indicating a clear role for the $P2Y_4$ receptor in this process (Robaye et al., 2003). This makes $P2Y_4$ receptor an attractive pharmacological target to relieve the intestinal abnormalities associated with cystic fibrosis. $P2Y_4$ receptor antagonists may

also be of therapeutic value. Bacterial infection of the gut is known to cause nucleotide release and chloride secretion. As excess luminal chloride secretion is a central mediator of diarrhea symptoms (Field et al., 1989;Kunzelmann and Mall, 2002), pharmacological inhibition of the $P2Y_4$ receptor (and likely the $P2Y_2$ receptor as well) may attenuate infection symptoms.

In addition to the intestine, the $P2Y_4$ receptor has a role in auditory neurotransmission. It is expressed in vestibular dark cell epithelium and strial marginal cells, where it controls K^+ secretion (Hur et al., 2007;Lee et al., 2006;Marcus and Scofield, 2001). The $P2Y_4$ receptor has also been implicated in vasodilation (Burnstock, 2002;McMillan et al., 1999), cell proliferation (Burnstock, 2002), and cardiac development (Horckmans et al., 2012).

$P2Y_6$ Receptor

The $P2Y_6$ receptor is a 328-amino acid protein encoded by a single exon on the forward strand of chromosome 11. There are eight splice variants, seven of which encode the same protein; they differ only in the 5'UTR (Genbank Accession Numbers NM_176797, NM_176798, NM_176796, NM_001277204, NM_001277205, NM_001277206, and NM_001277207). A single splice variant begins translation at an alternate start site and encodes additional amino acids at the N-terminus of the protein (Genbank Accession Number NM_001277208).

The $P2Y_6$ receptor is activated endogenously by UDP (EC_{50} = 300 nM), and to a lesser extent UTP (EC_{50} = 6 µM) and ADP (EC_{50} = 30 µM). ATP has little effect, even at millimolar concentrations (Communi et al., 1996;Nicholas et al., 1996). In addition, the synthetic ligands 5BrUTP (EC_{50} = 800 nM) and UDPβS (EC_{50} = 25 nM) (Communi et al., 1996;Malmsjo et al., 2000) are agonists. UDPβS is very selective for the $P2Y_6$ receptor over the $P2Y_2$ and $P2Y_4$ receptors (Goody et al., 1972;Malmsjo et al., 2000). More

recently, 5-OMe-UDP (EC_{50} = 0.08 μM) and N3-phenacyl-β,γ-dichloromethylene-UTP (EC_{50} = 0.142 μM) were synthesized and shown to be selective for the $P2Y_6$ receptor versus the $P2Y_4$ receptor but not the $P2Y_2$ receptor (El-Tayeb et al., 2011;Ginsburg-Shmuel et al., 2010). Additionally, three compounds have been synthesized that are insurmountable, selective antagonists of the $P2Y_6$ receptor; diisothiocyanate derivatives of 1,2-diphenylethane (MRS2567, IC_{50} = 126 nM), 1,4-di-(phenylthioureido)butane (MRS2578, IC_{50} = 37 nM), and 1,4-phenylendiisothiocyanate (MRS2575, IC_{50} = 155 nM, human only) (Mamedova et al., 2004).

The $P2Y_6$ receptor is expressed in particularly high levels in the spleen, and has also been detected in placenta, thymus, intestine, vascular smooth muscle, lung, kidney, bone, adipose, heart, and parts of the brain (Communi et al., 1996;Moore et al., 2001;Ralevic and Burnstock, 1998).

Like the receptors above, the $P2Y_6$ receptor also regulates ion flux in epithelial cells (Burnstock and Knight, 2004). Of particular interest, it seems to play a primary role in gallbladder epithelia, where it may be a therapeutic target to correct Cl^- secretion in cystic fibrosis patients (Lazarowski et al., 2001). Some evidence has been presented indicating that the $P2Y_6$ receptor also stimulates Cl^- secretion in various epithelial cells through a second mechanism involving the CFTR channel (Dulong et al., 2007;Kottgen et al., 2003;Schreiber and Kunzelmann, 2005;Wong et al., 2009). However, none of these studies directly demonstrates that the effects observed are dependent on $P2Y_6$ receptor activation, and each uses 100 μM UDP, which is more than 300-fold higher than the EC_{50} in other assays. Also, in early experiments with the $P2Y_6$ receptor, no direct coupling of $P2Y_6$ to G_s was observed (Chang et al., 1995).

In addition to its role in epithelial cells, the $P2Y_6$ receptor is involved in several physiological responses. Included are key roles in immune response and inflammation. The $P2Y_6$ receptor induces IL-6 and IL-8 expression in macrophages and monocytes,

respectively, and suppresses T-cell activation during allergic inflammation (Bar et al., 2008;Giannattasio et al., 2011;Warny et al., 2001). UDP, acting through the $P2Y_6$ receptor, has also been shown to induce chemokine production in microglia and astrocytes (Kim et al., 2011). In bone, the $P2Y_6$ receptor stimulates differentiation into osteoclasts and increases their resorptive activity (Orriss et al., 2011). In the vasculature, activation of the $P2Y_6$ receptor causes relaxation of endothelial cells and contraction of nitric-oxide-blocked vascular smooth muscle cells (Bar et al., 2008). Lastly, it has a cytoprotective role, preventing TNFα-induced apoptosis (Kim et al., 2003;Kim et al., 2003;Mamedova et al., 2008).

$P2Y_{11}$ Receptor

The $P2Y_{11}$ receptor is a 374-amino acid protein encoded by two exons on the forward strand of chromosome 19 (Genbank Accession Number AJ298334). Transcription of the $P2Y_{11}$ receptor has an uncommon feature. Through alternate splicing a chimeric protein can be formed between the $P2Y_{11}$ receptor and Ssf1, the neighboring gene on chromosome 19. This alters the extracellular N-terminus of the receptor, removing the first 5 amino acids and instead fusing the Ssf1 protein. Chimeric mRNA was detected in a variety of human tissues and the presence of a 90kDa protein product was identified from transfected CHO cells. ATP and other agonists have reduced potency and/or efficacy at the chimeric receptor, but the function of this fusion protein is unknown (Communi et al., 2001).

The $P2Y_{11}$ receptor is expressed in a wide range of cell types and has particularly high expression in the brain, pituitary, spleen, and lymphocytes (Moore et al., 2001). It is unique among the P2Y receptors because it couples strongly to two different classes of G protein alpha subunits, $G_{\alpha q}$ and $G_{\alpha s}$ (Communi et al., 1997). The human $P2Y_{11}$ receptor responds to adenine but not uridine nucleotides (though see (White et

al., 2003) regarding UTP), with a preference for ATP over ADP. In contrast, ADP is more potent than ATP at the canine receptor (Qi et al., 2001). Interestingly, agonist potency at the $P2Y_{11}$ receptor varies between the $G_{\alpha q}$ and $G_{\alpha s}$ pathways. Originally, it was reported that all agonists were more potent at stimulating cAMP production than IP (EC_{50} = 17.4 and 65 µM, respectively for ATP) (Communi et al., 1999). However, these two assays were performed in two different cell lines, CHO and 1321N1. It was later discovered that, when expressed in the same cell line, $P2Y_{11}$ agonists are more potent stimulating IP_3 production than cAMP production (EC_{50} = 3.6 and 62.4 µM, respectively for ATP in CHO cells, 8.5 and 130 µM in 1321N1 cells) (Qi et al., 2001). The $P2Y_{11}$ receptor also responds to the synthetic agonists, ATPγS, BzATP, dATP, ADPβS, 2MeSATP, and 2MeSADP in roughly that rank order, but again the exact EC_{50} values vary between assays (Communi et al., 1999;Qi et al., 2001). More recently, β-NAD+, and NAADP+ were shown to be $P2Y_{11}$ agonists (Moreschi et al., 2006;Moreschi et al., 2008). Also, a non-nucleotide agonist, NF546 (4,4'-(carbonylbis(imino-3,1-phenylene-carbonylimino-3,1-(4-methyl-phenylene)-carbonylimino))-bis(1,3-xylene-alpha,alpha'-diphosphonic acid) tetrasodium salt) (EC_{50} = 0.54 µM, Ca^{2+} assay) (Meis et al., 2010), and two antagonists, NF340 (4,4′-(carbonylbis(imino-3,1-(4-methyl-phenylene)carbonylimino)) bis(naphthalene-2,6-disulfonic acid) tetrasodium salt) (IC_{50} = 0.37 µM, Ca^{2+} assay) and NF157 (8,8′-[carbonylbis[imino-3,1-phenylenecarbonylimino(4-fluoro-3,1-phenylene)carbonylimino]]bis-1,3,5-naphthalene trisulfonic acid hexasodium salt) (IC_{50} = 0.46 µM, Ca^{2+} assay) were synthesized and shown to be antagonists at the $P2Y_{11}$ receptor, although the selectivity of these compounds is not remarkable (Meis et al., 2010;Ullmann et al., 2005).

Considering its almost ubiquitous expression, it is surprising that the $P2Y_{11}$ receptor has been linked with relatively few physiological processes. In epithelial cells, $P2Y_{11}$ stimulates electrolyte secretion in pancreatic duct cells, at least a portion of which

involves the cAMP pathway (Nguyen et al., 2001). Similarly, the $P2Y_{11}$ receptor has been shown to function in nasal epithelial cells and in MDCK cells (Kim et al., 2004;Torres et al., 2002). Outside of epithelial physiology, the $P2Y_{11}$ receptor is involved in immune responses, through modulation of cytokine production (Alkayed et al., 2012;Communi et al., 2000;Meis et al., 2010;Sakaki et al., 2013;Schnurr et al., 2003;Wilkin et al., 2001), it inhibits the proliferation of certain cells (Schafer et al., 2006;Xiao et al., 2011), and may have a cardioprotective role (Djerada et al., 2013).

$P2Y_{12}$ Receptor

The $P2Y_{12}$ receptor is a 342 amino acid protein encoded by a single exon on the reverse strand of chromosome 3. There are two splice variants, but they differ only in the 5'UTR; the encoded proteins are identical (Genbank Accession Numbers NM_022788 and NM_176876).

The $P2Y_{12}$ receptor was the first nucleotide receptor discovered that signals through G_i rather than G_q (Cooper and Rodbell, 1979). Interestingly, this activity was discovered more than twenty years before the molecular identity of the receptor was known (Hollopeter et al., 2001;Takasaki et al., 2001;Zhang et al., 2001). Expression of the $P2Y_{12}$ receptor has been detected in platelets and their precursors, spinal cord, brain (especially glia), differentiating osteoclasts, and nasal epithelial and inferior turbinate cells (Sasaki et al., 2003;Shirasaki et al., 2013;Su et al., 2012;Zhang et al., 2001).

Endogenously, the $P2Y_{12}$ receptor is potently activated by ADP (EC_{50} = 60.7 nM) (Zhang et al., 2001). ATP is a partial agonist with much lower potency (EC50 = ~26 µM) (Simon et al., 2001) and high ATP concentrations antagonize ADP-induced aggregation in platelets (Park and Hourani, 1999). Synthetic agonists include 2-MeSATP (EC_{50} = 3.4 nM), 2-MeSADP (EC_{50} = 14.1 nM), ATPγS (EC_{50} = 110 nM), ADPβS (EC_{50} = 20 nM), and 2-ClATP (EC_{50} = 636 nM) (Zhang et al., 2001). Synthetic antagonists of the $P2Y_{12}$

receptor are administered clinically as antithrombotics. Clopidogrel and prasugrel, as well as their clinical predecessor ticlopidine, are prodrugs, the active metabolites of which irreversibly bind and inactivate the $P2Y_{12}$ receptor (Gachet et al., 1992). Ticagrelor (AZD6140) is a reversible, non-competitive antagonist (Van Giezen et al., 2009) and cangrelor (AR-C69931MX, IC_{50} = 0.4 nM) is a competitive antagonist (Norgard, 2009), though the latter is also an antagonist of the $P2Y_{13}$ receptor (Marteau et al., 2003).

In addition to the well documented role in platelet aggregation, the $P2Y_{12}$ receptor may have a role in osteoclast function, as $P2Y_{12}$ knockout mice and mice treated with clopidogrel are protected from multiple conditions that trigger pathologic bone loss (Su et al., 2012). The full role of the $P2Y_{12}$ receptor in the nervous system has not been well characterized, but it has been implicated in microglial chemotaxis and the development of neuropathic pain (Ohsawa et al., 2007;Tozaki-Saitoh et al., 2008). Despite its striking basolateral polarity (Wolff et al., 2005) and expression in nasal epithelium (Shirasaki et al., 2013), no role has yet been established for the $P2Y_{12}$ receptor in epithelial cells.

$P2Y_{13}$ Receptor

The $P2Y_{13}$ receptor is a 354 amino acid protein encoded by two exons on the reverse strand of chromosome 3 (Genbank Accession Number NM_176894). This is an area where several P2Y receptor genes are encoded (including the $P2Y_1$ receptor), and the $P2Y_{13}$ receptor was discovered due to its homology with the nearby $P2Y_{12}$ receptor (Communi et al., 2001).

Like the $P2Y_{12}$ receptor, the $P2Y_{13}$ receptor responds with nanomolar potency to extracellular ADP (EC_{50} = 60 nM). ATP is also a potent agonist (EC_{50} = 261 nM), along with synthetic ligands 2-MeSADP (EC_{50} = 19 nM), ADPβS (EC_{50} = 31 nM), 2-MeSATP (EC_{50} = 32 nM), Ap3A (EC_{50} = 72 nM), and IDP (EC_{50} = 552 nM) (Zhang et al., 2002). As

mentioned above, the clinical drug cangrelor (AR-C69931MX, IC_{50} = 4.6 nM) is a potent antagonist of the $P2Y_{13}$ receptor (Marteau et al., 2003). A moderately selective (>20-fold vs. $P2Y_1$ or $P2Y_{12}$) antagonist of the $P2Y_{13}$ receptor was recently synthesized, MRS2211 (IC_{50} = 1.1 μM) (Kim et al., 2005).

The physiological roles of the $P2Y_{13}$ receptor are not well characterized. Various reports have suggested that the $P2Y_{13}$ receptor has a role in N-type calcium channel regulation (Wirkner et al., 2004), high-density lipoprotein and cholesterol transport (Fabre et al., 2010;Jacquet et al., 2005), neuroprotection (Espada et al., 2010), regulation of insulin secretion (Amisten et al., 2010), mast cell degranulation (Gao et al., 2010), inhibition of neuronal differentiation (Yano et al., 2012), and osteogenesis regulation (Wang et al., 2013).

$P2Y_{14}$ Receptor

The $P2Y_{14}$ receptor is a 338 amino acid protein encoded by a single exon on the reverse strand of chromosome 3 adjacent to $P2Y_{12}$ and $P2Y_{13}$ receptors. There are two splice variants, but they differ only in the 5'UTR; the encoded proteins are identical (Genbank Accession Numbers NM_001081455 and NM_014879).

The $P2Y_{14}$ receptor (formerly known as GPR105 or KIAA0001) is the most recently identified member of the P2Y receptor family (Abbracchio et al., 2003;Chambers et al., 2000) It also has the most unique pharmacological profile, responding to UDP (EC_{50} values ranged from 29 to 74 nM, depending on cell line) (Carter et al., 2009), UDP-glucose (EC_{50} = 80 nM), UDP-galactose (EC_{50} = 124 nM), UDP-glucuronic acid (EC_{50} = 370 nM), and UDP-*N*-acetylglucosamine (EC_{50} = 710 nM) (Chambers et al., 2000) Synthetic agonists include UDPβS (EC_{50} = 26 nM), 2-MeSUDP (EC_{50} = 2 nM), difluoro-α,β-methylene-UDP (MRS2802, EC_{50} = ~50 nM) and UDP-β-propylester (MRS2907, EC_{50} = ~50 nM), with the latter two showing high selectivity for the $P2Y_{14}$

receptor over the $P2Y_6$ receptor (Carter et al., 2009). A very potent, selective, competitive antagonist of the $P2Y_{14}$ receptor was also synthesized (4-((piperidin-4-yl)-phenyl)-7-(4-(trifluoromethyl)-phenyl)-2-naphthoic acid (PPTN, IC50 = 8 nM) (Barrett et al., 2013;Gauthier et al., 2011).

UDP-glucose has been shown to be released from a variety of cell types where it can act as an endogenous ligand for the $P2Y_{14}$ receptor (Lazarowski et al., 2003). $P2Y_{14}$ receptor mRNA has been detected at low levels in a wide range of cells and at higher levels in neutrophils, lymphocytes, and megakaryocytic cell lines (Chambers et al., 2000;Moore et al., 2003). The $P2Y_{14}$ receptor was also detected by immunohistochemistry on brain glia (Moore et al., 2003). Functionally, the $P2Y_{14}$ receptor has been associated with chemotaxis in hematopoietic stem cells (Lee et al., 2003) and neutrophils (Barrett et al., 2013;Sesma et al., 2012), gastric function (Bassil et al., 2009), release of pro-inflammatory cytokines (Muller et al., 2005) and mast cell degranulation (Gao et al., 2010). A recent study using $P2Y_{14}$ receptor knockout mice has identified a role for the receptor in the tolerance to radiation-induced genotoxic stress in utero. Paradoxically, exogenous application of UDP-glucose provided nearly identical levels of protection as gene deletion (Kook et al., 2013).

Epithelial Cells and Cell Polarization

Monolayers of epithelial cells line the lumens of essentially all of the body's organs, including those of the digestive, respiratory, urinary, and reproductive systems. They have three basic functions – absorption of nutrients, secretion of wastes, and protection from external pathogens. Depending on the subtype of epithelial cell, they may serve one, two, or all three of these functions.

Cell polarization – an asymmetry in shape, structure, or function - is an essential characteristic of many cell types, including neurons, endothelial, and epithelial cells. Cells create and maintain this polarity by specific sorting of lipids and proteins to different regions of the cell membrane (Giepmans and van Ijzendoorn, 2009). This involves a complex system of tightly regulated processes, the mechanisms of which are only beginning to be understood (Brown et al., 2009;Weisz and Rodriguez-Boulan, 2009).

Polarization in epithelial cells takes the form of two distinct membrane regions separated by a specialized protein structure known as the tight junction. The separation of the two regions formed by the tight junction is complete, preventing free diffusion of both water and ions across the monolayer. This is often called the "fence" function of the tight junction. As the tight junction exists at the apical end of the lateral membrane, the two membrane regions formed by the tight junctions are referred to as apical and basolateral. The apical membrane is the portion of the cell membrane that faces the organ lumen and is in contact with the external milieu. The basolateral membrane faces the underlying cells and basement membrane of the organ and is in direct contact with the interstitial fluid that fills the spaces between the cells.

In addition to separating the two membrane regions, the tight junction also connects epithelial cells to each other, forming a continuous sheet, or monolayer, of

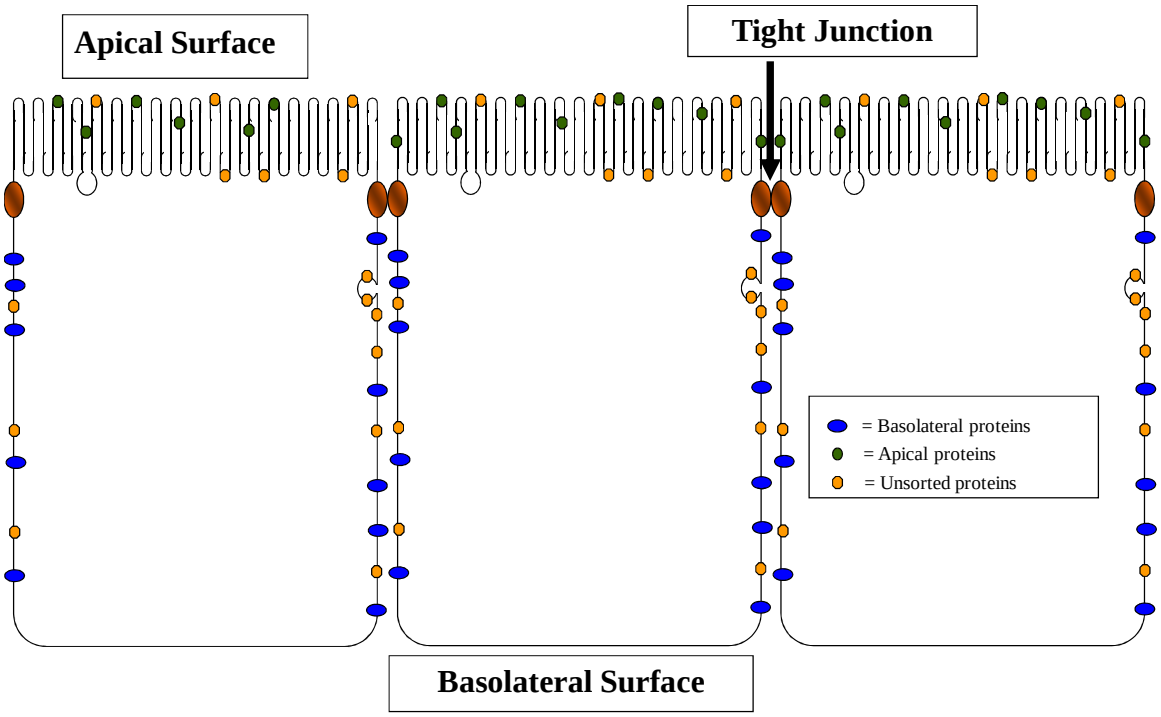

Figure 1.4. Epithelial cells have two distinct membrane domains. All epithelial cells have distinct apical (facing the lumen), and basolateral (facing the basement membrane and cell interstitium) membranes, separated by tight junctions. Some transmembrane proteins exist in both domains, while others are preferentially sorted either apically or basolaterally.

cells. The protein meshwork between the cells is water- and ion-tight, preventing paracellular diffusion between the lumen and the underlying tissues. This also helps protect the body from external pathogens, and is referred to as the “gate” or “barrier” function.

While the tight junction is a complex and impressive evolved structure, it would serve little purpose if the epithelial cells could not control the lipid and protein contents of each region. Epithelial cells deliver proteins to the correct membrane domains by a variety of mechanisms. The intracellular machinery acts on targeting signals contained within the amino acid sequence, or modifications of the individual proteins.

Sorting Signals in Transmembrane Proteins

The intracellular machinery of epithelial cells has evolved mechanisms to detect signals within many proteins that direct their expression to only one side of the tight junction. These signals take many forms; they can be post-translational modifications or primary sequences, they can be presented on either the cytoplasmic/extravesicular face or the extracellular/intravesicular face of vesicles, and they can be conserved among many different proteins, or unique to only one protein.

Apical-targeting signals

Apical-targeting signals fall into four categories: 1) Association with lipid rafts, 2) glycosylation, 3) GPI anchors, and 4) amino acid sequences (Folsch, 2008). As the mechanisms involved are poorly understood, these signals are not necessarily mutually exclusive. For example, a GPI anchor often makes a protein more likely to be associated with a lipid raft (Brown and Rose, 1992).

Cholesterol-rich and detergent-resistant lipid rafts are separated out of the trans-golgi network and targeted to the apical membrane of epithelial cells (Schuck and Simons, 2004). Some proteins associate with rafts by partitioning into these detergent-resistant membrane fractions and thus are delivered to the apical membrane (Schuck et al., 2003). This was the original theory of apical sorting in epithelial cells (van Meer and Simons, 1988). Only recently, however, has the formation of these lipid rafts in the trans-Golgi network been demonstrated, albeit in yeast (Klemm et al., 2009).

Glycosylation is a carbohydrate modification that is added to proteins in the endoplasmic reticulum and modified in the trans-Golgi network. Both N- and O-linked glycosylation modifications have been identified as apical-targeting signals. N-linked glycosylation is always added to asparagine residues within an Asn-X-Ser or Asn-X-Thr motif. O-linked glycosylation is a modification of serine or threonine residues, but there is

no consensus sequence for the attachment. The role of glycosylation in polarized trafficking was first demonstrated for the soluble protein clusterin (referred to then only as an 80 kD glycoprotein). Normally, clusterin is secreted only into the apical media, but following tunicamycin treatment (which inhibits N-glycosylation) it is secreted equally into the apical and basolateral compartments (Urban et al., 1987). It was later determined that many transmembrane glycoproteins were also sorted apically (Lisanti et al., 1989). Yeaman et al. found that O-linked glycosylation is necessary for the apical sorting of the p75 neurotrophin receptor tyrosine kinase (Yeaman et al., 1997). Both forms of glycosylation have been implicated in the sorting of several other proteins, including endolyn (Potter et al., 2004) and lactase-phlorizin hydrolase (Delacour et al., 2006).

A GPI anchor is a glycolipid modification that is added to the N-terminus of an otherwise soluble protein. GPI anchored proteins are generally expressed only on the apical membrane of epithelial cells, including MDCK cells (Lisanti et al., 1989), but this is not the case for all epithelial cells (Zurzolo et al., 1993). The apical targeting of GPI-anchored proteins was originally thought to be a product of their integration into lipid rafts (Brown and Rose, 1992). While this is likely the underlying mechanism for many proteins, more recent data has demonstrated apical targeting of a GPI-anchored protein independent of its raft association (Castillon et al., 2013). Furthermore, in the same cell line, the prion protein PrP(C), a GPI-anchored protein that is N-glycosylated and partitions into detergent-resistant lipid rafts, is targeted to the basolateral membrane (Puig et al., 2011;Sarnataro et al., 2002).

The final category of apical signals, based on amino acid sequences, is extremely diverse. While a variety of protein-based apical-targeting signals have been described, there is little consensus or knowledge of the underlying mechanisms to be found. Most of the signals identified are unique amino acid sequences, varying from a few amino acids to 20 or more and usually present in a cytoplasmic domain (Folsch,

2008). The closest example of a conserved apical targeting motif was described for three sodium-dependent acid transporter proteins. A peptide sequence from the rat sodium-dependent bile acid transporter containing the sequence NKGF was shown by NMR to adopt a β–turn conformation that was critical for apical delivery (Sun et al., 2003). Apical targeting of the related excitatory amino acid transporter-3 and the human sodium-dependent vitamin C transporter were shown to depend on similar sequences (NGGF and FKGF, respectively) and computer modeling suggested that they too form β–turn conformations (Cheng et al., 2002;Subramanian et al., 2004).

Amino acid-based sorting signals are the only type that has been shown to be involved in the polarized targeting of GPCRs, although this does not mean the other types of signals play no role in targeting. In addition to the P2Y receptors, apical-targeting signals have been described for the A1 adenosine receptor, two metabotropic glutamate receptors, mGluR1b and mGluR7, a serotonin receptor 5HT1B, a muscarinic acetylcholine receptor M2AchR, and rhodopsin (Chmelar and Nathanson, 2006;Chuang and Sung, 1998;Francesconi and Duvoisin, 2002;Jolimay et al., 2000;Wang et al., 2004). The rhodopsin targeting signal has the most well-defined mechanism for apical targeting. Portions of the rhodopsin C-tail interact directly with the microtubule motor dynein light chain Tctex-1, which directs it along the cytoskeleton to the apical surface (Tai et al., 2001).

In addition to targeting signals that promote direct delivery of newly synthesized proteins to its intended membrane domain, there are signals that direct trafficking after the protein has reached the plasma membrane. This involves selective internalization and movement to the opposite membrane region, a process called transcytosis. The best described apical transcytosis signal is from the polymeric immunoglobulin receptor (pIgR) (Luton et al., 2009). The pIgR is initially delivered to the basolateral membrane, and then accumulates at the apical membrane at steady-state, both constitutively and

when stimulated by immunoglobulins (Schaerer et al., 1990). Ligand binding stimulates transcytosis by inducing phosphorylation of a residue within the basolateral-targeting signal (Casanova et al., 1991), after which a separate signal drives the receptor to the apical surface (Luton et al., 2009).

Basolateral-targeting signals

Unlike apical signals, all known basolateral-targeting signals are amino acid sequences. There are three defined basolateral-targeting motifs and a large assortment of other signal sequences that are either unique or so poorly conserved that their similarities are not readily apparent.

The first basolateral-targeting signal described was within the pIgR C-tail, mentioned above, which is apparently unique to that protein (Casanova et al., 1991). This was shortly followed by the discovery of an NPVY basolateral-targeting signal in the cytoplasmic domain of the LDL receptor (as well as a second, less efficient signal) (Matter et al., 1992). This sequence overlaps the previously determined clathrin-mediated internalization signal of the receptor, which by species comparison was shown to depend on the same NPXY motif (where X is any amino acid) (Chen et al., 1990). Not surprisingly, the NPXY motif was shown to direct basolateral targeting by interacting with the epithelial-specific subunit (μ1B) of the AP-1 clathrin adaptor protein (Folsch et al., 1999). LLC-PK1, a porcine epithelial cell line, does not express μ1B and proteins containing NPXY-dependent signals are mis-sorted to the apical membrane. Exogenous expression of μ1B in LLC-PK1 cells corrects the sorting defect (Folsch et al., 1999).

The second conserved basolateral targeting motif also relies on a tyrosine residue, as demonstrated by mutational analysis of the VSV-G viral glycoprotein expressed in MDCK cells (Thomas et al., 1993). Similar basolateral targeting sequences from the asialoglycoprotein receptor (Geffen et al., 1993), and lysosomal acid

phosphatase (Prill et al., 1993) established the consensus sequence YXXΦ, where X is any amino acid and Φ is an amino acid with a bulky hydrophobic side chain (Thomas and Roth, 1994). As with the NPXY motif, YXXΦ signals also direct proteins to the basolateral membrane of polarized epithelial cells by interaction with the μ1B clathrin adaptor protein (Ohno et al., 1995;Ohno et al., 1999). YXXΦ-containing signals have also been identified as determinates for other types of vesicular sorting, including lysosomal (Guarnieri et al., 1993), endoplasmic reticulum (Mallabiabarrena et al., 1992), and trans-golgi network targeting (Bos et al., 1993;Humphrey et al., 1993;Wong and Hong, 1993), as well as endocytosis (Chang et al., 1991;Girones et al., 1991). Therefore, basolateral targeting cannot be assumed from the presence of a YXXΦ motif alone. These signals have been shown to interact with the μ-subunits of AP-1, AP-2, and AP-3, with some specificity derived from the amino acids surrounding the tyrosine residue (Ohno et al., 1998), which likely determines their intracellular functions.

The last class of conserved basolateral-targeting signals is based on a di-hydrophobic (often, but not always, a di-leucine) pair. This motif was first identified in the IgG Fc Receptor FcRII-B2 (Hunziker and Fumey, 1994;Matter et al., 1994). However, like the previous motifs, di-leucine motifs have also been shown to direct endocytosis and lysosomal targeting (Letourneur and Klausner, 1992;Pond et al., 1995). As with NPXY and YXXΦ motifs, di-leucine motifs were also shown to interact with clathrin adaptor proteins, the γ/σ1 subunits of AP-1 or δ/σ3 of AP-3 (Janvier et al., 2003).

Up to now, this discussion of basolateral-targeting signals has focused solely on conserved motifs. However, a number of labs, including our work with P2Y receptors, detailed below, have identified basolateral-targeting sequences that contain none of the above motifs. Furthermore, they appear to have very little in common with each other, suggesting a wider diversity of mechanisms than first envisioned. Notable proteins with apparently unique basolateral-targeting signals include the transferrin receptor (Odorizzi

and Trowbridge, 1997), metabotropic glutamate receptor-1a (Francesconi and Duvoisin, 2002), α2A, α2B and α2C adrenergic receptors (Wozniak and Limbird, 1996), follicle-stimulating hormone receptor (Beau et al., 1998), thyroid-stimulating hormone receptor and luteinizing hormone receptor (Beau et al., 2004), H/K-ATPase (Dunbar et al., 2000), and the M3 acetylcholine receptor (Nadler et al., 2001).

Polarized Expression of P2Y Receptors

Seven of the eight identified human P2Y receptors show polarized expression in cultured epithelial cell lines (Fig. 1.5) (Wolff et al., 2005). This is the largest number of related, polarized isoforms reported to date, making them a unique experimental model. Steady-state expression of $P2Y_2$, $P2Y_4$, and $P2Y_6$ receptors is almost entirely apical in kidney, colon, and bronchial epithelial cell lines (MDCK, Caco-2, and 16HBEo-, respectively) (Wolff et al., 2005). In contrast, the $P2Y_1$, $P2Y_{11}$, $P2Y_{12}$ and $P2Y_{14}$ receptors are localized to the basolateral membrane; only the $P2Y_{13}$ receptor is unsorted. One of the few restrictions to the study of P2Y receptors is the lack of high-affinity, isoform-specific antibodies (Yu and Hill, 2013). Thus, the authors generated cell lines that stably expressed P2Y receptor constructs with hemagglutinin (HA) epitope tags for confocal immunofluorescence. To ensure that there was no effect on receptor localization, pharmacological data for wild-type and HA-tagged receptors were collected in Ussing Chambers for apical and basolateral agonist administration (Wolff et al., 2005). As a number of polarized targeting signals had previously been isolated to the cytoplasmic tails of transmembrane proteins, initial experiments to identify the P2Y targeting signals consisted of the generation of a pair of mutant constructs for each polarized receptor. The first was a simple truncation just past the end of the seventh transmembrane domain, and the second a chimeric construct consisting of the main body of the unsorted bradykinin-2 (BK2) receptor with a P2Y replacement C-tail. The results, as illustrated in Figure 1.6, indicated the presence of apical-targeting signals in the main body of the $P2Y_1$, $P2Y_2$, and $P2Y_6$ receptors and the C-tail of the $P2Y_4$ receptor. Basolateral-targeting signals were found in the C-tails of the $P2Y_1$, $P2Y_{11}$, $P2Y_{12}$ and $P2Y_{14}$ receptors, as well as the main body of the $P2Y_{12}$ receptor (DuBose et al., 2013;Qi et al., 2005;Wolff et al., 2005).

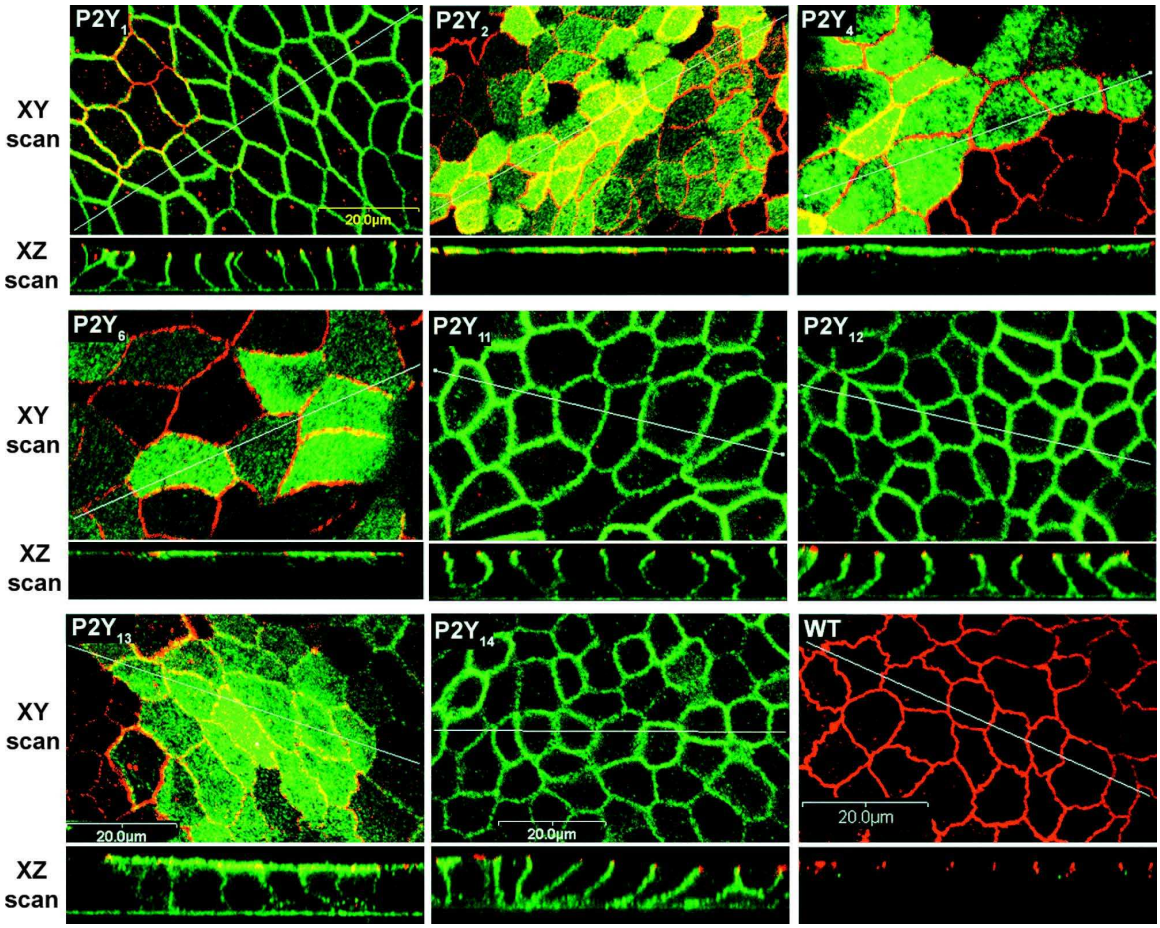

Figure 1.5. Confocal microscopy of wild-type (WT) MDCK(II) cells and MDCK(II) cells expressing HA-tagged human P2Y receptors. MDCK(II) epithelial cells expressing each of the HA-tagged P2Y receptor subtypes and WT MDCK(II) cells were examined using confocal microscopy. For each cell line, the top panel is a confocal image in which the focus plane was parallel to the monolayer (XY scan), whereas the bottom panel shows the focus plane as a vertical cross section of the monolayer (XZ scan). The white line in the XY scan indicates the path of the XZ scan. Green fluorescence represents HA-tagged P2Y receptor, and red fluorescence represents the ZO-1 subunit of the tight junction protein complex. The lack of green fluorescence in WT MDCK(II) cells demonstrates the specificity of the anti-HA antibody. Reprinted with permission from Wolff et al, AJP, 2005.

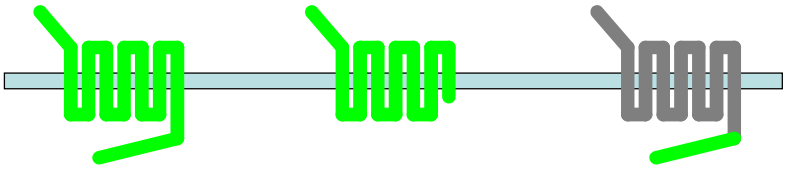

Receptor	Distribution	Nterm-TM7(Body)	C-tail
$P2Y_1$	Basolateral	Apical (1st ECL)	Basolateral
$P2Y_2$	Apical	Apical (1st ECL)	No Signal
$P2Y_4$	Apical	No Signal	Apical
$P2Y_6$	Apical	Apical (1st ECL)	Not Tested
$P2Y_{11}$	Basolateral	Not Expressed	Basolateral
$P2Y_{12}$	Basolateral	Basolateral	Basolateral
$P2Y_{13}$	Unsorted	N/A	N/A
$P2Y_{14}$	Basolateral	Not Expressed	Basolateral

Figure 1.6. P2Y receptor-targeting signals are contained within the main body and C-terminal tail of the receptors. Polarized sorting of three constructs are shown. The first is a full-length receptor, the second lacks the C-terminal tail, and the third is the C-terminal tail appended chimerically to the main body of the unsorted BK2 receptor.

The Apical-sorting signal of the $P2Y_2$ Receptor

Perhaps the most striking finding of these initial receptor constructs was the apparent difference in the mechanism of apical targeting of $P2Y_2$ and $P2Y_4$ receptors, despite their overall high homology (52% amino acid identity). This difference, coupled with the high homology of the two receptors, provided a useful approach to further delineate the $P2Y_2$ receptor apical-targeting signal. A series of chimeric constructs were created that contained the N-terminal region of the $P2Y_2$ receptor fused at various points to the corresponding region of the $P2Y_4$ receptor lacking its C-tail and thus its targeting signal. In this way, the location of the apical targeting sequence of the $P2Y_2$ receptor was narrowed down to the first extracellular loop (Qi et al., 2005).

Sequence alignment of the first extracellular loops of the $P2Y_2$ and $P2Y_4$ receptors narrowed the list of possible critical residues to just nine amino acids. These amino acids were mutated in the $P2Y_2$ receptor to the corresponding residue in the $P2Y_4$ receptor, allowing identification of four critical amino acids: Arg^{95}, Gly^{96}, Asp^{97}, and Leu^{108}. Interestingly, the RGD sequence is a well-characterized integrin-binding motif, suggesting that perhaps interactions with integrins are involved in apical targeting. However, further analysis was not consistent with this possibility. RGE and QGE mutations, both of which would not be expected to bind integrins, did not disrupt apical targeting (Qi et al., 2005).

Interestingly, it was later determined that this apical-targeting signal was conserved in the $P2Y_6$ receptor, where it is the only signal in the receptor (unpublished results), and the $P2Y_1$ receptor, where it is overridden by the basolateral signal in the $P2Y_1$ receptor C-terminal tail (Wolff et al., 2010) (see below). No other receptors to date have been found that share this targeting signal. In fact, it is still the only extracellular, amino acid-based targeting signal that has been described.

The Basolateral-sorting signal of the $P2Y_1$ Receptor

Initial studies as described above demonstrated that the $P2Y_1$ receptor contained two signals: a cryptic apical signal in the main body of the receptor (later shown to be in the first extracellular loop; see above) and a dominant basolateral signal in the C-terminal tail. The C-terminal tail, when used to replace the endogenous C-terminal tails of a variety of GPCRs, was capable of moving these receptors completely to the basolateral surface. While the extracellular apical-targeting signal appears to play no role in polarized sorting of the $P2Y_1$ receptor (See Chapter 3; DuBose *et al.*, in preparation), it did provide a useful tool for characterization of the dominant basolateral-targeting signal in the C-terminal tail (Wolff et al., 2010). As demonstrated by the $P2Y_1$ receptor ΔCT truncation construct, disruption of the basolateral targeting sequence uncovers the cryptic apical signal, and thus mutation of key amino acids required for basolateral sorting resulted in a receptor that not only was no longer basolateral, or even unsorted, but expressed entirely at the apical domain of epithelial monolayers.

The basolateral-targeting signal in the C-terminal tail of the $P2Y_1$ receptor is very unusual and unlike any signal characterized to date. Unlike the basolateral motifs described above, the signal is quite long (25 aa), and no single amino acid mutation is sufficient to disrupt basolateral targeting (Wolff et al., 2010). One of the most unusual properties of the signal is that it is sequence- and direction independent. The entire basolateral-targeting signal could be inverted N→C or even scrambled without disrupting basolateral targeting. An in-depth mutagenesis approach revealed that the targeting function of the signal is dependent on several factors: 1) the number of charged residues, but not the total charge of those residues, 2) the distance of the signal from the plasma membrane, and 3) a still unknown function of the non-charged residues, as mutation of all of those residues while leaving the charged residues intact also disrupted basolateral targeting (Wolff et al., 2010).

Polarized Sorting of Other P2Y Receptors

The apical-sorting signal of the $P2Y_4$ receptor is described herein in Chapter 2. Similar to the basolateral signal in the $P2Y_1$ receptor, the apical signal in the $P2Y_4$ receptor is unlike any previously described apical-targeting signal and appears to be unique to the $P2Y_4$ receptor (DuBose et al., 2013). The $P2Y_{12}$ receptor has two basolateral-targeting signals: one within its C-tail that appears to be dependent on the PDZ ligand (unpublished results), and one within the main body of the receptor that has yet to be explored further (DuBose et al., 2013). The $P2Y_{14}$ receptor C-tail contains a basolateral-targeting signal that shares many of the properties of the $P2Y_1$ receptor signal, although it bears little sequence homology. This signal, like that of the $P2Y_1$ receptor, is long (~23 amino acids), dependent on the number of charged residues, but it is also dependent on the type of charge (positive) and several hydrophobic residues (unpublished results). The $P2Y_{11}$ receptor basolateral-targeting signal has yet to be explored beyond its general location within the C-tail of the receptor.

The most interesting finding of these experiments is just how different the targeting signals are, even among such closely related receptors. Only $P2Y_2$ and $P2Y_6$ receptors appear to rely on the same mechanism for polarized targeting. It will be very interesting to learn whether these varied signals are simply different entry points into common sorting mechanisms, perhaps decoded by different adaptor proteins, or if these signals represent truly independent mechanisms for protein sorting that run in parallel within epithelial cells.

Trafficking Itineraries and Technological Limitations

A second area of interest for our lab, in addition to identifying and characterizing the targeting signals of P2Y receptors, has been to define the physical pathway that a receptor takes through the vesicular trafficking machinery to reach its final membrane destination. Ideally, this would include every subset of endosomal compartments that a protein traverses as well as every molecular interaction that drives it along its way. This type of experiment is, of course, quite technically challenging. In the broadest sense, all of these individual interactions can be summed up into one of two categories: direct and indirect.

Direct delivery refers to a mechanism in which a protein undergoes all of its polarized sorting during its biosynthesis before reaching the plasma membrane for the first time. In this pathway, all (or nearly all) of the newly synthesized protein appears on the same side of the tight junction where the protein is found at steady-state. With indirect targeting, newly synthesized proteins appear at both apical and basolateral membrane domains and are only later sorted to their polarized steady-state locations. There are many subdivisions and possible mechanisms that can underlie either of these mechanisms, but until recent technological advances even this distinction was difficult to make.

Historically, the way to distinguish between direct or indirect targeting was to perform an [^{35}S]cysteine/methionine pulse-chase experiment, then biotinylate extracellular proteins at either the apical or basolateral membranes at various times after the chase. Following biotinylation, the cell monolayers were lysed and the biotinylated proteins precipitated with (strept)avidin to separate the apical or basolateral proteins from the remaining cellular pool. These streptavidin-biotinylated protein complexes then had to be disrupted (a difficult process given the stability and extremely high affinity of

streptavidin for biotin), and the released material was then re-precipitated with a receptor-specific antibody to separate the receptor from the remaining biotinylated proteins. This 2nd precipitation was then separated by SDS-PAGE and detected by autoradiography. Western blotting could not be used as it would detect all of the proteins that were already present at the membrane of interest instead of just those that were labeled during the pulse.

While this technique has been used to study the delivery mechanisms of several polarized proteins (Anderson et al., 2005;Chmelar and Nathanson, 2006;Keefer and Limbird, 1993;Wozniak and Limbird, 1996), it suffers from three important drawbacks. First, the method relies on high expression of the protein of interest into sorting machinery that has been shown to be saturable (Marmorstein et al., 2000;Matter et al., 1992). Second, the method requires that the rates of transcytosis be slower than the rates of initial delivery, such that an accumulation of protein can be detected before moving to its final polarized location. Third, there is no direct demonstration that the trafficking itineraries observed are due to selective delivery or transcytosis rather than selective internalization and degradation.

In Chapter 3 (DuBose, in prep.), we describe a straightforward method for making these measurements using a recently developed covalent fluorophore attachment technology (see below) that avoids each of these limitations, and apply it to determine the trafficking itineraries of the $P2Y_1$, $P2Y_2$, and $P2Y_4$ receptors.

In Vivo Covalent Fluorophore Attachment

Several technologies have recently been developed for the covalent labeling of proteins in live cells. The first and simplest approach relies on the specific labeling of a tetra-cysteine motif within an alpha-helix by 4′,5′-bis(1,3,2-dithioarsolan-2-yl)fluorescein in the presence of $AsCl_3$ (Griffin et al., 1998). The benefit of this method is the relatively small genetic alteration necessary to create a target protein. The downside is that it is limited to a few fluorophore choices, the fluorophores are prohibitively expensive, and each site is capable of binding either one or two fluorophore molecules, complicating quantification.

Two methods, BioEase™ and AviTag™, rely on the specific biotinylation of relatively small (72 and 15 amino acids, respectively) tags by biotin protein ligases, followed by recognition by (strept)avidin probes (Ashraf et al., 2004;de Boer et al., 2003). While an improvement in many ways over previous methods, this technology is more suited to protein purification than fluorescence labeling.

The last two methods involve the attachment of a larger, enzyme-based “epitope” to the protein of interest. The enzymes react covalently with specific types of small molecules at a 1:1 stoichiometry, allowing the attachment of a wide variety of probes. The obvious downside to these techniques is that the presence of a large protein domain connected to the protein of interest may cause steric hindrance or otherwise impede its normal function.

The HALO-tag is a 34 kDa mutant of the *Rhodococcus rhodochrous* dehalogenase enzyme. A single histidine to phenylalanine substitution causes it to specifically react with probes displaying chloroalkane chains, forming an ester bond, rather than releasing the halogen-free product. These bonds are stable, form quickly at

room temperature and are suitable for both microscopy and biochemical applications (Los et al., 2008).

The SNAP-tag is a 20 kD derivative of the human O^6-alkylguanine-DNA alkyltransferase (Keppler et al., 2003). It has been engineered through directed evolution to react with O^6-benzylguanine derivatives rather than methylated guanosine residues (Gronemeyer et al., 2006;Juillerat et al., 2003). The reaction forms a stable thioether linkage between the protein of interest and a wide variety of fluorescent (or other) probes. Like the Halo-tag, this linkage is stable and forms quickly at room temperature. Additionally, a second derivative, CLIP-tag, has been developed that is selective for O^6-benzylcytosine derivatives, allowing for simultaneous two-color labeling of live cells (Gautier et al., 2008). Due to its smaller size and greater variety of labeling options, we found this system to be most appropriate for our current and future studies of P2Y receptor trafficking.

Chapter 2: Apical Targeting of the $P2Y_4$ Receptor is Directed by Hydrophobic and Basic Residues in the Cytoplasmic Tail

Overview

The $P2Y_4$ receptor is selectively targeted to the apical membrane in polarized epithelial cell lines and has been shown to play a key role in intestinal chloride secretion. In this study, we delimit a 23 amino acid sequence within the $P2Y_4$ receptor C-tail that directs its apical targeting. Using a mutagenesis approach, we found that four hydrophobic residues near the C-terminal end of the signal are necessary for apical sorting, whereas two basic residues near the N-terminal end of the signal are involved to a lesser extent. Interestingly, mutation of the key hydrophobic residues results in a basolateral enrichment of the receptor construct, suggesting that the apical targeting sequence may prevent insertion or disrupt stability of the receptor at the basolateral membrane. The signal is not sequence specific, as inversion of the 23 amino acid sequence does not disrupt apical targeting. We also show that the apical targeting sequence is an autonomous signal and is capable of redistributing the normally basolateral $P2Y_{12}$ receptor, suggesting that the apical signal is dominant over the basolateral signal in the main body of the $P2Y_{12}$ receptor. The targeting sequence is unique to the $P2Y_4$ receptor, and sequence alignments of the C-terminal tail of mammalian orthologs reveal that the hydrophobic residues in the targeting signal are highly conserved. These data define the novel apical-sorting signal of the $P2Y_4$ receptor, which may represent a common mechanism for trafficking of epithelial transmembrane proteins.

Introduction

Nucleotides are ubiquitous small molecules involved in a wide variety of biological processes. In addition to playing essential roles in phosphorylation, energy utilization and metabolism, and synthesis of nucleic acids and enzymatic co-factors, nucleotides are also released from cells where they serve as extracellular ligands for transmembrane receptors involved in signal transduction (Lazarowski et al., 2003;Lazarowski, 2012). Nucleotide receptors have been found in all cell types, where they mediate a broad range of cell activities. There are two distinct families of nucleotide receptors, P2X and P2Y. P2X receptors are ion channels that open in response to extracellular ATP, while the P2Y receptors are a family of G protein coupled receptors (GPCRs) that respond to extracellular nucleotides (Coddou et al., 2011;von Kugelgen and Harden, 2011). Eight P2Y receptors have been identified to date—$P2Y_1$, $P2Y_2$, $P2Y_4$, $P2Y_6$, $P2Y_{11}$, $P2Y_{12}$, $P2Y_{13}$, and $P2Y_{14}$. The numbering is not sequential because several receptors were reported to be P2Y receptors but later determined to either not respond to nucleotides or to be orthologs of existing mammalian P2Y receptors (Herold et al., 1997;Janssens et al., 1997;Li et al., 1998;Qi et al., 2004).

The P2Y receptors can be divided into two subclasses based on their downstream signaling properties. The $P2Y_1$-like receptors ($P2Y_1$, $P2Y_2$, $P2Y_4$, $P2Y_6$, and $P2Y_{11}$) signal primarily through $G_{\alpha q}$, while the $P2Y_{12}$-like receptors ($P2Y_{12}$, $P2Y_{13}$, and $P2Y_{14}$) signal primarily through $G_{\alpha i}$. The $P2Y_{11}$ receptor also signals through $G_{\alpha s}$ to stimulate adenylyl cyclase (Communi et al., 1997;Qi et al., 2001). The receptors can also be characterized by their activating ligands: $P2Y_1$, $P2Y_{11}$, $P2Y_{12}$, and $P2Y_{13}$ receptors are activated by adenine nucleotides (either ADP or ATP), $P2Y_4$, $P2Y_6$, and $P2Y_{14}$ receptors are activated by uracil nucleotides (UDP or UTP), and the $P2Y_2$ receptor is activated equally by ATP and UTP. The $P2Y_{14}$ receptor is unusual as it is activated by both UDP and UDP-sugars (Carter et al., 2009).

P2Y receptors are expressed in a variety of tissue types, and the subtype and density of the receptors varies significantly. $P2Y_4$ receptor mRNA is widely distributed and most abundant in the intestine (Moore et al., 2001), where it has been shown to play a role in luminal Cl^- secretion (Robaye et al., 2003). Since bacterial invasion can induce nucleotide release (Crane et al., 2002;McNamara et al., 2001;Tran Van Nhieu et al., 2003) and Cl^- secretion is the known mediator of diarrhea symptoms (Field et al., 1989;Field et al., 1989;Kunzelmann and Mall, 2002), antagonists of the $P2Y_4$ receptor may have therapeutic value for the treatment of infectious diarrhea. Agonists of the $P2Y_4$ receptor may also be useful as it has been hypothesized that stimulation of the Cl^- secretory pathway may alleviate intestinal abnormalities associated with cystic fibrosis (Robaye et al., 2003). Unfortunately, there are currently no selective ligands for the $P2Y_4$ receptor available. The $P2Y_4$ receptor has also been implicated in the control of K^+ secretion in vestibular dark cell epithelium and in mouse colon (Marcus and Scofield, 2001;Matos et al., 2005).

Epithelial cells are specialized cells that form water- and ion-impermeable barriers between organ lumens and underlying cells and tissues (Brown et al., 2009). This impermeable barrier is created by tight junctions, which are multi-protein complexes that surround and connect the cells that form the epithelial monolayer, as well as separate the epithelial cell plasma membrane into two distinct compartments (Giepmans and van Ijzendoorn, 2009). The apical membrane faces the lumen and contacts the external milieu, while the basolateral membrane faces the underlying cells and is in contact with the interstitial fluid. Formation of this barrier allows epithelial cell monolayers to regulate absorption and excretion of water, salts, nutrients, and toxins by selective expression and distribution of transmembrane channels, pumps, and receptors. The proper targeting of these proteins to the correct membrane surface is critical for the proper function of the monolayer. Our lab has investigated the targeting of the entire

family of P2Y receptors, and shown that seven of the eight P2Y receptors are strongly polarized when expressed in epithelial cell lines (Wolff et al., 2005).

Despite the fact that aberrant protein sorting is often associated with disease states, the mechanisms by which epithelial cells establish and maintain these polarized distributions are poorly understood (Keitel et al., 2003;Kleizen et al., 2000;Marr et al., 2002;Marr et al., 2002;Rotin et al., 2001). It is well established that many proteins contain amino acid sequences that act as trafficking signals to direct the protein to the appropriate membrane (Folsch, 2008;Rodriguez-Boulan et al., 2004;Weisz and Rodriguez-Boulan, 2009). Tyrosine- and di-hydrophobic-based signals have been shown to interact with clathrin adaptor complex proteins and to direct basolateral targeting (Folsch et al., 1999;Hunziker et al., 1991;Hunziker and Fumey, 1994;Matter et al., 1994;Ohno et al., 1995). In contrast, post-translational modification, such as glycosylation or glypiation, is often sufficient to confer apical targeting (Lisanti et al., 1989;Scheiffele et al., 1995;Vagin et al., 2009;Wilson et al., 1990;Yeaman et al., 1997). Oligomerization and lipid raft association have also been suggested to direct apical trafficking (Lingwood and Simons, 2010;Paladino et al., 2004;Paladino et al., 2006;Schuck and Simons, 2004).

Beyond these conserved signals, a wide array of seemingly unrelated sorting signals have been described (Folsch, 2008;Weisz and Rodriguez-Boulan, 2009). Our lab has described such signals for the $P2Y_1$ and $P2Y_2$ receptor. The $P2Y_1$ receptor is directed to the basolateral membrane by a 25-amino-acid signal located within its C-terminal tail, whose function depends on nine charged residues. The signal functions even after inverting or scrambling the sequence in the context of the full receptor, indicating that it is sequence independent (Wolff et al., 2010). The $P2Y_2$ receptor is sorted to the apical membrane of MDCK(II) cells and contains an apical-targeting signal in its first extracellular loop that is dependent on four amino acids: Arg95, Gly96, Asp97,

and Leu108 (Qi et al., 2005). This signal is highly unusual because, following receptor synthesis, it is located on the inside of vesicles and therefore inaccessible to intracellular sorting machinery. This is the only protein-based extracellular apical-targeting signal identified in any protein to date.

The $P2Y_4$ receptor is expressed almost exclusively at the apical surface at steady-state in MDCK(II), Caco-2, and 16HBE14o- cells (Wolff et al., 2005). Even though $P2Y_2$ and $P2Y_4$ receptors are 52% identical and both are targeted to the apical membrane in MDCK(II) cells, they do not share a common sorting signal. We have previously shown that the apical-sorting signal of the $P2Y_4$ receptor, in contrast to the $P2Y_2$ receptor, is located within its C-terminal tail (Qi et al., 2005). When the C-terminal tail of the $P2Y_4$ receptor is deleted, the truncated receptor is unsorted, whereas fusion of the $P2Y_4$ C-tail to the unsorted BK2 receptor just after transmembrane segment 7 (TM7) results in its expression at the apical membrane. In this study, we delimit the $P2Y_4$ targeting signal, identify key amino acids within this signal that are responsible for apical targeting, and demonstrate its dominance over a basolateral signal in the main body of the $P2Y_{12}$ receptor. These data add to the known targeting signals by which P2Y receptors are sorted to distinct membrane surfaces, and may represent a novel mechanism for polarized trafficking.

Methods

Construction of Mutant and Chimeric Receptors—Construction and cloning of HA-tagged $P2Y_4$ and $BK2/Y_4$ receptors into the retroviral vector pLXSN was accomplished as described previously (Qi et al., 2005;Wolff et al., 2005). Targeted mutations were introduced into the $P2Y_4$ receptor C-tail of these constructs by overlap-extension PCR (Ho et al., 1989), whereas $P2Y_4$ receptor truncation constructs were made using PCR with a 5' vector primer and 3' primers containing a stop codon at the appropriate location followed by a XhoI site to facilitate cloning.

The $P2Y_{12}/P2Y_4$ receptor chimera was constructed using overlap extension PCR. One set of primers amplified the $P2Y_{12}$ receptor coding sequence from the second codon (with an MluI site to facilitate cloning) through the codon for Ser304, the start of the C-tail, and also included the first seven codons of the $P2Y_4$ receptor C-tail starting at Asp311. The second set of primers amplified the C-tail of the $P2Y_4$ receptor starting at Asp311 through the end of the gene and contained a XhoI site at the end of the downstream primer. After the initial amplification, the two PCR products were isolated, then combined and amplified with only the outside primers. The resulting product was digested with MluI and XhoI and ligated into a similarly digested modified pLXSN vector that added an HA-tag to the N-terminus of the chimera.

The $P2Y_4$ receptor C-tail invert construct was created using two long primers (68 and 69 nucleotides) whose respective 3' ends overlapped by 30 nucleotides. These primers encoded the $P2Y_4$ receptor C-tail in which the codons for the targeting signal were inverted N$\rightarrow$C and included SalI and SbfI restriction sites at the ends of the primers. The primers were annealed, filled in with the Klenow fragment of DNA polymerase I (New England Biolabs, Ipswich, MA), and digested with SalI and SbfI. The digested fragment was cloned into a modified pLXSN-HA-$P2Y_4$ plasmid in which SalI

and SbfI sites were introduced by incorporating silent mutations into the codons for Arg314/Arg315 and Ser345, respectively.

We initially created receptor mutants in the context of either the BK2-$P2Y_4$ C-tail chimeric receptor or the $P2Y_4$ receptor. While confocal microscopy revealed essentially identical targeting as observed with modified $P2Y_4$ receptor constructs described below, cell surface expression was often too low for accurate quantification of apical versus basolateral receptor distribution (data not shown). Therefore, we introduced a cleavable signal sequence (MKTIIALSYIFCLVPA) and FLAG epitope tag (DYKDDDDA) immediately upstream of the HA-tag to increase receptor expression (Guan et al., 1992). All of the constructs shown in Figure 2.3A, with the exception of the BK2/$P2Y_4$-C321S receptor, contained this addition. Inclusion of the signal sequence increased steady-state receptor levels, which facilitated imaging and quantification, without having an appreciable effect on localization in polarized monolayers.

Cell culture—All cells were grown in a humidified incubator at 37℃ in a 5% CO_2/95% air atmosphere. Type II Madin-Darby canine kidney cells (MDCK(II); ATCC, Rockville, MD) were maintained in 1:1 DMEM/F12 medium containing 5% fetal bovine serum and 1X pen/strep. PA317 cells were maintained in DMEM containing 10% fetal bovine serum and 1X pen/strep.

Retroviral infection—Recombinant retroviruses were produced by calcium phosphate-mediated transfection of PA317 cells with pLXSN plasmids as previously described (Comstock et al., 1997). Retroviral particles in the culture supernatant were harvested 3 days after transfection and used to infect MDCK(II) cells. Infected cells were selected for 7-10 days in medium containing 1 mg/mL G418. After selection, cells were maintained in medium containing 0.4 mg/mL G418. Surface expression of receptors was confirmed by radioimmunoassay with an antibody directed against the HA-epitope tag as described previously (Brinson and Harden, 2001).

Confocal Fluorescence Microscopy—MDCK(II) cells were seeded at 6 x 10^5 cells/well in 12 mm Transwell inserts (Corning Life Sciences, Acton, MA) and grown for 5-7 days with daily medium changes to allow the cells to form polarized monolayers. Cells were prepared for confocal microscopy as described previously (Wolff et al., 2005). Briefly, cells were washed and fixed in 2% PFA in PBS with 2 mM $CaCl_2$ and 2 mM $MgCl_2$ for 30 minutes at 4 ºC. After fixation, cells were permeabilized with cold (-20 ºC) methanol for 30 seconds. Cells were then quenched by three washes of 150 mM sodium acetate in 1% non-fat dry milk (NFDM) and blocked by three more washes in 1% NFDM. Cells were incubated with a 1:1000 dilution of mouse monoclonal anti-HA antibody (HA.11; Covance, Berkeley, CA) and a 1:500 dilution of rabbit anti-ZO-1 antibody (Zymed Laboratories Inc., South San Francisco, CA) in 1% NFDM overnight at 4 ºC. Cells were then washed three times and incubated with both goat anti-mouse Alexa-488 and goat anti-rabbit Alexa-594 (Molecular Probes, Eugene, OR), each diluted 1:500 in 1% NFDM, for one hr at room temperature. After washing five times in PBS and once in Molecular Probes Equilibration Buffer, the polyester membranes were removed from the transwell inserts with a scalpel and mounted under cover slips in Slow Fade A mounting media (Invitrogen, Carlsbad, CA).

Confocal images were acquired using an Olympus Fluoview 300 laser scanning microscope system equipped with a PlanApo 60x oil-immersion objective. Multiple representative XY (parallel to the apical cell membrane) and XZ (vertical cross-section) images were acquired from each monolayer. For apically sorted or unsorted receptors an XY slice through the apical membrane is shown, whereas for basolaterally sorted receptors an XY slice below the level of the apical membrane is shown. In both instances, the XZ image shows the relative receptor expression at the two membrane regions. The brightness and contrast of the resulting images were adjusted in Adobe Photoshop with the goal of highlighting membrane expression while minimizing

background fluorescence. In most cases, auto-fluorescence of the polyester membrane has been removed for clarity. Representative images are shown for each receptor construct.

Polarized Cell-surface Biotinylation—MDCK(II) cells were seeded on 12 mm (6 x 10^5 cells/well) or 24 mm (1.2 x 10^6 cells/well) Transwell inserts and grown for 5-7 days with daily medium changes to allow the cells to form a polarized monolayer. A polarized biotinylation assay was used to quantify cell-surface expression of HA-tagged receptors essentially as described previously (Wolff et al., 2005). Briefly, cells were carefully cooled to 4ºC and kept cold for the entire assay to avoid potential nucleotide release and redistribution due to receptor activation. Cells were washed twice in PBS++ (phosphate-buffered saline, pH 8.0, plus 2 mM $CaCl_2$ and 2 mM $MgCl_2$), then PBS++ containing 2 mg/mL Sulfo-NHS-SS-Biotin (Pierce, Rockford, IL) was applied to either the apical or basolateral surface, and the reaction was allowed to proceed for 20 min. Following aspiration of the biotinylation solution, the cells were incubated with PBS++ containing 100 mM glycine (pH 8.0) for 10 minutes to quench the reaction, and then washed three times with PBS++.

Proteins extracts were prepared by adding RIPA lysis buffer (50 mM Tris HCl pH 8.0, 100 mM NaCl, 5 mM EDTA, 1% Triton X-100, 0.5% deoxycholate, and 0.1% SDS) to washed cells and passing the lysate through a 25-gauge needle 7-10 times to ensure complete disaggregation. Insoluble materials were removed by centrifugation at 13,000 x *g* for 30 minutes, and the resulting supernatant was incubated for 90 minutes with 35 µL (for 12 mm inserts) or 50 µL (for 24 mm inserts) of immobilized NeutrAvidin resin (Pierce). The resin was washed twice with Tris-Triton buffer (50 mM Tris•HCl, pH 7.4, 100 mM NaCl, 5 mM EDTA, and 1% Triton X-100) and biotinylated proteins were released from the resin by incubating with 30 µL of 2× SDS-PAGE sample buffer containing 100 mM dithiothreitol for 10 minutes at 37ºC. Eluted proteins were separated

on a 10% SDS-PAGE gel and transferred to a PVDF membrane overnight at 4ºC. HA-tagged proteins were detected with a peroxidase-conjugated monoclonal antibody (3F10, Roche Biochemicals, Indianapolis, IN) at 1:500 dilution and visualized with SuperSignal West Pico chemiluminescent substrate (Pierce). Bands were quantified from scanned images with ImageJ software (Schneider et al., 2012).

Results

Delimitation of the apical-targeting signal of the $P2Y_4$ receptor—We showed previously that the human $P2Y_4$ receptor is sorted to the apical membrane of three different epithelial cell types (MDCK(II), 16HBE14o$^-$, and Caco-2 cells), and that the apical targeting sequence is located within the C-tail of the receptor (Qi et al., 2005;Wolff et al., 2005). To delimit the C-terminal end of the apical-targeting signal, we constructed a series of HA-tagged human $P2Y_4$ receptors in which increasing amounts of the C-terminus were truncated. The truncated receptors were expressed in MDCK(II) cells and their steady-state localization was determined by confocal microscopy (Fig. 2.1). XZ scans of the full-length human $P2Y_4$ receptor and $P2Y_4$ receptors truncated at amino acids 355 or 343 revealed that these receptors were localized to the apical membrane at steady state, indicating that the signal remained intact (Fig. 2.1). In contrast, the $P2Y_4$ receptor truncated at amino acid 332 resulted in an unsorted phenotype. These data indicate that the C-terminal end of the apical targeting sequence is no further downstream than amino acid 343.

The C-tail of the $P2Y_4$ receptor confers apical targeting to the normally unsorted BK2 receptor when fused to the receptor just past TM7 (Qi et al., 2005). To delimit the N-terminal end of the apical targeting sequence, we created chimeric receptors comprised of the body of the BK2 receptor (N-terminus through TM7) fused with progressively smaller portions of the $P2Y_4$ C-tail (Fig. 2.2). The longest of these constructs has a C-tail that starts at the putative beginning of the $P2Y_4$ C-tail (Asp311) and ends at the end of the apical-targeting signal (Asp343) as determined in Fig. 2.1. The other two chimeric receptors have shorter lengths of the $P2Y_4$ C-tail fused to the body of the BK2 receptor, beginning at Cys321 and Lys325 respectively. Fusion of

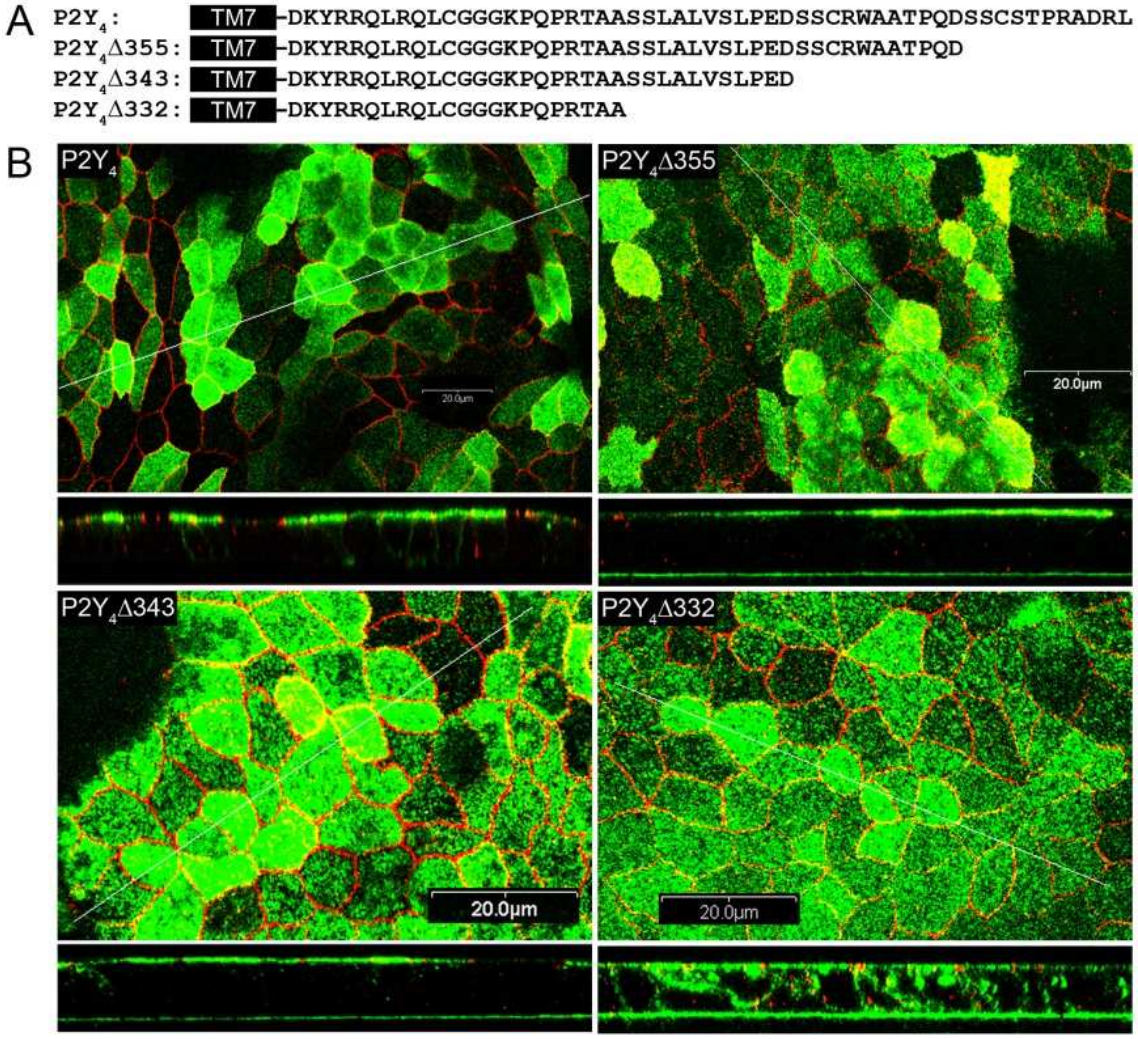

Figure 2.1. The $P2Y_4$ apical-targeting signal ends before Asp343. *A,* HA-tagged wild type and truncated $P2Y_4$ receptors with the C-tail sequences shown were stably expressed in MDCK(II) cells. *B,* subcellular localization of the receptor constructs in polarized monolayers was analyzed by confocal microscopy. The receptor tags are marked by green fluorescence while red fluorescence marks ZO-1, a tight junction protein. For all fluorescence micrographs in this study, the lager images are scans of the XY plane (parallel to the apical membrane) and the smaller images are XZ scans along the white line shown in the XY scan.

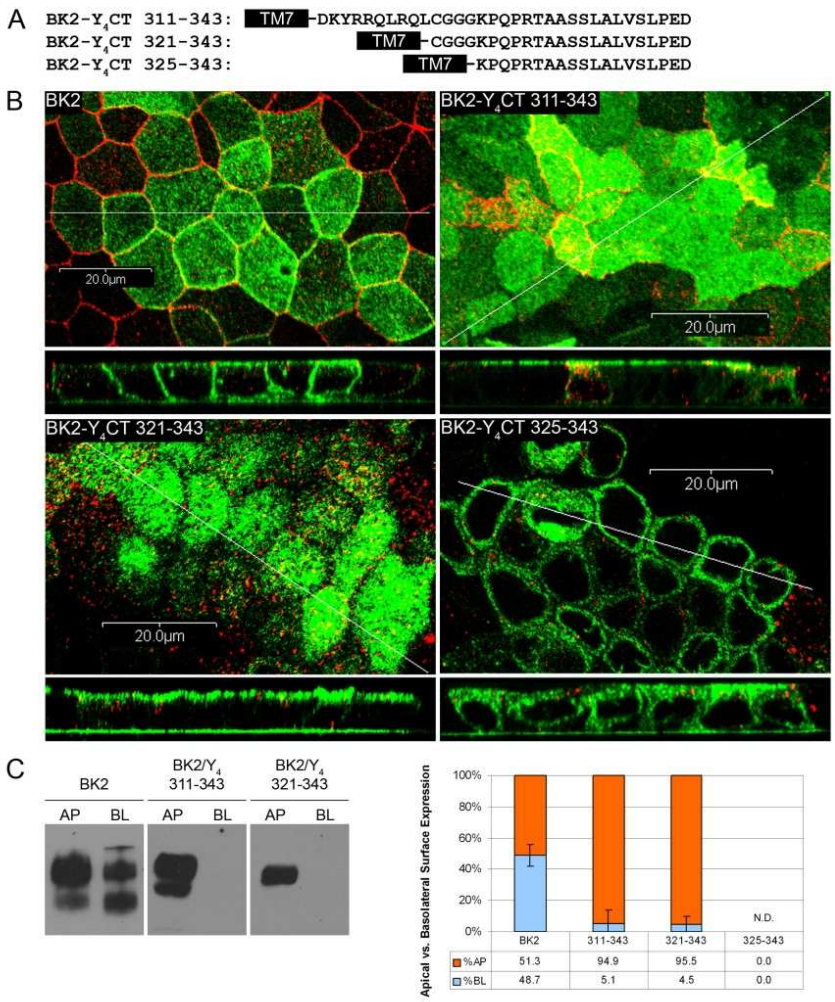

Figure 2.2. The $P2Y_4$ apical-targeting signal begins after Cys321. *A*, HA-tagged BK2-$P2Y_4$ chimeric receptors with the indicated C-tail sequences were stably expressed in MDCK(II) cells. *B,* subcellular localization of the receptor constructs in polarized monolayers was analyzed by confocal microscopy. *C,* surface expression of the receptor constructs was determined by a polarized biotinylation assay (see Methods). Quantification is based on densitometry data of apical (AP) and basolateral (BL) bands (n≥3). Error bars represent the standard deviation of each data set. The BK2-Y_4CT 325-343 construct was not detected in our biotinylation assay, presumably because it does not reach the cell surface in sufficient quantities.

amino acids 311-343 or 321-343 of the $P2Y_4$ C-tail was sufficient to confer polarized sorting of the BK2 receptor to the apical surface of MDCK(II) cells (Fig. 2.2B), and the apical localization of these chimeric receptors revealed by confocal microscopy was confirmed by an established polarized cell-surface biotinylation assay (Fig. 2.2C) (Keefer and Limbird, 1993;Qi et al., 2005;Wolff et al., 2005). In contrast to the other chimeras, the BK2 receptor with the fewest number of amino acids (325-343) of the $P2Y_4$ C-tail was not sorted to the apical membrane. This receptor construct was presumably unstable and failed to reach the cell surface, as we were unable to pull down sufficient quantities of receptor to produce a visible band in our biotinylation assay. These data indicate that the N-terminal end of the apical-targeting signal of the $P2Y_4$ receptor is no farther upstream than amino acid 321.

Taken together, these experiments defined a 23-amino-acid sequence (Cys321 to Asp343) that is both necessary and sufficient to target the $P2Y_4$ or the BK2 receptor to the apical surface. This sequence is unique to the $P2Y_4$ receptor, bears no similarity to any known sorting signal, and does not contain any known binding motifs or conserved domains.

Identification of key amino acids in the $P2Y_4$ apical targeting sequence—Because its length made single residue mutational analysis unlikely to yield useful information, we mutagenized amino acid groups (e.g. charged, polar, non-polar, etc.) to discern their role in apical targeting (Fig. 2.3) as we have done previously for the basolateral targeting sequence of the $P2Y_1$ receptor (Wolff et al., 2010). We began by analyzing a $P2Y_4$ receptor construct in which all of the serine and threonine residues in the C-tail were mutated to alanine. Previous work had established that agonist-dependent phosphorylation of Ser333 and Ser334 within the apical targeting sequence is required for $P2Y_4$ receptor desensitization and internalization (Brinson and Harden, 2001), which

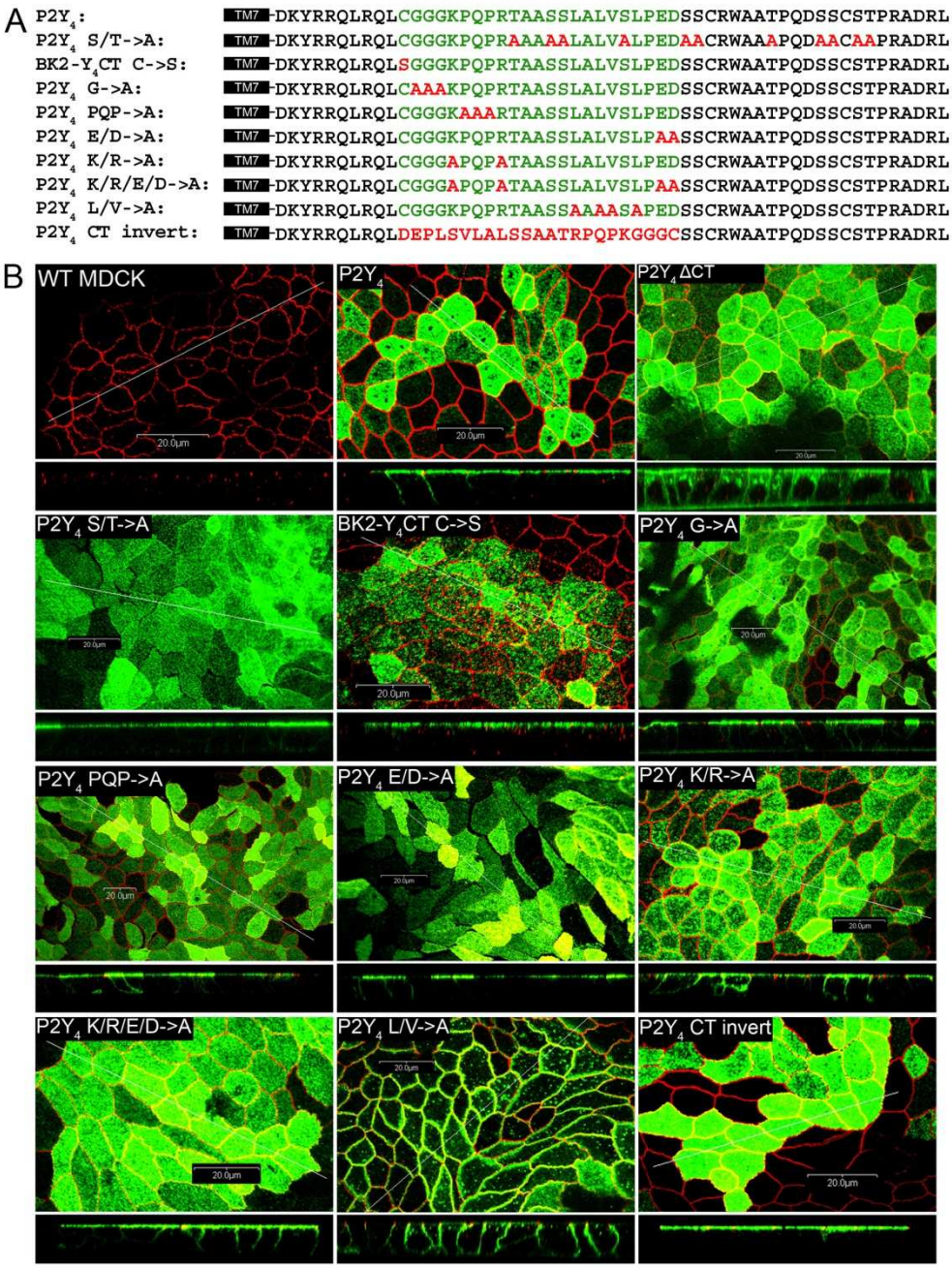

Figure 2.3. Subcellular localization of receptor constructs with mutant $P2Y_4$ C-tails. *A,* mutant receptors with the C-tail sequences shown were stably expressed in MDCK(II) cells. The delimited apical-targeting sequence is marked in green and the amino acid mutations of each construct are marked in red. *B,* subcellular localization of the receptor constructs in polarized monolayers was analyzed by confocal microscopy.

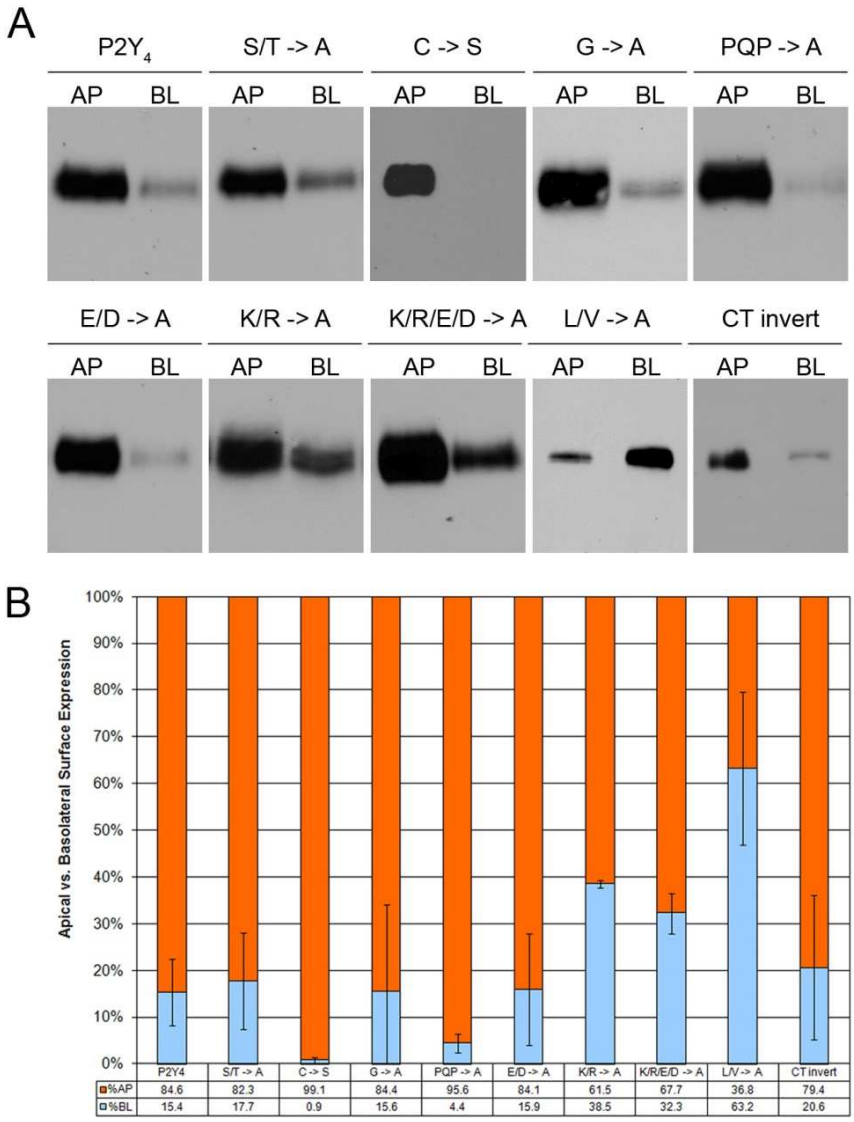

Figure 2.4. Surface expression of receptor constructs with mutant $P2Y_4$ C-tails. Mutant receptors (see Figure 2.3 for specific sequences) were stably expressed in MDCK(II) cells. *A,* surface expression of the mutant receptor constructs was determined by polarized biotinylation. *B,* Quantification is based on densitometry data of apical (AP) and basolateral (BL) bands (n≥3). Error bars represent the standard deviation of each data set.

potentially could affect steady-state receptor distribution. However, these mutations had no effect on the polarized expression of the $P2Y_4$ receptor (Figs. 2.3 & 2.4).

We next targeted the single cysteine residue (Cys321) in the apical targeting sequence, as palmitoylation of cysteines has been implicated in protein stability as well as trafficking (Huang and El-Husseini, 2005;Linder and Deschenes, 2007). We found that a C321S mutation had no effect on receptor localization of the BK2/$P2Y_4$ C-tail chimeric receptor (Figs. 2.3 & 2.4). Likewise, mutation of three consecutive glycines or the PQP triad near the beginning of the sequence to alanines in the context of the $P2Y_4$ receptor had no effect on apical targeting (Figs. 2.3 & 2.4).

Charged residues within the basolateral targeting sequence of the $P2Y_1$ receptor are critical to its function (Wolff et al., 2010). To address the role of charged residues in the $P2Y_4$ receptor apical-targeting signal, we mutated the acidic and/or basic residues of the apical targeting sequence to alanine. Mutation of the glutamate and aspartate residues to alanine had no effect on targeting, whereas mutation of lysine and arginine residues to alanine reduced apical polarization by 24% (61% apical versus 85% apical for wild-type $P2Y_4$). Mutation of both the basic and acidic amino acids to alanine closely matched the results of mutating the basic residues alone.

We also made mutations to a small hydrophobic region in the latter half of the apical targeting sequence (one valine and three leucine residues within six residues). Mutation of these four amino acids to alanine markedly disrupted the apical targeting of the $P2Y_4$ receptor and in fact promoted pronounced (but not complete) basolateral targeting (63% basolateral). These data highlight the importance of these four hydrophobic residues for proper apical targeting of the $P2Y_4$ receptor.

The apical-targeting signal of the $P2Y_4$ receptor is sequence-independent-We previously showed that the 25-amino acid basolateral-targeting signal of the $P2Y_1$ receptor was functional either in its normal N->C direction or inverted in a C->N direction

(i.e. where the last amino acid of the signal becomes the first amino acid in the inverted construct's signal sequence), suggesting that the basolateral-targeting signal was sequence-independent (Wolff et al., 2010). To determine if there is any sequence or directional specificity to the apical targeting sequence of the $P2Y_4$ receptor, the signal was inverted in the context of the full-length receptor and its localization was determined by confocal microscopy (Figs. 2.3 & 2.4). Surprisingly, the inverted signal was still able to direct complete apical targeting to the $P2Y_4$ receptor. This lack of sequence- and direction-specificity may indicate that only a few key amino acids within the sequence and/or a particular structure of the $P2Y_4$ receptor C-tail (which is preserved upon inversion) are necessary for proper polarization.

The $P2Y_4$ receptor apical targeting sequence redistributes a basolaterally targeted receptor—There are numerous examples of membrane proteins that have more than one targeting signal, and these signals can be either redundant or opposing. For opposing signals, it has been generally assumed that when both apical and basolateral signals reside within the same protein, the basolateral signal is dominant (Matter et al., 1994). For example, we have shown that the $P2Y_1$ receptor contains both an apical signal in the main body of the receptor and a basolateral-targeting signal in the C-tail, with the basolateral-targeting signal completely dominant over the apical signal (Wolff et al., 2010). However, dominance of a basolateral signal over an apical signal is not always observed (Chuang and Sung, 1998).

To address whether the apical-targeting signal of the $P2Y_4$ receptor can be dominant over a basolateral-targeting signal, we fused the C-tail of the $P2Y_4$ receptor to the main body of the $P2Y_{12}$ receptor. Unpublished work in our lab has shown that the $P2Y_{12}$ receptor contains two redundant basolateral-sorting signals; one in its C-tail, and one in the main body (N-terminus to TM7) of the receptor. The HA-tagged $P2Y_{12}$ receptor truncated at the start of its C-tail is targeted to the basolateral membrane

($P2Y_{12}\Delta CT$; 95% basolateral; Fig. 2.5). Fusion of the C-tail of the $P2Y_4$ receptor to the $P2Y_{12}$ receptor results in a protein that is mostly, but not completely, redirected to the apical surface of MDCK(II) cells (76% apical; Fig. 2.5).

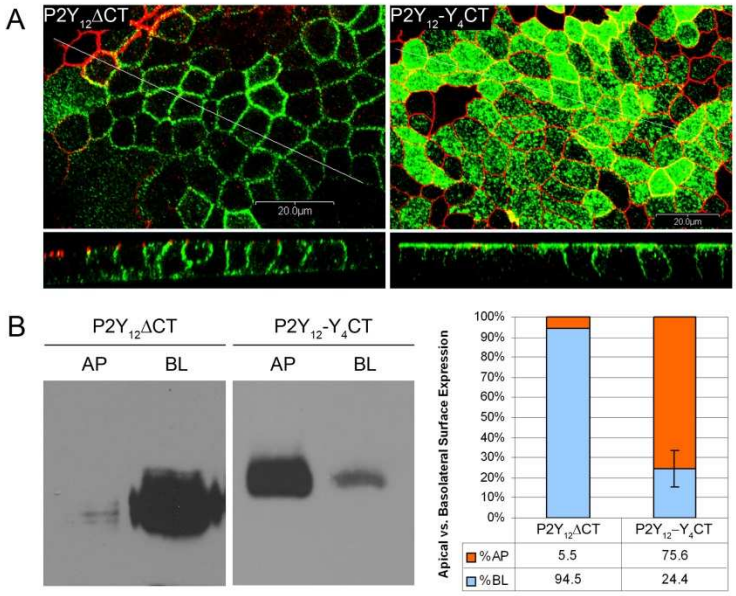

Figure 2.5. The $P2Y_4$ apical-targeting signal is dominant over a basolateral signal. The HA-tagged $P2Y_{12}$ receptor lacking its C-tail and $P2Y_{12}$-$P2Y_4$ C-tail chimera were stably expressed in MDCK(II) cells. *A,* subcellular localization of the receptor constructs in polarized monolayers was analyzed by confocal microscopy. *B,* surface expression of the receptor constructs was determined by polarized biotinylation. Quantification is based on densitometry data of apical (AP) and basolateral (BL) bands (n≥3). Error bars represent the standard deviation of each data set.

Discussion

Seven of the eight known P2Y receptors are sorted to distinct membrane surfaces when expressed in polarized epithelial cells, including the $P2Y_4$ receptor. We show here that the $P2Y_4$ receptor contains a 23-amino-acid sequence in its C-tail that is both necessary and sufficient to direct apical targeting in MDCK(II) cells. The signal is autonomous, as it is functional even when fused to other GPCRs. The signal depends primarily on the presence of 4 hydrophobic residues near the C-terminal end of the sequence, and less so on basic amino acids. Other amino acids in this sequence appear to have little to no effect on apical targeting. Surprisingly, the apical-targeting signal functions normally even when inverted and is capable of redirecting a basolaterally targeted GPCR to the apical membrane. The properties of this novel apical-sorting signal have not been described for any apical signal identified to date.

Alignment of the C-terminal tail of the $P2Y_4$ receptor from a broad range of mammalian orthologs indicates that the most important residues of the signal (i.e. basic and hydrophobic residues) are conserved. For example, the four key hydrophobic residues are highly conserved, with only slight variations (L→R in *M. domestica* (opossum) and *S. harrisii* (tasmanian devil), and V→G in *A. melanoleuca* (panda)) (Fig. 2.6). Conservation of the basic amino acids is not as strong as with the hydrophobic residues, but when they are not conserved, other nearby residues are changed to basic amino acids such that there is at least one basic amino acid within the N-terminal region of the signal (the exceptions, *T. belangeri* (tree shrew) and *O. cuniculus* (European rabbit), have no basic residues within the same region). This may indicate that the specific position of these amino acids is not critical, as long as positive charges are located nearby. Consistent with this idea, inversion the targeting sequences in the $P2Y_4$ receptor (Fig. 2.3) and the $P2Y_1$ receptor (Wolff et al., 2010), or scrambling the

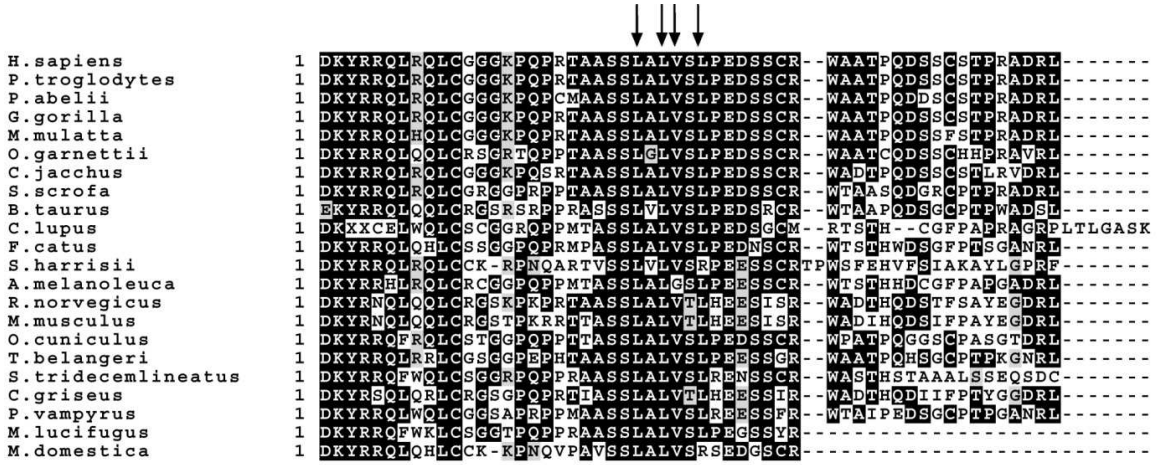

Figure 2.6. Conservation of the apical-targeting sequence of the $P2Y_4$ receptor. Known mammalian $P2Y_4$ receptor C-tail amino acid sequences are shown. Sequences were aligned using ClustalW and shaded using Boxshade 3.21, both available on the World Wide Web (http://www.ch.embnet.org/). Residues that are conserved in greater than 50% of the sequences are shaded black. Positions with similar residues in greater than 50% of the sequences are shaded grey. The key hydrophobic amino acids for apical targeting are marked with red arrows. Protein sequence accession numbers or ensembl.org identification numbers are as follows: *Homo sapiens* (human), P51582.1; *Pan troglodytes* (chimpanzee), XP_003317560.1; *Pongo abelii* (orangutan), XP_002834732.1; *Gorilla gorilla* (gorilla), ENSGGOP00000000615; *Macaca mulatta* (macaque), NP_001185632.1; *Otolemur garnettii* (bush baby), ENSOGAP00000021789; *Callithrix jacchus* (marmoset), XP_002807938.1; *Sus scofra* (pig), NP_001231097.1; *Bos Taurus* (cow), NP_001243486.1; *Canis lupus familiaris* (dog), XP_003640305.1; *Felis catus* (cat), ENSFCAP00000007557; *Sarcophilus harrisii* (Tasmanian devil), ENSSHAP00000006770; *Ailuropoda melanoleuca* (panda), ENSAMEP00000021321; *Rattus norvegicus* (rat), NP_113868.1; *Mus musculus* (mouse), NP_065646.1; *Oryctolagus cuniculus* (rabbit), XP_002720124.1; *Tupaia belangeri* (tree shrew), ENSTBEP00000001285; *Spermophilus tridecemlineatus* (squirrel),

ENSSTOP00000015075; *Cricetulus griseus* (Chinese hamster), XP_003509162.1; *Pteropus vampyrus* (megabat), ENSPVAP00000013535; *Myotis lucifugus* (microbat), ENSMLUP00000018666; and *Monodelphis domestica* (opossum), XP_001362915.1.

basolateral targeting sequence in the $P2Y_1$ receptor, had little to no effect on steady-state localization, indicating that the absolute positions of important residues are not critical and that these sorting signals function in a sequence-independent manner. Taken together, these data suggest that other orthologs of the $P2Y_4$ receptor are also trafficked to the apical membrane of epithelial cells in their respective hosts by a similar mechanism involving the C-tail of the receptor.

The apical-sorting signal of the $P2Y_4$ receptor is a member of a large group of heterogeneous sequences of various lengths with little sequence homology, characteristic motifs, or known common-binding partners (Francesconi and Duvoisin, 2002;Takeda et al., 2003). Several studies with three apically expressed sodium-dependent acid transporters suggest that a beta-turn secondary structure motif may be important in apical sorting. A 14-amino-acid sequence in the C-tail of the rat ileal sodium-dependent bile acid transporter (Abst) was shown to direct apical targeting, and NMR studies indicated that a 4-amino acid tetramer (NKGF) within this sequence formed a beta-turn that was suggested to be important in apical targeting (Sun et al., 2003). Apical targeting of two other members of this family, the human sodium-dependent vitamin C transporter and the excitatory amino acid transporter-3, was shown to depend on similar sequences for apical sorting (Cheng et al., 2002), and computer modeling suggested that these sequences also form β–turns (Subramanian et al., 2004). However, both potential phosphorylation sites within the apical signal of Abst and its interaction with the 16 kDa subunit c of the vacuole proton pump were also shown to be important in apical targeting, suggesting a more complex sorting mechanism than simple recognition of a secondary structure element (Sun et al., 2003;Sun et al., 2004).

The mechanism of apical sorting directed by the apical signal in the $P2Y_4$ receptor appears to be distinct from that of the acid transporters. Hydrophobic and basic amino acids are the most important for proper apical targeting of the $P2Y_4$ receptor, and

our experiments rule out a role of phosphorylation in this process. We have not ruled out the possibility that the $P2Y_4$ apical targeting sequence forms a beta-turn (albeit with a different sequence of amino acids than the acid transporters) or other secondary structure that is selectively stabilized by lipids or proteins at the apical membrane, although modeling programs do not predict a beta turn in the region comprising the hydrophobic cluster (data not shown).

Four members of the G protein coupled receptor family (including the $P2Y_4$ receptor) have been shown to contain apical sorting sequences within their C-tails. Even among receptors from the same superfamily, there is no apparent common mechanism for apical targeting. The final 32 amino acids of rhodopsin, the best characterized of the four apical signals, interact with the Tctex-1 dynein light chain, a minus-end microtubule motor, presumably directing rhodopsin to the apical membrane along the cell's cytoskeleton (Tai et al., 2001). The exact amino acids responsible for targeting rhodopsin are unknown, but there are no hydrophobic clusters or sequence similarity to $P2Y_4$. While we have shown that apical targeting of the $P2Y_4$ receptor is most dependent on hydrophobic residues, apical targeting of the metabotropic glutamate receptor 1b isoform is dependent on three basic residues (Francesconi and Duvoisin, 2002). The C-tail of the serotonin 5-HT_{1B} receptor operates as an apical-targeting signal through an as yet unknown mechanism (Jolimay et al., 2000). This sequence also appears to be distinct from the $P2Y_4$ receptor, but there is a group of two hydrophobic residues flanked by two charged residues.

Taken together, the diversity of cytoplasmic apical-targeting signals may simply reflect a diverse set of adaptor proteins that may be resolved by common sorting mechanisms, as others have speculated (Hodson et al., 2006). However, relatively few sorting signals and even fewer binding partners and mechanisms are currently known. It is possible that as more signals are discovered and characterized, more commonalities

will begin to appear. What is emerging from our studies of the sorting signals in the $P2Y_1$ and $P2Y_4$ receptors is that there is a set of sorted proteins that do not interact with proteins in the sorting machinery in a manner that depends on specific protein-protein interactions; instead, these sorting proteins likely recognize a secondary structure or physiochemical state, but how this is achieved is not clear. If the apical-targeting sequence does interact directly with another protein, it seems more likely that it would resemble the interaction of a GPCR with arrestin proteins, which are involved in receptor internalization (Benovic et al., 1987;Lohse et al., 1990). Arrestin proteins bind to a broad range of different receptors in a manner that is dependent on charged residues (usually through phosphorylation) but is sequence independent (Ferguson et al., 1996).

The two P2Y receptors with the highest identity (52%), $P2Y_2$ and $P2Y_4$, are both located at the apical membrane, but their targeting sequences are markedly different (Qi et al., 2005). The $P2Y_2$ receptor has an apical-targeting signal located in the first extracellular loop that is absent in the $P2Y_4$ receptor. In contrast, the C-terminus of the $P2Y_4$ receptor directs apical targeting, whereas the C-terminus of the $P2Y_2$ receptor does not contain any targeting information (Qi et al., 2005). This difference has important mechanistic implications. For example, once the $P2Y_2$ receptor is synthesized and inserted into the endoplasmic reticulum, the apical signal in the extracellular loop becomes inaccessible to cytosolic sorting proteins, whereas the apical signal in the C-terminus of the $P2Y_4$ receptor is available. Given the distinct locations of the apical signals, it will be informative to examine the mechanistic similarities (and differences) by which these receptors reach steady-state.

Curiously, many membrane proteins contain more than one targeting sequence, and these signals can be either redundant or opposing. In at least two proteins, mGluR1 and PMCA2, alternative splicing determines their distribution, indicating a functional and physiological reason for multiple targeting signals (Chicka and Strehler,

2003;Francesconi and Duvoisin, 2002). Within the P2Y family, we have shown that the $P2Y_1$ receptor contains a cryptic apical targeting sequence in addition to its dominant basolateral targeting sequence (Wolff et al., 2010), and the $P2Y_{12}$ receptor contains redundant basolateral sequences (unpublished results). It was thought that when opposing targeting sequences are present in the same protein, the basolateral signal is always dominant, as is the case for the $P2Y_1$ receptor. However, we show here that the $P2Y_4$ receptor apical-targeting signal is able to override most (but not all) of the basolateral targeting encoded in the $P2Y_{12}$ receptor lacking its C-tail. These data are consistent with those from Chuang et al. who showed that the apical targeting sequence in the C-tail of rhodopsin can overcome the basolateral signal in the single pass protein, CD7 (Chuang and Sung, 1998). Thus, both apical and basolateral-targeting signals can overcome an opposing signal elsewhere in the protein, and likely depend on context and location.

Our studies of the $P2Y_4$ receptor have shown strong apical polarization in cell lines derived from kidney, lung, and colon epithelia, suggesting that the sorting mechanism for this receptor is common to all epithelial cells (Wolff et al., 2005). Even so, it is possible that epithelial cells exist that do not sort the $P2Y_4$ receptor in the same manner or to the same extent as in MDCK(II) cells. Indeed, one group has shown $P2Y_4$ receptor-mediated functional responses at both the apical and basolateral membranes in a study of nucleotide-stimulated Cl^- secretion in mouse jejunum and colon (Ghanem et al., 2005). There are caveats to these experiments – the measurements were taken using only a single, saturating dose of UTP in a “leaky” membrane preparation – but they may demonstrate a variation in the location of the $P2Y_4$ receptor in different epithelial cells. In contrast, using $P2Y_2$ and $P2Y_4$ receptor knock-out mice, members of this same group found no evidence of basolateral $P2Y_4$ receptor function in mouse colon when studying nucleotide-induced K^+ secretion (Matos et al., 2005). Unfortunately, the lack of

selective, high affinity antibodies makes it impossible to directly detect the native $P2Y_4$ receptor.

Our studies have provided important information about the steady-state localization of P2Y receptors, but how they achieve steady state is not clear. Previous work showed that the $P2Y_4$ receptor undergoes internalization and recycling much faster than other P2Y receptors (Brinson and Harden, 2001), but the lack of an effect on apical targeting from mutating the two Ser residues (Ser 333 and Ser 334) responsible for desensitization and internalization strongly suggests that internalization and recycling is not important in the establishment of the steady-state apical localization. It is further unclear when and where the sorting of P2Y receptors and most other polarized transmembrane proteins occurs. Recent improvements in fluorescence microscopy technology should make it possible to answer not only these questions of spatial regulation, but also the regulation of these proteins over time, and these experiments are in progress.

Chapter 3: Distinct Trafficking Itineraries of the $P2Y_1$, $P2Y_2$, and $P2Y_4$ Receptors in Polarized Madin-Darby Canine Kidney Epithelial Cells

Overview

Multiple nucleotide-activated P2Y receptors are expressed in a polarized manner in epithelial cells, where they regulate ion transport. We previously illustrated that the $P2Y_1$ receptor is expressed exclusively at the basolateral membrane, whereas $P2Y_2$ and $P2Y_4$ receptors are expressed at the apical membrane. While the steady state locations and protein sorting signals of these receptors are firmly established, little is known about the mechanism(s) whereby polarized distribution is achieved. For example, it is unknown whether sorting occurs during protein synthesis and transport to the membrane surface or via transcytosis after cell surface delivery. To distinguish between these pathways, we developed a novel method utilizing commercial SNAP-tag technology and applied it to determine the trafficking itineraries of these P2Y receptors. SNAP-tagged receptors present at the plasma membrane of MDCK cell monolayers were blocked with non-fluorescent substrate, different membrane-impermeable fluorescent substrates were added to the apical and basolateral surfaces, and the membrane region where newly synthesized proteins first appeared was determined by confocal microscopy and image analysis. These data reveal that the basolaterally located $P2Y_1$ receptor is delivered directly to the basolateral surface of MDCK cells, while apically located $P2Y_2$ and $P2Y_4$ receptors reach the apical surface via unsorted delivery followed by selective basolateral to apical transcytosis. An estimate of the molar quantity of each receptor delivered to each membrane surface also is provided by this technology.

Introduction

Polarity is a crucial characteristic of neurons, endothelial cells, and epithelial cells that enables spatially specific inputs and cell-specific physiological responses. Cells establish and maintain polarity by mechanisms that stringently sort and traffic proteins and lipids to specific membrane compartments. Polarized epithelial cells form a monolayer with distinct apical and basolateral membrane regions separated by a protein complex called the tight junction. Proper maintenance of these membrane regions allows epithelial cells to perform their primary function of selective exchange of nutrients and waste between the body and external milieu.

The mechanisms underlying apical versus basolateral sorting of transmembrane proteins are poorly understood. We and others have identified sorting signals in several G protein-coupled receptors (GPCRs) (Beau et al., 1998;Beau et al., 2004;DuBose et al., 2013;Iverson et al., 2005;Nadler et al., 2001;Qi et al., 2005;Saunders et al., 1998;Wolff et al., 2010). Multiple subtypes of the family of nucleotide-activated P2Y receptors are widely expressed on epithelial cells, and our lab illustrated that seven of the eight P2Y receptor subtypes exhibit polarized distribution at steady-state when expressed in Madin-Darby Canine Kidney (MDCK) epithelial cells (Wolff et al., 2005). $P2Y_2$, $P2Y_4$, and $P2Y_6$ receptors are located on the apical membrane, and $P2Y_1$, $P2Y_{11}$, $P2Y_{12}$, and $P2Y_{14}$ receptors are located on the basolateral membrane. The targeting signals of the $P2Y_1$ and $P2Y_4$ receptors are in the C-terminal tails of these signaling proteins, are relatively long (between 20-25 amino acids), and are functional even when inverted N->C in the primary sequence (DuBose et al., 2013;Wolff et al., 2010). In contrast, the apical signal of the $P2Y_2$ receptor is located in the first extracellular loop (Qi et al., 2005) and is the first extracellular, protein-based sorting signal identified. While these studies defined the location, sequence, and characteristics of the signal within

each P2Y receptor protein, they offered little insight into how cells read these structure-based signals to traffic the receptor to its eventual location at steady-state.

Membrane proteins in epithelial cells undergo a normal protein life-cycle – synthesis at the endoplasmic reticulum, post-translational modification during movement through the trans-Golgi network, vesicular delivery to the cell surface, internalization and recycling, and eventual lysosomal degradation. At some point during these steps, sorted proteins are directed specifically toward one of the two membrane regions. Sorting occurs either intracellularly (in the trans-Golgi network or by subdivision of vesicles) prior to direct delivery of the protein to its final surface destination or by delivery of the protein from its initial surface destination to the opposite membrane compartment through internalization into vesicles and membrane fusion in a process known as transcytosis (Apodaca et al., 2012). Techniques that differentiate between these two basic possibilities help classify and define the mechanisms for the various sorting signals.

Existing techniques that address these sorting mechanisms, however, are either cumbersome, interfere with cell function, require high levels of recombinant receptor expression, require specialized equipment and/or software, or require incubation temperatures that markedly slow rates of vesicle delivery and transcytosis (Hua et al., 2006;Paladino et al., 2006;Polishchuk et al., 2004;Wozniak and Limbird, 1996). With the goal of defining the trafficking itineraries of basolaterally versus apically localized P2Y receptors, we developed methodology that enables quantification of existing cell surface receptors versus newly synthesized receptors in a straightforward and readily accessible manner. This system employs fusion of the N-terminus of each receptor with the SNAP tag protein, a 20 kDa variant of human O^6-alkylguanine-DNA-alkyltransferase engineered to react specifically with O^6-benzylguanine derivatives (Gronemeyer et al., 2006). Fusion of the SNAP tag to the N-termini of the $P2Y_1$, $P2Y_2$, or $P2Y_4$ receptors did

not affect steady-state targeting, downstream signaling, or regulation of these receptors in MDCK cells. By first blocking cell-surface receptors in polarized monolayers, then adding different fluorescent SNAP-tag substrates to the apical and basolateral compartments and allowing newly synthesized receptors to approach steady-state, we were able to determine the trafficking itineraries of the three P2Y receptors. Advantages of this labeling system over traditional immunofluorescence approaches include the small size and variety of fluorescent substrates, the rapid rate at which proteins are labeled, and the formation of a long-lived covalent bond between fluorophore and protein. Application of this technology unambiguously demonstrates that the basolateral $P2Y_1$ receptor is targeted directly to the basolateral membrane, whereas the $P2Y_2$ and $P2Y_4$ receptors are delivered to both membrane surfaces but then undergo transcytosis from the basolateral to the apical membrane during the progression to steady-state. This approach not only provides assessment of trafficking mechanisms, but presumably can be applied to estimate apical:basolateral ratios at steady-state of any protein of interest using standard techniques.

Materials and Methods

Construction of SNAP-HA-P2Y Receptors – To produce SNAP-HA-P2Y receptor constructs, we amplified the SNAP-tag sequence fused to an N-terminal, cleavable signal sequence from pSNAP-ADRβ2 (New England Biolabs, Ipswich, MA). The upstream primer contained an EcoRI site and a consensus Kozak site (ACCATGG, with the start codon underlined) at its 5' end (Kozak, 1984), while the downstream primer contained at its 5' end an MluI site, an HA-epitope tag sequence, and 12 bp encoding a Gly-Ser-Gly-Ser linker. The amplified fragment was digested with EcoRI and MluI and ligated into similarly digested pLXSN plasmids containing $P2Y_1$, $P2Y_2$, or $P2Y_4$ sequences, fusing the SNAP-HA tag sequence in-frame with the receptor coding sequences.

Cell Culture – All cells were maintained in a humidified 37℃ incubator under 5% CO_2. Growth media for Type II MDCK cells (ATCC, Rockville, MD) was 1:1 DMEM:F12 containing 5% fetal bovine serum and 1X pen/strep. PA317 cells (for producing retroviral particles) and 1321N1 cells (for assessing signaling properties) were grown in DMEM containing 4.5 g/L glucose, 10% fetal bovine serum, and 1X pen/strep.

Retroviral Infection – Retroviruses were produced by calcium phosphate-mediated transfection of PA317 packaging cells with pLXSN plasmids as described previously (Comstock et al., 1997;DuBose et al., 2013). Media containing recombinant virus was harvested three days after transfection and used to infect MDCK or 1321N1 cells. After incubating for 24 hours, the media was replaced with media containing 1 mg/mL G418 for 7-10 days (until mock-infected cells were dead) to select for infected cells. The presence of receptor protein was confirmed by radioimmunoassay with an antibody that detects the HA-tag. In all cases, G418-resistant cell populations were used for experiments.

SNAP-tag Labeling – Stock solutions of SNAP reagents (New England Biolabs, Ipswich, MA) were made by dissolution in DMSO, and working solutions were made by 200-fold dilution into growth media (supplemented to 50 mM HEPES to maintain the pH at 7.4). The non-fluorescent blocking reagent (SNAP-Surface Block, C8 propanoic acid benzylguanine) was used at a final concentration of 20 µM, while the fluorescent reagents (SNAP-Surface Alexafluor 488, based on Alexafluor 488; SNAP-Surface 488, based on Atto-Tec 488; and SNAP-Surface 549, based on Dyomics Dy549) were each used at 5 µM. MDCK cell monolayers were formed by seeding 5×10^5 cells/cm^2 on Transwell support membranes (Corning Life Sciences, Acton, MA) and growing for 7 days with daily media changes. Live cell monolayers were labeled for 30 minutes at 19℃ to reduce vesicle movement. Potato apyrase (Sigma-Aldrich, St. Louis, MO) was added to the media at 0.5 units/mL to reduce autocrine activation of P2Y receptors. Excess reagent was removed by two 5 min and one 30 min wash in growth media at 19℃.

Confocal Fluorescence Microscopy – Following SNAP-tag labeling, cell monolayers in the Transwell inserts were fixed in 4% paraformaldehyde for 30 min at 4℃, rinsed in 1X phosphate-buffered saline (PBS), and the membranes were removed from their supports and mounted under coverslips in Slow Fade A mounting media (Invitrogen, Carlsbad, CA). Some monolayers (e.g. those in Fig. 3.1) were counter-labeled with a monoclonal antibody against the HA-tag (HA.11; Covance, Berkeley, CA) and a fluorescent secondary antibody (Goat anti-mouse Alexafluor 594; Molecular Probes, Eugene, OR) before mounting. These monolayers underwent further processing after fixation as described previously (DuBose et al., 2013;Wolff et al., 2010). Briefly, cells were permeabilized in methanol at -20℃ for 30 sec and then washed with 150 mM sodium acetate plus 1% non-fat dry milk (NFDM) in PBS containing 2 mM $CaCl_2$ and 2

mM $MgCl_2$ (PBS++). Cells were further blocked in 1% NFDM in PBS++, and then labeled overnight at 4℃ with HA.11 at a 1:1000 dilution. S econdary antibody was applied in the same buffer at a 1:500 dilution for 1 hour at room temperature.

Fluorescence micrographs were acquired using an Olympus Fluoview 300 laser-scanning microscope system through a PlanApo 60X oil immersion objective. Multiple surface and cross-sectional images were acquired for each monolayer, and representative images are shown. Quantification was accomplished by comparing average pixel density of highlighted apical and lateral sections using ImageJ software (Schneider et al., 2012). Selections were highlighted with the 'Selection Brush Tool', the width of which was kept constant (25 pixels) so that area quantified was proportional to the length of selected membrane segments, to account for variations in the height of the monolayers. Non-specific fluorescence from SNAP-surface-labeled MDCK cells expressing HA-$P2Y_1$ receptors lacking the SNAP-tag was quantified and subtracted from the values determined for each of the labeled SNAP-tagged receptors.

SNAP-HA-P2Y Receptor Signaling – The signaling responses of the SNAP-tagged receptors were quantified using a FLIPR calcium flux assay (Sullivan et al., 1999). MDCK cells expressing the SNAP-tagged receptors could not be used for this assay, as they natively express $P2Y_1$, $P2Y_2$, and $P2Y_{11}$ receptors (Insel et al., 1996;Post et al., 1996;Post et al., 1998). Instead, retrovirally infected 1321N1 cells expressing SNAP-HA-tagged $P2Y_1$, $P2Y_2$, or $P2Y_4$ receptors were plated at 5000 cells/well in a 384 well plate 24 hr prior to assay. Cells were loaded with Calcium Plus Assay Kit dye and responses to the cognate natural agonist (ADP for $P2Y_1$ and UTP for $P2Y_2$ and $P2Y_4$ receptors) were measured using a FLIPR Tetra fluorescence image plate reader (Molecular Devices, Sunnyvale, CA). Concentration-response curves were created by plotting mean peak fluorescence (+/- SEM) of quadruplicate readings versus the

logarithm of agonist concentration. Response from a buffer-only addition was subtracted as background. Curves were fitted and EC_{50} values calculated with GraphPad Prism (La Jolla, CA) using least squares nonlinear regression and holding the Hill Slope fixed at 1.0 for concentrations between $10^{-10.5}$ and 10^{-5} M.

SNAP-HA-P2Y Agonist Induced Internalization – Agonist-promoted internalization of SNAP-HA-P2Y constructs in MDCK cells was quantified by a cell surface radioimmunoassay as described previously (Brinson and Harden, 2001;Qi et al., 2005). Briefly, MDCK cells expressing SNAP-HA-P2Y or HA-P2Y receptors were plated at 1×10^5 cells per well 48 hr prior to performing the assay. Agonists (ADP for the $P2Y_1$ receptor, UTP for $P2Y_2$ and $P2Y_4$ receptors) were added directly to cells without a media change at a final concentration of 100 μM and incubated for times between 2 min and 60 min. Cells were then chilled on ice, fixed in 4% paraformaldehyde for 30 min, and then blocked in DMEM with 50 mM HEPES (pH 7.4) and 10% fetal bovine serum. The cells were then incubated in blocking buffer containing a 1:1000 dilution of the HA.11 antibody at room temperature for 1 hr, washed, and blocking buffer containing a 1:500 dilution of ^{125}I-labeled goat anti-mouse antibody (Perkin-Elmer, Waltham, MA) was added at room temperature for 2 hr. Following thorough washing with PBS, the cells were solubilized overnight in 1 M NaOH and the amount of ^{125}I-antibody bound was quantified by gamma counting.

Construction and Purification of GST-SNAP Protein – To produce a GST-SNAP control protein, the SNAP coding sequence was amplified using pLXSN-SNAP-HA-$P2Y_1$ plasmid as template and the resulting amplified fragment was subcloned into pGEX-2V (Fedarovich et al., 2006). The upstream primer contained an in-frame BamHI site, codons for a seven amino acid linker (GSGSKLT), and the first seven codons of the SNAP tag, while the downstream primer comprised the complementary sequence of the

last six codons and the stop codon of the SNAP tag, and an EcoRI site. Following PCR amplification, the fragment was digested with BamHI and EcoRI and ligated into a similarly digested pGEX2V vector. The pGEX-2V-SNAP plasmid was transformed into *E. coli* BL21*, the cells were grown to an OD_{600} = 0.8 and then induced with 500 µM IPTG for 4 hr at 37℃. GST-SNAP protein was purified by a single pass over a 5 mL glutathione-sepharose FPLC column (GE Healthcare, Piscataway, NJ). GST-SNAP-containing fractions were identified by SDS-PAGE, pooled, and dialyzed into PBS containing 50 mM DTT. Protein concentration was determined using a standard Bradford assay (Bradford, 1976).

Analysis of SNAP reaction kinetics – The kinetics of GST-SNAP reacting with SNAP-Surface 488 or SNAP-Surface 549 (5 µM final concentration) were determined in vitro at 37℃. Samples were removed from the reaction tube at various times and added directly to 0.5 vol of 3X SDS sample buffer to stop the reaction. Labeled proteins were separated by electrophoresis on an SDS-10% polyacrylamide gel and detected sequentially in two wavelength-filtered channels (526 nm short-pass emission filter with 488 nm excitation and 580 nm band-pass-30 emission filter with 532 nm excitation) using a Typhoon fluorescence scanner. Fluorescence intensities of the bands were quantified using ImageJ software. One-phase exponential association curves were fit using Graphpad Prism. To determine the stability of the thioether bond between the SNAP protein and fluorophores, GST-SNAP labeled with SNAP-Surface 488 or SNAP-Surface 549 was added to MDCK growth media and incubated at 37℃ under 5% CO_2 in a humidified incubator. Samples were taken and diluted into 3X SDS sample buffer at various times up to 24 hrs. Labeled proteins were separated by electrophoresis on an SDS-10% polyacrylamide gel and fluorescence intensity was quantified as described above. One-phase exponential decay curves were fit using Graphpad Prism. Prior to this

experiment, the GST-SNAP proteins were dialyzed into PBS to remove excess fluorophore reagents, eliminating the possibility of SNAP tags re-labeling with excess reagent during the experiment.

Initial delivery and post-delivery movement of SNAP-HA-P2Y Receptors – We utilized the capacity of the SNAP-tag to undergo a single covalent reaction with cell-impermeable fluorescent benzylguanine substrates to determine the initial delivery locations of SNAP-HA-P2Y receptors. Polarized monolayers were first incubated with a non-fluorescent blocking reagent to prevent subsequent fluorescent labeling of receptors already at the cell surface. After washing out excess blocking reagent, different SNAP fluorescent dyes (5 μM) in growth media were added to the apical and basolateral compartments. Cells were incubated for up to 12 hr; at each timepoint, samples of the apical and basolateral media were taken and fluorescence was measured to ensure that the two dyes were not leaking across the monolayer. Excess fluorophore was washed out at 19℃, then the cells were fixed and prepared for confocal microscopy as described above. Fluorescence intensity of the two different fluorophores and their movement between the apical and basolateral membranes over time were used to assess receptor delivery itineraries. To balance intensity between the two color channels during each experiment, two wells of SNAP-HA-P2Y receptor expressing cells were labeled at steady state. One well was labeled with SNAP-Surface Alexafluor-488 (shown in green) in the apical compartment and SNAP-Surface 549 (shown in red) in the basolateral compartment, whereas the additions in other well were reversed (SNAP-Surface 549 apical, SNAP-Surface Alexafluor-488 basolateral). The ratio of intensities at the dominant membrane (basolateral for $P2Y_1$, apical for $P2Y_2$ and $P2Y_4$) was used to correct for signal output throughout the experiment.

Immunoprecipitation of SNAP-HA-P2Y Receptors – Polarized monolayers of MDCK expressing one of the three SNAP-HA-P2Y receptors were grown in 24 mm Transwell inserts and labeled for 30 min at 19^{o}C with fluorescent substrate. The cells were washed three times with growth media, also at 19^{o}C, and then lysed in ice cold RIPA buffer (50 mM Tris HCl pH 8.0, 100 mM NaCl, 5 mM EDTA, 1% Triton X-100, 0.5% deoxycholate, and 0.1% SDS) containing a protease-inhibitor cocktail (Sigma-Aldrich, St. Louis, MO). Membranes were disaggregated by 7 passages through a 25-gauge needle followed by several bursts of sonication, and receptors were extracted overnight at 4℃ with constant oscillation. Insoluble material was removed by centrifugation at 13,000 $\times$ *g* for 30 min. The supernatant was incubated with HA.11 antibody at a 1:150 dilution for 1.5 hours at 4℃ with constant oscillation, followed by the addition of 35 µL of a 50% slurry of protein A/G beads (pre-incubated with 0.1% BSA), and the mixture was incubated an additional 1.5 hours at 4℃ with constant oscillation. The beads were washed extensively in RIPA buffer, and bound proteins were released from the beads by addition of 15 µL of 2X SDS loading buffer containing 100 mM DTT. The entire sample was then submitted to electrophoresis on an SDS-10% polyacrylamide gel and fluorescent bands were detected using a Typhoon fluorescence scanner as described above. Fluorescence intensities of the bands were quantified using ImageJ software.

These experiments were originally performed with SNAP-Surface Alexafluor-488 as the green fluorophore, but these experiments were disregarded due to unacceptable levels of intracellular accumulation when the substrate was added to the basolateral compartment for 12 hours. This artifact was confirmed by confocal microscopy and was not detected with either SNAP-Surface 549 or SNAP-Surface 488.

Quantification of labeled receptors - Molar quantities of protein were estimated using fluorescently labeled GST-SNAP proteins to create a standard curve. GST-SNAP

protein was labeled in vitro with SNAP-Surface 488 or SNAP-Surface 549 fluorescent substrate (forming GST-SNAP-ATTO-488 and GST-SNAP-DY-549, respectively), amounts from 11 fmol to 1.4 pmol were separated on SDS-10% polyacrylamide gels, and the resulting fluorescent bands were visualized using a Typhoon scanner as described above. We observed that the fluorescence intensity plateaued at higher protein concentrations and thus used least-squares nonlinear regression to fit rectangular hyperbolic curves to our standards. The GST-SNAP-DY-549 standard produced no detectable background in the green channel, while there was significant cross-channel background in the red channel produced by the GST-SNAP-ATTO-488 standard.

In order to use the standard curves to estimate the moles of receptors, we assumed that the protein attached to the SNAP-tag does not affect either the ability to bind substrate or the fluorescence quantum yield. If so, the moles of receptor labeled with each fluorophore (g and r in the equations below) can be calculated for each immunoprecipitated sample by taking measurements in each fluorescence channel and then solving a system of two equations after the background signal is manually subtracted:

$$F_g = S_g(g) + X_g(r)$$

$$F_r = S_r(r) + X_r(g)$$

F_g and F_r are the fluorescence intensities measured in the two channels for a sample, S_g and S_r are the functions of the two standard curves (GST-SNAP-ATTO-488 and GST-SNAP-DY-549, respectively, in our experiments), and X_g and X_r are the cross-channel background functions calculated for each fluorophore. Note that these four functions are of only two unknowns, g and r, the moles of each fluorophore in a sample. We used

Mathematica 9 (Wolfram, Champaign, IL) to evaluate this system of equations. This provides a solution that can be used for molar quantification of samples labeled with any fluorophore and filter set combination, provided that there is some resolution between the S and X functions. However, because $X_g = 0$ for the fluorophores in our experiments, the solution is simplified as follows (also calculated using Mathematica 9).

$$\text{If } S_g = \frac{B_1 * g}{k_1 + g} \; ; X_g = 0 \; ; \; S_r = \frac{B_2 * r}{k_2 + r} \text{ and } X_r = \frac{B_3 * g}{k_3 + g}$$

$$\text{Then } F_g = \frac{B_1 * g}{k_1 + g} \text{ and } F_r = \frac{B_2 * r}{k_2 + r} + \frac{B_3 * g}{k_3 + g}$$

$$\text{Solving for g and r yields } g = \frac{F_g * k_1}{B_1 - F_g} \text{ and}$$

$$r = -\frac{k_2(B_3 F_g k_1 - F_g F_r k_1 - B_1 F_r k_3 + F_g F_r k_3)}{B_2 F_g k_1 + B_3 F_g k_1 - F_g F_r k_1 + B_1 B_2 k_3 - B_2 F_g k_3 - B_1 F_r k_3 + F_g F_r k_3}$$

We used this solution, with specific B and k values from our standard curves, to calculate the moles of each fluorophore (which correlates 1:1 with moles of receptor if we assume 100% binding) in each immunoprecipitated sample.

Results

Overall strategy. In order to determine the trafficking itineraries of $P2Y_1$, $P2Y_2$, and $P2Y_4$ receptors, we developed an approach that met the following criteria: i) capacity to distinguish receptors already at the cell surface (and likely at steady-state) from newly synthesized receptors; ii) capacity to label receptors with different probes at the two membrane domains of polarized cells; and iii) capacity to label receptors in a stable manner at a single site with fast kinetics. We settled on fusing a SNAP tag domain, which reacts covalently with O^6-benzylguanine derivatives in a 1:1 stoichiometry (Keppler et al., 2003), to the N-termini of the three P2Y receptors. The experimental design was straightforward: initially block existing cell surface receptors in a polarized monolayer with a non-fluorescent derivative, add different cell-impermeable fluorescent substrates at the two surfaces, and allow the cells to reach steady state. Importantly, newly synthesized receptors will be labeled with the fluorescent substrate present at the membrane surface to which they are initially delivered irrespective of where the receptors reside at steady state.

Analysis of SNAP-HA-tagged P2Y receptors. Each SNAP-receptor construct comprised a cleavable signal sequence, the SNAP-tag domain, a four amino acid linker, and an HA-epitope tag fused in-frame to the second amino acid of the native receptor (Fig. 3.1A). These constructs were cloned into the retroviral plasmid pLXSN and stably expressed in MDCK and 1321N1 human astrocytoma cells. Although we have not quantified the level of expression of these receptors, previous work from our laboratory showed that HA-$P2Y_1$ receptors were expressed at ~180 fmol/mg protein, and based on RIA analysis, the SNAP-HA fusion proteins were expressed at similar levels. We first examined the steady-state distribution of the SNAP-HA receptors in polarized monolayers by labeling both sides of the monolayer with SNAP-Surface Alexafluor 488,

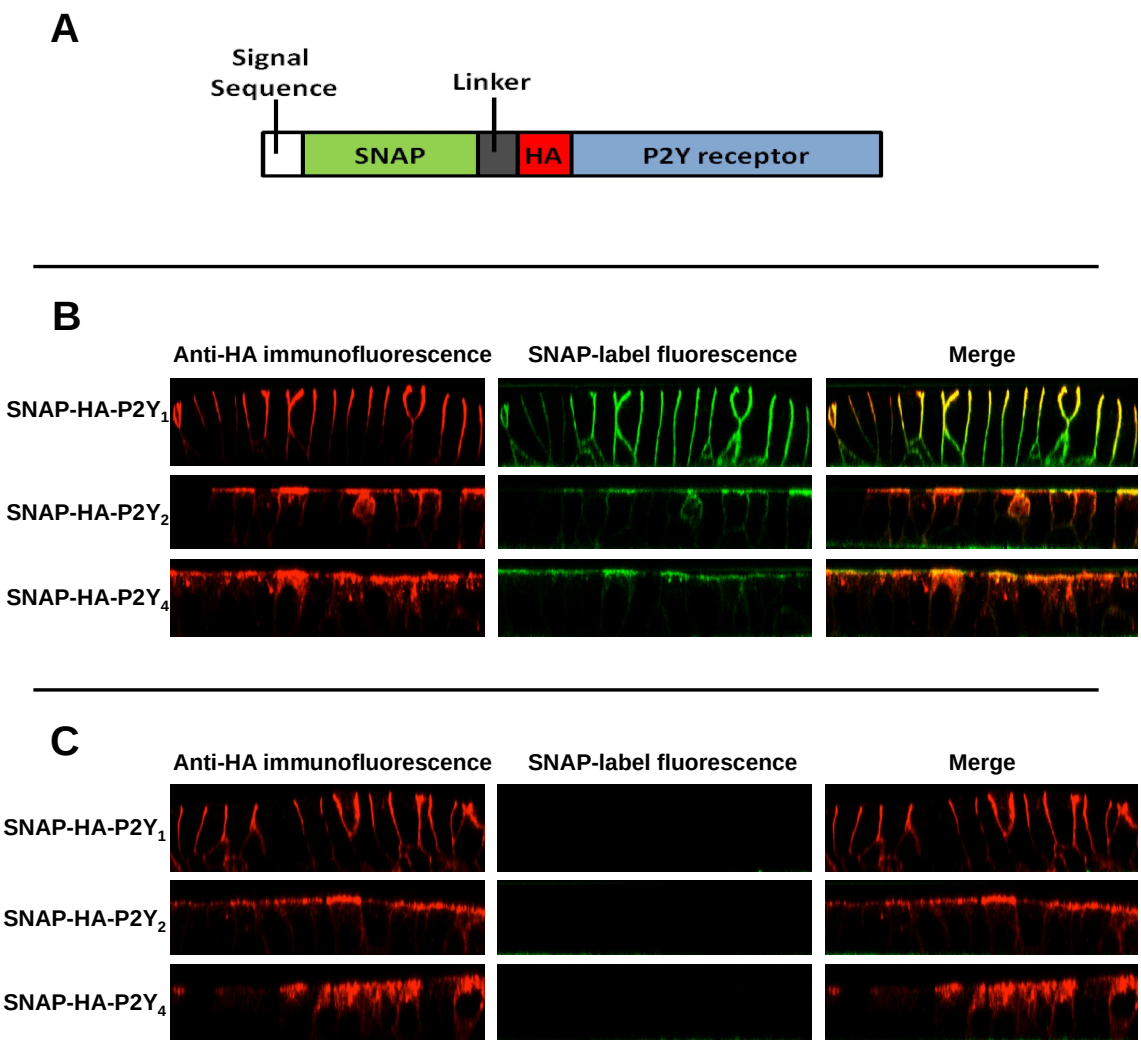

Figure 3.1. Design and Labeling of SNAP-HA-P2Y Receptors. A) Each receptor construct consisted of a cleavable signal sequence, the SNAP tag, a short linker segment, an HA epitope, and a P2Y receptor. B) Z-stack images of polarized MDCK cells expressing SNAP-HA-P2Y$_1$, SNAP-HA-P2Y$_2$, or SNAP-HA-P2Y$_4$ labeled with SNAP-Surface Alexafluor 488 and immunostained at the HA epitope. C) Z-stack images of polarized MDCK cells expressing SNAP-HA-P2Y$_1$, SNAP-HA-P2Y$_2$, or SNAP-HA-P2Y$_4$ pre-treated with SNAP-Surface Block, then labeled with SNAP-Surface Alexafluor 488 and immunostained at the HA epitope. Representative images are shown in all cases.

fixing the cells, incubating with primary HA and fluorescently labeled secondary antibodies, and then examining the monolayers by confocal microscopy. SNAP-HA-$P2Y_1$ and SNAP-HA-$P2Y_4$ receptors were localized nearly 100% to the basolateral and apical surfaces, respectively, consistent with previous results for the same receptors bearing only an N-terminal HA-tag (Wolff et al., 2005). SNAP-HA-$P2Y_2$ also was localized to the apical membrane, but perhaps less completely than previously observed for HA-$P2Y_2$ (Fig. 3.1B). Pretreatment with a non-fluorescent SNAP-tag substrate (C8 propanoic acid benzylguanine) completely abolished the SNAP-fluorophore signal, but did not block the binding of anti-HA antibody (Fig. 3.1C).

To ensure that the SNAP tag did not interfere with receptor function, we compared the activities of SNAP-HA-P2Y receptors to those of HA-P2Y receptors measuring downstream signaling responses and agonist-dependent receptor internalization. Agonist-promoted Ca^{2+} mobilization responses of each receptor were quantified in 1321N1 cells since unlike MDCK cells, these cells do not express endogenous P2Y receptors that would confound interpretation (Filtz et al., 1994). As shown in Figure 3.2A, the responses of the two variants of each P2Y receptor were nearly identical. We also examined agonist-promoted internalization of the receptors using a cell-intact radioimmunoassay with the anti-HA antibody (Brinson and Harden, 2001). MDCK cells expressing either SNAP-HA-P2Y or HA-P2Y receptors were treated with cognate agonists (100 μM ADP for $P2Y_1$ and 100 μM UTP for $P2Y_2$ and $P2Y_4$) for times up to 60 min, and the kinetics and extent of agonist-promoted internalization were similar for the two variants of the three different receptors (Fig. 3.2B). Thus, the presence of SNAP-HA at the N-termini of the P2Y receptors does not alter their signaling properties, capacity to undergo agonist-promoted internalization, or steady-state localization in polarized

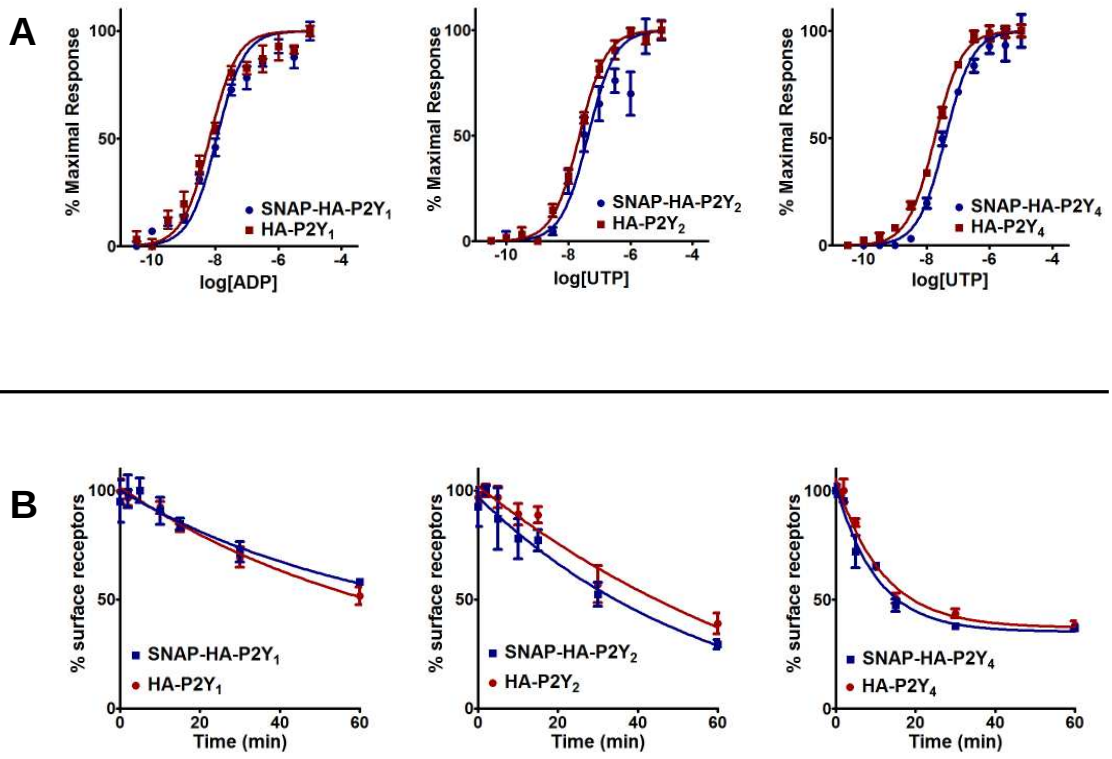

Figure 3.2. Activity of SNAP-HA-P2Y Receptors. A) Calcium signaling in response to cognate agonists in 1321N1 cells expressing SNAP-HA-P2Y or HA-P2Y receptors. The graphs show mean ± SEM of representative experiments. Measurements were performed in quadruplicate, and the experiment was repeated three times. B) Internalization of SNAP-HA-P2Y or HA-P2Y receptors in response to 100 µM agonists in MDCK cells. These measurements were performed in triplicate and the experiment was repeated three times. A representative data set is shown. Curves were fit and 'half-life' calculated using least squares nonlinear regression one-phase decay.

monolayers. These results strongly suggest that the presence of a SNAP-HA domain does not alter the trafficking itineraries of the three P2Y receptors in MDCK cells.

We purified a GST-SNAP fusion protein to assess the kinetics of labeling and to confirm the stability of the fluorescent label attached to the SNAP tag. Incubation of the fusion protein with 5 μM SNAP-Surface 488 or SNAP-Surface 549 (the same concentration used in the experiments described below) at 37^{o}C resulted in essentially complete labeling of the protein within the first minute of exposure (Fig. 3.3A). The stability of the covalent labeling of the protein was determined by incubating the GST-SNAP protein with 5 μM SNAP reagent for 30 min, dialyzing the protein to remove excess reagent, and then incubating the protein with cell medium at 37^{o}C for various times before assessing the amount of bound label by SDS-PAGE (Fig. 3.3B). These data show that the fluorescent tag remains covalently attached to the SNAP enzyme for at least 24 hours at 37^{o}C.

Trafficking itineraries of P2Y receptors. Polarized monolayers of MDCK cells expressing SNAP-HA-P2Y$_1$, -P2Y$_2$, or -P2Y$_4$ receptors were first incubated at 19^{o}C on both sides of the monolayers with a non-fluorescent substrate (SNAP-Surface Block, C8 propanoic acid benzylguanine) to block all cell surface receptors. The surface block-containing medium was removed and the monolayers were washed with fresh medium. SNAP-Surface Alexafluor-488 (shown in green) then was added to the apical surface, and SNAP-Surface 549 (based on Dyomics DY-549; shown in red) was added to the basolateral surfaces. The cells were returned to 37^{o}C and incubated for up to 12 hours. Receptors newly synthesized during the 12 hour incubation are labeled with fluorescent substrate present at the membrane surface where the receptors first appear (Figs. 3.4A, 3.5A, & 3.6A). Importantly, the SNAP-reagents do not diffuse between the apical and basolateral

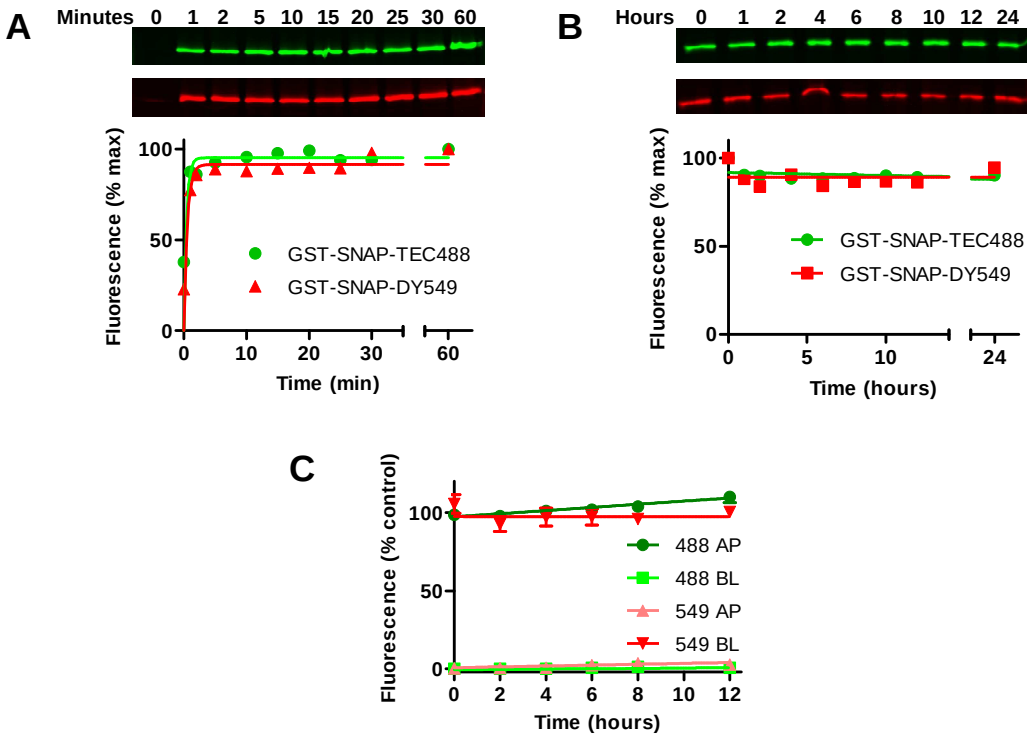

Figure 3.3. SNAP-tag Kinetics, Stability, and Membrane Leak. A) Binding kinetics for purified GST-SNAP and 5 µM SNAP-Surface 488 or SNAP-Surface 549 at 37℃. At each time point, samples were diluted into 3X SDS sample buffer to stop the reaction. B) Stability of GST-SNAP-488 or GST-SNAP-549 in MDCK growth media at 37℃. In both A and B, labeled proteins were separated by electrophoresis on an SDS-10% polyacrylamide gel and detected using a Typhoon fluorescence scanner. Fluorescence intensities of the bands were quantified using ImageJ software and one-phase exponential curves were fit using Graphpad Prism. C) Leak of SNAP-Surface Alexafluor 488 or SNAP-Surface 549 across polarized MDCK monolayers. Apical and Basolateral media samples were taken during each of the time points of the experiments in Figures 3.4 through 3.6. Fluorescence in two wavelength-filtered channels was measured using a Polarstar 96-well platereader.

compartments (<3% leak after 12 hours, Fig. 3.3C), and therefore, covalent labeling is membrane surface-specific.

DY-549 fluorescence accumulated at the basolateral membrane of SNAP-HA-$P2Y_1$ cells within 2 hours of labeling, and the amount of labeling increased to steady-state levels in 8 to 12 hours (Fig. 3.4A,B). These data suggest that new SNAP-HA-$P2Y_1$ receptors are primarily sorted intracellularly and traffic directly to the basolateral membrane. Very little Alexafluor-488 fluorophore accumulated during this time, although low levels of fluorescence were observed at later times of incubation. This fluorescence also was primarily at the basolateral membrane, suggesting that a secondary mechanism rescues mis-targeted receptors. An identical distribution of receptors at steady state was observed when SNAP-Surface Alexafluor-488 was added to the basolateral surface and SNAP-Surface 549 to the apical surface or vice versa, indicating that labeling was not influenced by the properties of the two substrates (Fig. 3.4B). These images were used to calibrate the quantification for differences in the two color channels as described in Materials and Methods. Quantification is shown as total apical vs basolateral signal with red and green colored bars to indicate contributions from each channel (Fig. 3.4C).

In contrast to the SNAP-HA-$P2Y_1$ receptor, the SNAP-HA-$P2Y_2$ and SNAP-HA-$P2Y_4$ receptors were labeled equally with both SNAP-Surface Alexafluor-488 (apical) and SNAP-Surface 549 (basolateral) within as little as 2 hours (Figs. 3.5 & 3.6). For the SNAP-HA-$P2Y_2$ receptor, the levels of Alexafluor-488 fluorescence (representing receptors delivered to the apical membrane) never seemed to reach steady state, and nearly all of these receptors remained at the apical membrane. Receptors labeled at the basolateral membrane with SNAP-Surface 549 increased steadily over 12 hours, and by

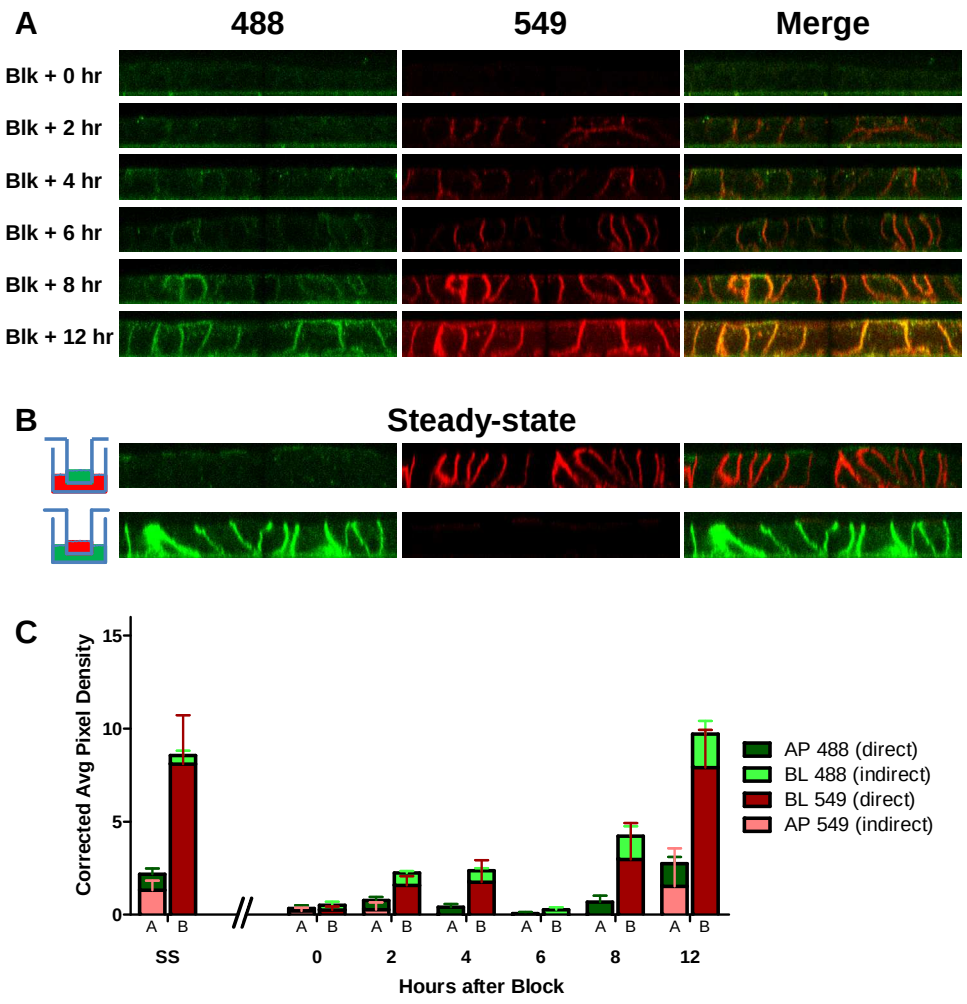

Figure 3.4. Cell Surface Delivery of SNAP-HA-P2Y$_1$. A) Following SNAP-Surface Block pre-treatment, SNAP-Surface Alexafluor 488 was applied apically and SNAP-Surface 549 was applied basolaterally for various times to MDCK cells expressing SNAP-HA-P2Y$_1$. B) SNAP-HA-P2Y$_1$ MDCK cells at steady-state were labeled with the two fluorophores in both the same and reverse orientations. These images were used to correct for differences in the two color channels and provide a reference point for quantification. Representative Z-stack confocal micrographs are shown in all cases. C) Fluorophore accumulation was quantified using ImageJ software. Mean corrected average pixel density results from 6 images per time point are shown.

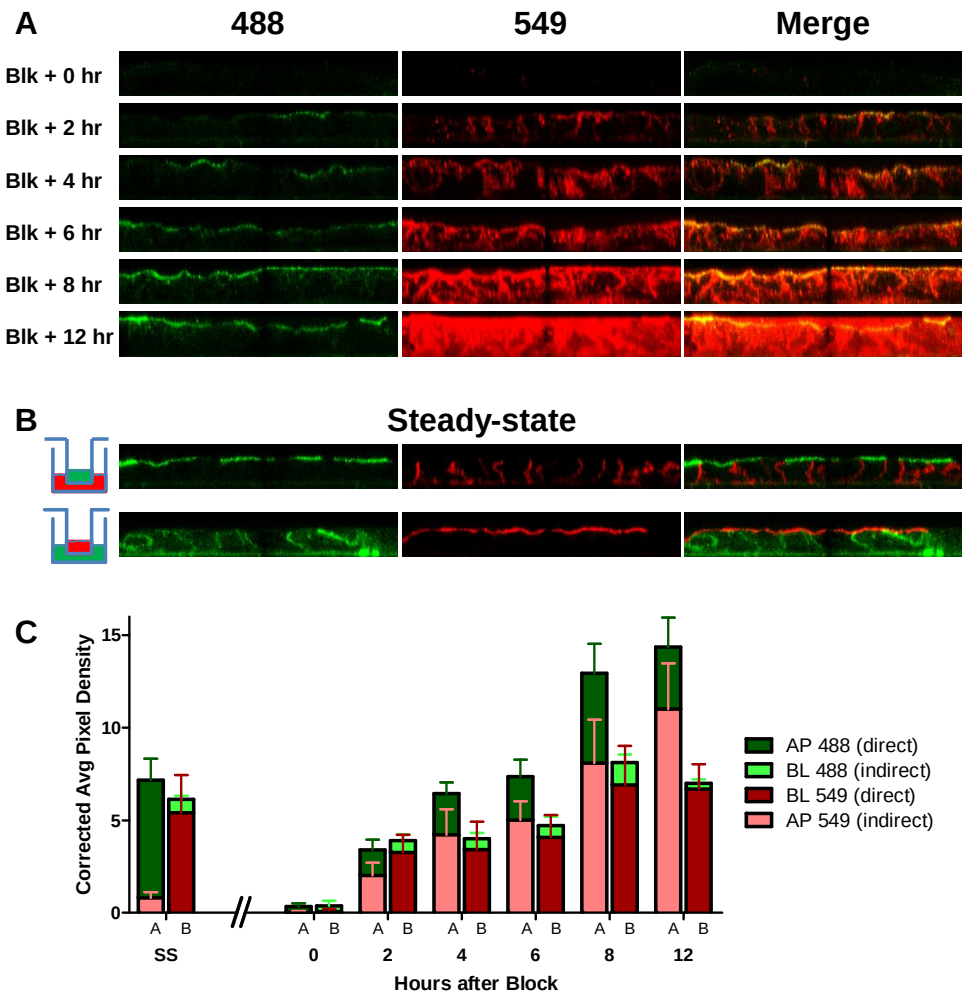

Figure 3.5. Cell Surface Delivery of SNAP-HA-P2Y$_2$. A) Accumulation of apical and basolateral fluorophores over time. B) SNAP-HA-P2Y$_2$ MDCK cells at steady-state. C) Quantification of fluorescence accumulation. See Figure 3.4 legend for more detail.

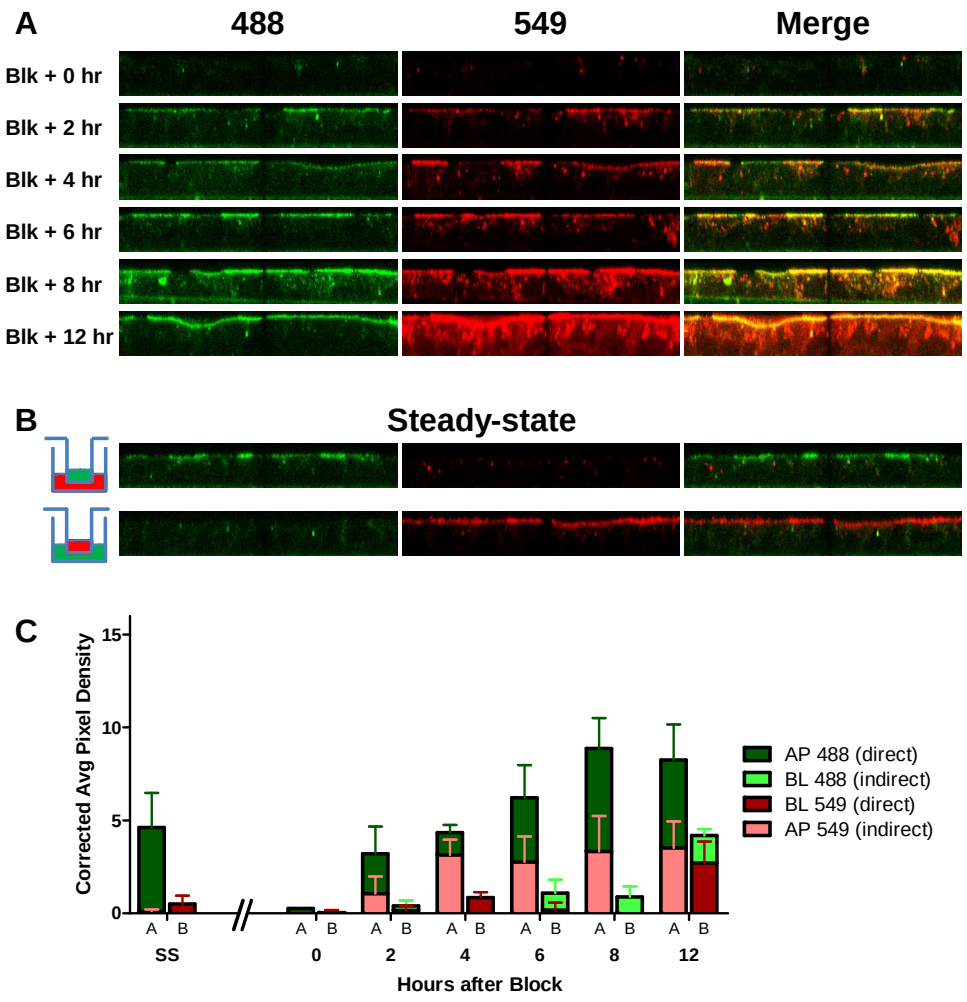

Figure 3.6. Cell Surface Delivery of SNAP-HA-P2Y$_4$. A) Accumulation of apical and basolateral fluorophores over time. B) SNAP-HA-P2Y$_4$ MDCK cells at steady-state. C) Quantification of fluorescence accumulation. See Figure 3.4 legend for more detail.

12 hours more of the signal was present at the apical membrane than the basolateral membrane. This result strongly suggests that the $P2Y_2$ receptor is delivered to the cell surface in an unsorted manner and achieves its apical localization primarily through basolateral to apical transcytosis. SNAP-HA-$P2Y_4$ receptors were nearly equally labeled with DY-549 (basolateral) and Alexafluor-488 (apical) within 2 hours and the fluorescence intensity increased to a maximum over 8 hours (Fig. 3.6), which also is consistent with delivery of the $P2Y_4$ receptor to both membrane regions followed by basolateral to apical transcytosis that results in steady-state apical distribution. Almost all of the fluorescence (in both channels) was at the apical membrane, even at the earliest time point, indicating that the process of transcytosis for the $P2Y_4$ receptor is much more rapid than observed with the $P2Y_2$ receptor.

Biochemical analysis of receptor delivery in MDCK monolayers. To extend the utility of the SNAP-tag method for analyzing the trafficking itineraries of polarized proteins, we also applied this technology for biochemical quantification using whole MDCK monolayers. Polarized monolayers (on 24 mm transwell inserts) of MDCK cells expressing SNAP-HA-P2Y constructs were treated similarly to the method described above, and then were washed, lysed and the receptors immunoprecipitated with anti-HA antibody as described in Materials and Methods. The immunoprecipitates were treated with SDS-PAGE sample buffer, separated by electrophoresis, and submitted to fluorescent scanning on a Typhoon imaging system. This technique has two distinct advantages over microscopy: 1) it eliminates any potential investigator bias, as the sample is an entire population of cells rather than hand-selected cell patches for imaging, and 2) it provides molar quantification of the receptors.

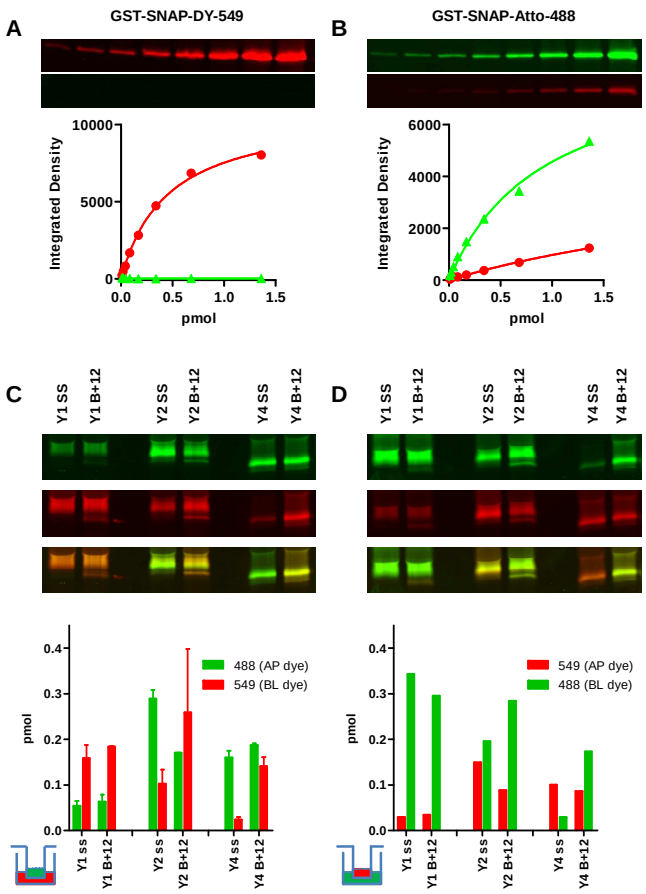

Figure 3.7. Biochemical Quantification of SNAP-HA-P2Y Receptors. A) Standard curve of GST-SNAP protein labeled with SNAP-Surface 549. B) Standard curve of GST-SNAP protein labeled with SNAP-Surface 488. C) HA immunoprecipitation of SNAP-HA-P2Y receptors from MDCK monolayers labeled with SNAP-Surface 488 in the apical media and SNAP-Surface 549 in the basolateral media, either at steady state or after surface receptor block followed by 12 hours of fluorophore accumulation. Image analysis and quantification were performed as described in Materials and Methods. Mean ± SEM of two independent experiments are shown. D) HA immunoprecipitation of SNAP-HA-P2Y receptors from MDCK monolayers labeled with SNAP-Surface 549 in the apical media and SNAP-Surface 488 in the basolateral media. Quantification from a single experiment is shown.

To quantify receptor levels, we labeled the GST-SNAP protein *in vitro* with the same fluorescent substrates used in the immunoprecipitation experiments. The reaction mixtures were then separated by SDS-PAGE and scanned on the Typhoon imager (at the same settings as the immunoprecipitates) to produce standard curves for each fluorophore (Fig. 3.7 A,B).

MDCK monolayers expressing the SNAP-HA-P2Y receptors were pretreated with SNAP-Surface Block and then were labeled for 12 hours at the apical and basolateral surfaces with SNAP-Surface 488 (based on ATTO-488) and SNAP-Surface 549, respectively. This approach allowed quantification of the mass of the three SNAP-HA-P2Y receptors from the polarized surfaces of monolayers at steady state as well as quantification of the accumulation of new, fluorophore-labeled receptors at each surface over the 12-hour incubation period (Fig. 3.7C). Results from this experiment correlate well with the results from confocal microscopy. SNAP-HA-$P2Y_1$ receptors were labeled to a much higher level with the basolateral (SNAP-Surface 549, red) fluorophore than with the apical (SNAP-Surface 488) fluorophore, both at steady state (0.16 ± 0.03 fmol DY-549 vs 0.05 ± 0.01 fmol ATTO-488) and after block + 12 hour accumulation (0.18 ± 0.002 fmol DY-549 vs 0.06 ± 0.02 fmol ATTO-488). In contrast, whereas SNAP-HA-$P2Y_2$ and SNAP-HA-$P2Y_4$ receptors were more strongly labeled with the apical fluorophore (SNAP-Surface 488) at steady-state (0.29 ± 0.02 fmol ATTO-488 vs. 0.10 ± 0.03 fmol DY-549 for SNAP-HA-$P2Y_2$ and 0.16 ± 0.02 fmol ATTO-488 vs. 0.02 ± 0.006 fmol DY-549 for SNAP-HA-$P2Y_4$), both receptors showed nearly equivalent labeling with the two different fluorophores in the block + 12 hour accumulation samples (0.17 ± 0.001 fmol ATTO-488 vs. 0.26 ± 0.14 fmol DY-549 for SNAP-HA-$P2Y_2$ and 0.19 ± 0.004 fmol ATTO-488 vs. 0.14 ± 0.02 fmol DY-549 for SNAP-HA-$P2Y_4$). These results again are consistent with direct delivery to the basolateral membrane of the $P2Y_1$ receptor, and random

delivery of the $P2Y_2$ and $P2Y_4$ receptor followed by basolateral to apical transcytosis. To ensure that the labeling was not due to an artifact of the individual fluorescent substrates, we repeated the experiment with the apical and basolateral fluorophores reversed (Fig. 3.7D), and the results were very similar.

Discussion

Historically, the experimental approaches used to address sorting mechanisms have suffered from significant limitations. The earliest experiments to distinguish between direct delivery and transcytosis relied on metabolic labeling of newly synthesized proteins with [^{35}S]methionine combined with biotin labeling at either the apical or basolateral surface. For example, Wozniak and Limbird showed that α2A and α2C adrenergic receptors are targeted directly to the basolateral membrane, while α2B receptors are delivered to the cell membrane unsorted, then enriched at the basolateral membrane (Wozniak and Limbird, 1996). While straightforward, this technique relies on high expression levels (α2 receptors were expressed at 2-25 pmol/mg protein; (Wozniak and Limbird, 1996)), at which saturation of some sorting mechanisms may occur (Marmorstein et al., 2000;Matter et al., 1992), and slow enough rates of transcytosis to allow detectable levels of protein at the non-enriched surface. Also, this technique lacks any direct demonstration that proteins are being moved from one membrane surface to the other rather than being mis-targeted, internalized and degraded.

Using a different approach, Polishchuk et al. (Polishchuk et al., 2004) showed by confocal microscopy that a GPI-anchored YFP construct was dependent on a transcytotic pathway by inhibiting apical delivery with a basolateral application of tannic acid, a cross-linking agent that prevents vesicle fusion. However, these experiments are controversial and have been difficult to reproduce, with a subsequent study coming to the opposite conclusion (Paladino et al., 2006). This approach is also highly invasive, and the effects of tannic acid beyond those on vesicle fusion are unknown.

More recently, Hua et al. (Hua et al., 2006) demonstrated that Ng-Cam-GFP, but not GPI-anchored YFP, was transcytosed from the basolateral to the apical membrane using an assay that involved binding of fluorescently labeled antibody to the protein in

question at the basolateral compartment, and subsequent movement of the fluorescent antibody to the apical membrane (Hua et al., 2006). This approach eliminates many of the issues highlighted above, but requires complex image analysis and suffers from limited temporal resolution due to the time necessary for antibody labeling. Moreover, unpublished experiments from our lab showed that labeling of basolateral receptors (e.g. the $P2Y_1$ receptor) with anti-HA-Ab followed by ^{125}I-labeled secondary antibody in intact monolayers on a transwell insert was markedly reduced compared to apical receptors (e.g. the $P2Y_2$ receptor). These results were not consistent with the distributions revealed by fluorescent anti-HA Ab binding in fixed and permeabilized monolayers (Fig. 1B), suggesting that diffusion of antibodies into the basolateral space between cells is limited. Finally, this approach cannot be done on the biochemical level due to the poor efficiency of transfection in polarized monolayers.

With these limitations in mind, we report here the development of a straightforward method using the commercially available SNAP tag to determine how polarized receptors arrive at their steady-steady location in epithelial cell monolayers. This method was used to investigate the trafficking itineraries of three P2Y receptors. Our results indicate that the $P2Y_1$ receptor is delivered directly to the basolateral membrane, while $P2Y_2$ and $P2Y_4$ receptors are delivered randomly and basolateral receptors are then transcytosed to the apical surface. The SNAP tag method also provides biochemical quantification of delivery. Its salient advantages suggest that it can supplement or supplant other methods that are more problematic or require expensive equipment or software.

Validation of the experimental constructs for these experiments was an important consideration, as the SNAP-tag adds significant bulk to the extracellular N-terminus of the receptors. All three receptor constructs showed normal agonist-promoted signaling and internalization, suggesting that the SNAP-tag does not interfere with these

processes. However, we did observe that the SNAP-HA-P2Y$_2$ construct was somewhat less polarized at steady state than we had previously reported for the HA-P2Y$_2$ receptor (Wolff et al., 2005). It is unlikely that overexpression causes the decreased polarization of the SNAP-HA-P2Y$_2$ receptor, as radioimmunoassays showed similar expression levels to the HA-P2Y$_2$ receptor, which is sorted normally. Instead, the less robust targeting is potentially due to the presence of the targeting signal of the P2Y$_2$ receptor in the 1st extracellular loop of the receptor (Qi et al., 2005). We surmise that the bulk of the SNAP-tag domain causes steric hindrance to the P2Y$_2$ receptor targeting signal, reducing its efficiency to direct transcytosis. Therefore, any discussion of the P2Y$_2$ receptor signal based on these experiments must have the caveat that the results may be influenced by the presence of the tag itself. In contrast, the SNAP-HA-P2Y$_1$ and SNAP-HA-P2Y$_4$ receptors displayed no problems in targeting, and consistent with our thinking, the targeting signals are located on the cytoplasm side of these GPCR and would not be hindered by the N-terminal tag.

A concern specific to the study of P2Y receptor trafficking is agonist-induced internalization caused by the autocrine release of nucleotides. As our experiments quantify the net result of all trafficking of a receptor, excessive agonist-induced internalization caused by manipulations that induce nucleotide release could affect the observed receptor distributions. To minimize this possibility, all experiments were carried out in the presence of apyrase, an enzyme that rapidly converts nucleoside di- and triphosphates into nucleoside monophosphates, which do not activate P2Y receptors. Local concentration spikes of nucleotide within the unstirred layer (Joseph et al., 2003) could still lead to some receptor activation, but extended activation should be prevented. Indeed, a much higher incidence of labeled intracellular vesicles occurred in experiments carried out in absence of apyrase (data not shown).

Despite the utility of this method, some experimental protocols proved intractable. One goal was to label and monitor intracellular receptors and evaluate their intracellular movement in polarized monolayers using cell-permeable versions of the SNAP reagents. Although these reagents successfully labeled receptors in nonpolarized cells, they were highly inefficient when labeling receptors in fully polarized cell monolayers. Specifically, we attempted labeling with SNAP-Cell-TMR Star and SNAP-Cell-Oregon Green. Additionally, the cell-permeable blocking reagent, SNAP-Cell-Block (bromothenylpteridine) did not efficiently wash out of polarized cells, preventing further labeling.

We also attempted to directly determine the rates of transcytosis by performing pulse-chase experiments using the SNAP-Surface reagents, but the signal-to-noise ratio was too low for meaningful quantification. The SNAP-HA-$P2Y_4$ receptor also was particularly problematic since a 30 minute pulse at 37℃ from the basolateral side was sufficient time for receptors to accumulate at the apical membrane, and thus a longer pulse time to increase the signal was not an option. Unfortunately, pulsing at a restrictive temperature provided too little signal for quantification. Nonetheless, we anticipate that these types of experiment are still viable with this technology in a system with higher protein expression levels or slower turnover rates.

The trafficking itineraries of the P2Y receptors were somewhat unexpected. We speculated that because the $P2Y_1$ receptor contains a cryptic apical signal (Wolff et al., 2010), it might take an indirect path to the basolateral membrane, whereas the $P2Y_2$ and $P2Y_4$ receptors, which contain solitary sorting signals, might be directly delivered to the apical membrane. However, the cryptic apical signal in the $P2Y_1$ receptor plays no obvious role, as nearly all of the SNAP-HA-$P2Y_1$ receptors first appeared at the basolateral surface; strongly suggesting that these receptors were sorted intracellularly and delivered directly to the basolateral membrane. We did observe that a small fraction

of $P2Y_1$ receptors were initially delivered to the apical membrane, but these mis-targeted receptors rapidly accumulated at the basolateral membrane, suggesting the existence of an additional scavenging mechanism to redirect wayward receptors to the correct membrane surface. The small portion of receptors initially delivered to the apical membrane may be a normal part of the receptor's cellular trafficking, due to the cryptic apical signal present in the main body of the $P2Y_1$ receptor, or to saturation of the intracellular vesicle sorting machinery. In contrast to the $P2Y_1$ receptor, the SNAP-HA-$P2Y_2$ and SNAP-HA-$P2Y_4$ receptors appeared in roughly equal levels at both membrane regions, but receptors at the basolateral membrane were redirected to the apical membrane, where they reside at steady state. This suggests that these two receptors contain transcytosis signals and are not sorted as part of their vesicular delivery, but rather through selective retention and/or active loading of transcytotic vesicles.

The assays described here should be highly applicable for the discovery of mechanisms of polarized sorting. For example, now that we have evidence for intracellular sorting of the $P2Y_1$ receptor it will be interesting to determine if its sorting signal is dependent on clathrin adapter proteins, as are proteins with NPXY and YXXΦ basolateral sorting motifs (Matter et al., 1992;Ohno et al., 1995) (the sorting signal in the $P2Y_1$ receptor does not contains either of these two motifs). Additionally, the covalent fluorophore attachment technology can be further exploited to explore the details of vesicular trafficking. An altered SNAP-tag (dubbed CLIP) is available that is selective for benzylcytosine derivatives and can be expressed and labeled concurrently with SNAP-tagged proteins (Gautier et al., 2008). This type of system could allow for a very precise examination of the vesicular sorting and delivery system, simply by observation of when and where labeled cargo proteins become separated.

Proper apical vs. basolateral protein sorting is critical for epithelial cell function. For example, reversed polarity trafficking of the Na,K-ATPase and other transmembrane

proteins drive the symptoms of polycystic kidney disease (Wilson, 2011). Still, many of the sorting mechanisms involved are unknown. One reason is that there appears to be a plethora of specialized and individualized mechanisms for protein sorting. For example, our results indicate that the cryptic apical signal of the $P2Y_1$ receptor plays no role in sorting, as the receptor is delivered directly to the basolateral membrane. This is not because the signal is non-functional, since deletion of the C-terminal basolateral signal results in apical sorting of the receptor (Wolff et al., 2010). Additionally, the $P2Y_2$ receptor is sorted to the apical membrane by this same signal sequence (Qi et al., 2005), and our results suggest that the apical signal is active as a transcytosis signal at the basolateral membrane. These results further suggest that the $P2Y_1$ receptor basolateral targeting sequence not only directs its initial, vesicular delivery, but also inhibits the basolateral to apical transcytosis signal, as basolaterally labeled receptors were not observed at the apical surface. This is a feature not previously observed for any sorting signal, and is one more level of complexity that must be considered in order to fully understand the mechanisms that underlie cell polarity.

Chapter 4: Conclusions and Future Directions

Conclusions

The results of our original data presented here are focused on two related aspects of P2Y receptor trafficking in a polarized epithelial cell line. In the first project (Chapter 2), we delimited and characterized the amino acid sequence that is both necessary and sufficient for the apical targeting of the $P2Y_4$ receptor. In the second project (Chapter 3), we developed a novel and straightforward method to determine the sorting mechanism, i.e. direct delivery or random delivery and transcytosis, and used this method to determine the sorting mechanisms of $P2Y_1$, $P2Y_2$, and $P2Y_4$ receptors.

The first set of experiments (Chapter 2) delimited the apical-targeting signal of the $P2Y_4$ receptor to a 23-amino acid sequence, CGGGKPQPRTAASSLALVSLPED, within its cytoplasmic C-terminal tail (DuBose et al., 2013). Furthermore, our results show that only the four hydrophobic residues (three L and one V) are critical to the signal's function, with a lesser contribution of two basic residues (one each K and R). Several interesting features of the targeting signal were discovered during the course of these experiments. First, and most strikingly, the entire sequence can be reversed N->C without any loss of apical localization. This had only been observed previously for the basolateral targeting signal of the $P2Y_1$ receptor (Wolff et al., 2010), and the underlying mechanisms behind such flexible targeting signals are still unclear. Second, the signal functions autonomously, as it was capable of directing a chimeric BK2/Y4 C-tail receptor to the apical membrane and even overcoming the basolateral-targeting signal present in the main body of the $P2Y_{12}$ receptor. The signal was determined to be unique to the

$P2Y_4$ receptor, although with so few critical amino acids, other proteins may well use the same mechanism. Lending further support to their critical nature, the key hydrophobic residues are well conserved among all mammalian species for which sequence data were available.

Our results from the second set of experiments validate and utilize a method to determine the trafficking itinerary of P2Y receptors using fluorescent SNAP-tag probes. In order to use this method, cell lines were generated expressing the P2Y receptors with the SNAP-tag fused to the extracellular N-terminus. Cell surface receptors at steady-state in a fully polarized monolayer were blocked with a non-fluorescent reagent, and newly synthesized receptors were allowed to be transported to the cell surface, where they were exposed to different fluorophores at either the apical and basolateral membrane. Because there is a single, covalent binding site on each SNAP-tag, only the first fluorophore that a receptor is exposed to will react and remain bound regardless of where it moves within the cell. A combination of confocal microscopy and immunoprecipitation with fluorescence detection were used to determine if receptors are delivered directly or via transcytosis and to estimate the molar quantity of receptors at each membrane region.

The results from these experiments indicated that the $P2Y_1$ receptor is delivered directly to the basolateral membrane, while $P2Y_2$ and $P2Y_4$ receptors are delivered unsorted and eventually reach the apical membrane via selective transcytosis. Quantification of immunoprecipitated receptors indicated that between 0.2 and 0.4 pmol of each receptor were expressed per 24 mm transwell, or between 120,000 and 240,000 molecules per cell.

Future Directions

The most obvious extension of this project is the examination of the remaining P2Y receptor targeting signals and trafficking itineraries. Thus far, we have defined the targeting signals for four of the P2Y receptors: $P2Y_1$ (Wolff et al., 2010), $P2Y_2$ (Qi et al., 2005), $P2Y_4$ (DuBose et al., 2013), and $P2Y_6$ (unpublished results). Remaining are four basolateral signals, one in the C-tail of the $P2Y_{11}$ receptor, the two basolateral signals of the $P2Y_{12}$ receptor (one in the C-terminal tail and one in the main body of the receptor), and one in the C-tail of the $P2Y_{14}$ receptor (unpublished results).

Additionally, we should be able to use the method developed in Chapter 3 to determine the trafficking itineraries of the remaining P2Y receptors. The $P2Y_6$ receptor will almost certainly follow the same itinerary as the $P2Y_2$ receptor, as they share a common sorting signal (unpublished results). Because I have shown that the $P2Y_{14}$ receptor basolateral-targeting signal is similar in its properties to that of the $P2Y_1$ receptor targeting signal (unpublished results), it would be very surprising if they did not share a common delivery mechanism. The $P2Y_{11}$ and $P2Y_{12}$ receptor trafficking itineraries remain complete unknowns, though it will be particularly interesting to learn if one of the two $P2Y_{12}$ receptor basolateral-targeting signals is responsible for direct targeting and the other for transcytosis, or if they are completely redundant signals.

Future experiments should also incorporate the alternate SNAP-tag (dubbed CLIP-tag) that is selective for benzylcytosine derivatives and allows for coexpression and concurrent labeling alongside a SNAP-tagged protein (Gautier et al., 2008). A very simple experiment would be to determine if the $P2Y_2$ and $P2Y_4$ receptors follow the same vesicular path during their basolateral to apical transcytosis. So long as differently colored fluorophores are used for the benzylguanine and benzylcytosine reagents, the two proteins could be tracked through the same cell, potentially in real-time if sufficient

signal-to-noise ratios could be maintained. If we could solve the permeability issues described in Chapter 3, this technique could also be used to evaluate the initial biogenesis of the receptors.

Beyond the limits of our P2Y model, we could apply these techniques to the many transmembrane proteins involved in epithelial pathologies. For example, it could help determine the mechanism of basolateral targeting of the V2R receptor, another GPCR, in kidney epithelia, as well as the mutant forms (which fail to accumulate properly at the basolateral membrane), responsible for X-linked diabetes insipidus (Oksche et al., 1996).

These techniques should also be useful for non-GPCRs, such as the CFTR chloride channel, which can harbor any one of several mutations that cause cystic fibrosis, the most common fatal autosomal recessive disease among Caucasians (Barrett et al., 2012). Wild type CFTR accumulates at the apical membrane of epithelial cells, but its trafficking itinerary is not well defined. Furthermore, CFTR contains both dilucine and tyrosine basolateral targeting signals and C-terminal truncated proteins reside at the basolateral membrane (Kleizen et al., 2000). Although the most common mutation, ΔF508, results in ER retention of CFTR, there are a group of mutations that allow cell-surface delivery, but the protein is unstable at the apical membrane (Haardt et al., 1999). Furthermore, when the ΔF508 mutant is rescued by reduced temperature processing, it too is destabilized at the apical membrane (Sharma et al., 2004). Thus, improved tools to analyze trafficking of CFTR selectively at the apical membrane may help to elucidate the underlying deficiencies.

Perhaps the most relevant disease state to our apical versus basolateral targeting studies is polycystic kidney disease (PKD). PKD is a group of genetic diseases characterized by the formation of large, fluid-filled cysts instead of normal kidney tubules (Wilson, 2011). These malformations appear to be driven by the reversed-polarity sorting

of a number of proteins, including EGF receptors, Na^+/K^+ATPase, E-cadherin, integrins, and the NKCC1 cotransporter. However, a number of other polarized proteins are sorted normally, including the H^+-ATPase, CFTR, and Aquaporin 1 and 2 water channels. The mechanisms underlying this partial breakdown of cell polarity remain largely unknown.

If combined with an effective gene transduction system, our SNAP-tag method could possibly be applied to study protein trafficking within an intact kidney. By cannulating the renal artery, we could circulate the basolateral dye through the entire kidney and use the leaky endothelium to our advantage to deliver the dye to the basolateral side of the tubule epithelia. Meanwhile, the tubules themselves could be filled with the apical dye. Maximum labeling times would likely be much shorter than in cell culture, as the kidney's normal function would quickly mix the two dyes. However, the much higher expression levels of these proteins of interest (relative to P2Y receptors) would likely still allow for sufficient fluorescent signal for microscopy of tissue sections and biochemical analysis. In this way, the same construct could be expressed and observed under normal kidney function or during polycystic pathogenesis, either from transgenic models (Nagao et al., 2012) or in human kidneys removed from PKD transplant patients.

Thus, in addition to being an interesting and physiologically important set of polarized proteins in their own right, the P2Y receptors have provided an excellent model for the development of techniques for apical versus basolateral protein targeting.

References

Abbracchio, M. P., Boeynaems, J. M., Barnard, E. A., Boyer, J. L., Kennedy, C., Miras-Portugal, M. T., King, B. F., Gachet, C., Jacobson, K. A., Weisman, G. A. et al. (2003). Characterization of the UDP-glucose receptor (re-named here the P2Y14 receptor) adds diversity to the P2Y receptor family. *Trends Pharmacol. Sci.* **24,** 52-55.

Albert, P. R. and Robillard, L. (2002). G protein specificity: Traffic direction required. *Cell. Signal.* **14,** 407-418.

Alkayed, F., Kashimata, M., Koyama, N., Hayashi, T., Tamura, Y. and Azuma, Y. (2012). P2Y11 purinoceptor mediates the ATP-enhanced chemotactic response of rat neutrophils. *J. Pharmacol. Sci.* **120,** 288-295.

Amisten, S., Meidute-Abaraviciene, S., Tan, C., Olde, B., Lundquist, I., Salehi, A. and Erlinge, D. (2010). ADP mediates inhibition of insulin secretion by activation of P2Y13 receptors in mice. *Diabetologia* **53,** 1927-1934.

Anderson, E., Maday, S., Sfakianos, J., Hull, M., Winckler, B., Sheff, D., Folsch, H. and Mellman, I. (2005). Transcytosis of NgCAM in epithelial cells reflects differential signal recognition on the endocytic and secretory pathways. *J. Cell Biol.* **170,** 595-605.

Apodaca, G., Gallo, L. I. and Bryant, D. M. (2012). Role of membrane traffic in the generation of epithelial cell asymmetry. *Nat. Cell Biol.* **14,** 1235-1243.

Ashraf, S. S., Benson, R. E., Payne, E. S., Halbleib, C. M. and Gron, H. (2004). A novel multi-affinity tag system to produce high levels of soluble and biotinylated proteins in escherichia coli. *Protein Expr. Purif.* **33,** 238-245.

Ayata, C. K., Ganal, S. C., Hockenjos, B., Willim, K., Vieira, R. P., Grimm, M., Robaye, B., Boeynaems, J. M., Di Virgilio, F., Pellegatti, P. et al. (2012). Purinergic P2Y(2) receptors promote neutrophil infiltration and hepatocyte death in mice with acute liver injury. *Gastroenterology* **143,** 1620-1629.e4.

Bar, I., Guns, P. J., Metallo, J., Cammarata, D., Wilkin, F., Boeynams, J. M., Bult, H. and Robaye, B. (2008). Knockout mice reveal a role for P2Y6 receptor in macrophages, endothelial cells, and vascular smooth muscle cells. *Mol. Pharmacol.* **74,** 777-784.

Barrett, M. O., Sesma, J. I., Ball, C. B., Jayasekara, P. S., Jacobson, K. A., Lazarowski, E. R. and Harden, T. K. (2013). A selective high-affinity antagonist of the P2Y14 receptor inhibits UDP-glucose-stimulated chemotaxis of human neutrophils. *Mol. Pharmacol.* **84,** 41-49.

Barrett, P. M., Alagely, A. and Topol, E. J. (2012). Cystic fibrosis in an era of genomically guided therapy. *Hum. Mol. Genet.* **21,** R66-71.

Bassil, A. K., Bourdu, S., Townson, K. A., Wheeldon, A., Jarvie, E. M., Zebda, N., Abuin, A., Grau, E., Livi, G. P., Punter, L. et al. (2009). UDP-glucose modulates

gastric function through P2Y14 receptor-dependent and -independent mechanisms. *Am. J. Physiol. Gastrointest. Liver Physiol.* **296,** G923-30.

Beau, I., Groyer-Picard, M. T., Desroches, A., Condamine, E., Leprince, J., Tome, J. P., Dessen, P., Vaudry, H. and Misrahi, M. (2004). The basolateral sorting signals of the thyrotropin and luteinizing hormone receptors: An unusual family of signals sharing an unusual distal intracellular localization, but unrelated in their structures. *Mol. Endocrinol.* **18,** 733-746.

Beau, I., Groyer-Picard, M. T., Le Bivic, A., Vannier, B., Loosfelt, H., Milgrom, E. and Misrahi, M. (1998). The basolateral localization signal of the follicle-stimulating hormone receptor. *J. Biol. Chem.* **273,** 18610-18616.

Benovic, J. L., Kuhn, H., Weyand, I., Codina, J., Caron, M. G. and Lefkowitz, R. J. (1987). Functional desensitization of the isolated beta-adrenergic receptor by the beta-adrenergic receptor kinase: Potential role of an analog of the retinal protein arrestin (48-kDa protein). *Proc Natl Acad Sci U S A* **84,** 8879-82.

Bird, J. E., Wang, X., Smith, P. L., Barbera, F., Huang, C. and Schumacher, W. A. (2012). A platelet target for venous thrombosis? P2Y1 deletion or antagonism protects mice from vena cava thrombosis. *J. Thromb. Thrombolysis* **34,** 199-207.

Bos, K., Wraight, C. and Stanley, K. K. (1993). TGN38 is maintained in the trans-golgi network by a tyrosine-containing motif in the cytoplasmic domain. *EMBO J.* **12,** 2219-2228.

Boucher, I., Kehasse, A., Marcincin, M., Rich, C., Rahimi, N. and Trinkaus-Randall, V. (2011). Distinct activation of epidermal growth factor receptor by UTP contributes to epithelial cell wound repair. *Am. J. Pathol.* **178,** 1092-1105.

Bourdon, D. M., Mahanty, S. K., Jacobson, K. A., Boyer, J. L. and Harden, T. K. (2006). (N)-methanocarba-2MeSADP (MRS2365) is a subtype-specific agonist that induces rapid desensitization of the P2Y1 receptor of human platelets. *J. Thromb. Haemost.* **4,** 861-868.

Boyer, J. L., Adams, M., Ravi, R. G., Jacobson, K. A. and Harden, T. K. (2002). 2-chloro N(6)-methyl-(N)-methanocarba-2'-deoxyadenosine-3',5'-bisphosphate is a selective high affinity P2Y(1) receptor antagonist. *Br. J. Pharmacol.* **135,** 2004-2010.

Bradford, M. M. (1976). A rapid and sensitive method for the quantitation of microgram quantities of protein utilizing the principle of protein-dye binding. *Anal. Biochem.* **72,** 248-254.

Brinson, A. E. and Harden, T. K. (2001). Differential regulation of the uridine nucleotide-activated P2Y4 and P2Y6 receptors. SER-333 and SER-334 in the carboxyl terminus are involved in agonist-dependent phosphorylation desensitization and internalization of the P2Y4 receptor. *J Biol Chem* **276,** 11939-48.

Brown, D., Breton, S., Ausiello, D. A. and Marshansky, V. (2009). Sensing, signaling and sorting events in kidney epithelial cell physiology. *Traffic* **10,** 275-284.

Brown, D. A. and Rose, J. K. (1992). Sorting of GPI-anchored proteins to glycolipid-enriched membrane subdomains during transport to the apical cell surface. *Cell* **68,** 533-544.

Burnstock, G. (2002). Potential therapeutic targets in the rapidly expanding field of purinergic signalling. *Clin. Med.* **2,** 45-53.

Burnstock, G. (2002). Purinergic signaling and vascular cell proliferation and death. *Arterioscler. Thromb. Vasc. Biol.* **22,** 364-373.

Burnstock, G. and Knight, G. E. (2004). Cellular distribution and functions of P2 receptor subtypes in different systems. *Int. Rev. Cytol.* **240,** 31-304.

Burrell, H. E., Bowler, W. B., Gallagher, J. A. and Sharpe, G. R. (2003). Human keratinocytes express multiple P2Y-receptors: Evidence for functional P2Y1, P2Y2, and P2Y4 receptors. *J. Invest. Dermatol.* **120,** 440-447.

Carter, R. L., Fricks, I. P., Barrett, M. O., Burianek, L. E., Zhou, Y., Ko, H., Das, A., Jacobson, K. A., Lazarowski, E. R. and Harden, T. K. (2009). Quantification of gi-mediated inhibition of adenylyl cyclase activity reveals that UDP is a potent agonist of the human P2Y14 receptor. *Mol. Pharmacol.* **76,** 1341-1348.

Casanova, J. E., Apodaca, G. and Mostov, K. E. (1991). An autonomous signal for basolateral sorting in the cytoplasmic domain of the polymeric immunoglobulin receptor. *Cell* **66,** 65-75.

Castillon, G. A., Michon, L. and Watanabe, R. (2013). Apical sorting of lysoGPI-anchored proteins occurs independent of association with detergent-resistant membranes but dependent on their N-glycosylation. *Mol. Biol. Cell* **24,** 2021-2033.

Chambers, J. K., Macdonald, L. E., Sarau, H. M., Ames, R. S., Freeman, K., Foley, J. J., Zhu, Y., McLaughlin, M. M., Murdock, P., McMillan, L. et al. (2000). A G protein-coupled receptor for UDP-glucose. *J. Biol. Chem.* **275,** 10767-10771.

Chang, C. P., Kao, J. P., Lazar, C. S., Walsh, B. J., Wells, A., Wiley, H. S., Gill, G. N. and Rosenfeld, M. G. (1991). Ligand-induced internalization and increased cell calcium are mediated via distinct structural elements in the carboxyl terminus of the epidermal growth factor receptor. *J. Biol. Chem.* **266,** 23467-23470.

Chang, K., Hanaoka, K., Kumada, M. and Takuwa, Y. (1995). Molecular cloning and functional analysis of a novel P2 nucleotide receptor. *J. Biol. Chem.* **270,** 26152-26158.

Chen, W. J., Goldstein, J. L. and Brown, M. S. (1990). NPXY, a sequence often found in cytoplasmic tails, is required for coated pit-mediated internalization of the low density lipoprotein receptor. *J. Biol. Chem.* **265,** 3116-3123.

Cheng, C., Glover, G., Banker, G. and Amara, S. G. (2002). A novel sorting motif in the glutamate transporter excitatory amino acid transporter 3 directs its targeting in madin-darby canine kidney cells and hippocampal neurons. *J Neurosci* **22,** 10643-52.

Chicka, M. C. and Strehler, E. E. (2003). Alternative splicing of the first intracellular loop of plasma membrane Ca2+-ATPase isoform 2 alters its membrane targeting. *J Biol Chem* **278,** 18464-70.

Chmelar, R. S. and Nathanson, N. M. (2006). Identification of a novel apical sorting motif and mechanism of targeting of the M2 muscarinic acetylcholine receptor. *J Biol Chem* **281,** 35381-96.

Chorna, N. E., Santiago-Perez, L. I., Erb, L., Seye, C. I., Neary, J. T., Sun, G. Y., Weisman, G. A. and Gonzalez, F. A. (2004). P2Y receptors activate neuroprotective mechanisms in astrocytic cells. *J. Neurochem.* **91,** 119-132.

Christofi, F. L., Wunderlich, J., Yu, J. G., Wang, Y. Z., Xue, J., Guzman, J., Javed, N. and Cooke, H. (2004). Mechanically evoked reflex electrogenic chloride secretion in rat distal colon is triggered by endogenous nucleotides acting at P2Y1, P2Y2, and P2Y4 receptors. *J. Comp. Neurol.* **469,** 16-36.

Chuang, J. Z. and Sung, C. H. (1998). The cytoplasmic tail of rhodopsin acts as a novel apical sorting signal in polarized MDCK cells. *J Cell Biol* **142,** 1245-56.

Communi, D., Gonzalez, N. S., Detheux, M., Brezillon, S., Lannoy, V., Parmentier, M. and Boeynaems, J. M. (2001). Identification of a novel human ADP receptor coupled to G(i). *J. Biol. Chem.* **276,** 41479-41485.

Communi, D., Govaerts, C., Parmentier, M. and Boeynaems, J. M. (1997). Cloning of a human purinergic P2Y receptor coupled to phospholipase C and adenylyl cyclase. *J Biol Chem* **272,** 31969-73.

Communi, D., Janssens, R., Robaye, B., Zeelis, N. and Boeynaems, J. M. (2000). Rapid up-regulation of P2Y messengers during granulocytic differentiation of HL-60 cells. *FEBS Lett.* **475,** 39-42.

Communi, D., Parmentier, M. and Boeynaems, J. M. (1996). Cloning, functional expression and tissue distribution of the human P2Y6 receptor. *Biochem. Biophys. Res. Commun.* **222,** 303-308.

Communi, D., Pirotton, S., Parmentier, M. and Boeynaems, J. M. (1995). Cloning and functional expression of a human uridine nucleotide receptor. *J. Biol. Chem.* **270,** 30849-30852.

Communi, D., Robaye, B. and Boeynaems, J. M. (1999). Pharmacological characterization of the human P2Y11 receptor. *Br. J. Pharmacol.* **128,** 1199-1206.

Communi, D., Suarez-Huerta, N., Dussossoy, D., Savi, P. and Boeynaems, J. M. (2001). Cotranscription and intergenic splicing of human P2Y11 and SSF1 genes. *J. Biol. Chem.* **276,** 16561-16566.

Comstock, K. E., Watson, N. F. and Olsen, J. C. (1997). Design of retroviral expression vectors. *Methods Mol Biol* **62,** 207-22.

Cooper, D. M. and Rodbell, M. (1979). ADP is a potent inhibitor of human platelet plasma membrane adenylate cyclase. *Nature* **282,** 517-518.

Crane, J. K., Olson, R. A., Jones, H. M. and Duffey, M. E. (2002). Release of ATP during host cell killing by enteropathogenic E. coli and its role as a secretory mediator. *Am J Physiol Gastrointest Liver Physiol* **283,** G74-86.

da Silva, C. G., Specht, A., Wegiel, B., Ferran, C. and Kaczmarek, E. (2009). Mechanism of purinergic activation of endothelial nitric oxide synthase in endothelial cells. *Circulation* **119,** 871-879.

de Boer, E., Rodriguez, P., Bonte, E., Krijgsveld, J., Katsantoni, E., Heck, A., Grosveld, F. and Strouboulis, J. (2003). Efficient biotinylation and single-step purification of tagged transcription factors in mammalian cells and transgenic mice. *Proc. Natl. Acad. Sci. U. S. A.* **100,** 7480-7485.

Delacour, D., Cramm-Behrens, C. I., Drobecq, H., Le Bivic, A., Naim, H. Y. and Jacob, R. (2006). Requirement for galectin-3 in apical protein sorting. *Curr. Biol.* **16,** 408-414.

Djerada, Z., Peyret, H., Dukic, S. and Millart, H. (2013). Extracellular NAADP affords cardioprotection against ischemia and reperfusion injury and involves the P2Y11-like receptor. *Biochem. Biophys. Res. Commun.* **434,** 428-433.

Drews, J. (2000). Drug discovery: A historical perspective. *Science* **287,** 1960-1964.

DuBose, D. R., Wolff, S. C., Qi, A. D., Naruszewicz, I. and Nicholas, R. A. (2013). Apical targeting of the P2Y(4) receptor is directed by hydrophobic and basic residues in the cytoplasmic tail. *Am. J. Physiol. Cell. Physiol.* **304,** C228-39.

Dulong, S., Bernard, K. and Ehrenfeld, J. (2007). Enhancement of P2Y6-induced cl-secretion by IL-13 and modulation of SK4 channels activity in human bronchial cells. *Cell. Physiol. Biochem.* **20,** 483-494.

Dunbar, L. A., Aronson, P. and Caplan, M. J. (2000). A transmembrane segment determines the steady-state localization of an ion-transporting adenosine triphosphatase. *J. Cell Biol.* **148,** 769-778.

El-Tayeb, A., Qi, A., Nicholas, R. A. and Muller, C. E. (2011). Structural modifications of UMP, UDP, and UTP leading to subtype-selective agonists for P2Y2, P2Y4, and P2Y6 receptors. *J. Med. Chem.* **54,** 2878-2890.

Espada, S., Ortega, F., Molina-Jijon, E., Rojo, A. I., Perez-Sen, R., Pedraza-Chaverri, J., Miras-Portugal, M. T. and Cuadrado, A. (2010). The purinergic P2Y(13) receptor activates the Nrf2/HO-1 axis and protects against oxidative stress-induced neuronal death. *Free Radic. Biol. Med.* **49,** 416-426.

Fabre, A. C., Malaval, C., Ben Addi, A., Verdier, C., Pons, V., Serhan, N., Lichtenstein, L., Combes, G., Huby, T., Briand, F. et al. (2010). P2Y13 receptor is critical for reverse cholesterol transport. *Hepatology* **52,** 1477-1483.

Fang, X., Hu, H. Z., Gao, N., Liu, S., Wang, G. D., Wang, X. Y., Xia, Y. and Wood, J. D. (2006). Neurogenic secretion mediated by the purinergic P2Y1 receptor in guinea-pig small intestine. *Eur. J. Pharmacol.* **536,** 113-122.

Fedarovich, A., Tomberg, J., Nicholas, R. A. and Davies, C. (2006). Structure of the N-terminal domain of human CEACAM1: Binding target of the opacity proteins during invasion of neisseria meningitidis and N. gonorrhoeae. *Acta Crystallogr. D Biol. Crystallogr.* **62,** 971-979.

Ferguson, S. S., Downey, W. E.,3rd, Colapietro, A. M., Barak, L. S., Menard, L. and Caron, M. G. (1996). Role of beta-arrestin in mediating agonist-promoted G protein-coupled receptor internalization. *Science* **271,** 363-6.

Field, M., Rao, M. C. and Chang, E. B. (1989). Intestinal electrolyte transport and diarrheal disease (1). *N Engl J Med* **321,** 800-6.

Field, M., Rao, M. C. and Chang, E. B. (1989). Intestinal electrolyte transport and diarrheal disease (2). *N Engl J Med* **321,** 879-83.

Filippov, A. K., Brown, D. A. and Barnard, E. A. (2000). The P2Y(1) receptor closes the N-type ca(2+) channel in neurones, with both adenosine triphosphates and diphosphates as potent agonists. *Br. J. Pharmacol.* **129,** 1063-1066.

Filtz, T. M., Li, Q., Boyer, J. L., Nicholas, R. A. and Harden, T. K. (1994). Expression of a cloned P2Y purinergic receptor that couples to phospholipase C. *Mol. Pharmacol.* **46,** 8-14.

Folsch, H. (2008). Regulation of membrane trafficking in polarized epithelial cells. *Curr Opin Cell Biol* **20,** 208-13.

Folsch, H., Ohno, H., Bonifacino, J. S. and Mellman, I. (1999). A novel clathrin adaptor complex mediates basolateral targeting in polarized epithelial cells. *Cell* **99,** 189-98.

Francesconi, A. and Duvoisin, R. M. (2002). Alternative splicing unmasks dendritic and axonal targeting signals in metabotropic glutamate receptor 1. *J Neurosci* **22,** 2196-205.

Fumagalli, M., Brambilla, R., D'Ambrosi, N., Volonte, C., Matteoli, M., Verderio, C. and Abbracchio, M. P. (2003). Nucleotide-mediated calcium signaling in rat cortical astrocytes: Role of P2X and P2Y receptors. *Glia* **43,** 218-203.

Gachet, C., Savi, P., Ohlmann, P., Maffrand, J. P., Jakobs, K. H. and Cazenave, J. P. (1992). ADP receptor induced activation of guanine nucleotide binding proteins in rat

platelet membranes--an effect selectively blocked by the thienopyridine clopidogrel. *Thromb. Haemost.* **68,** 79-83.

Gao, Z. G., Ding, Y. and Jacobson, K. A. (2010). P2Y(13) receptor is responsible for ADP-mediated degranulation in RBL-2H3 rat mast cells. *Pharmacol. Res.* **62,** 500-505.

Gauthier, J. Y., Belley, M., Deschenes, D., Fournier, J. F., Gagne, S., Gareau, Y., Hamel, M., Henault, M., Hyjazie, H., Kargman, S. et al. (2011). The identification of 4,7-disubstituted naphthoic acid derivatives as UDP-competitive antagonists of P2Y14. *Bioorg. Med. Chem. Lett.* **21,** 2836-2839.

Gautier, A., Juillerat, A., Heinis, C., Correa, I. R.,Jr, Kindermann, M., Beaufils, F. and Johnsson, K. (2008). An engineered protein tag for multiprotein labeling in living cells. *Chem. Biol.* **15,** 128-136.

Geffen, I., Fuhrer, C., Leitinger, B., Weiss, M., Huggel, K., Griffiths, G. and Spiess, M. (1993). Related signals for endocytosis and basolateral sorting of the asialoglycoprotein receptor. *J. Biol. Chem.* **268,** 20772-20777.

Ghanem, E., Robaye, B., Leal, T., Leipziger, J., Van Driessche, W., Beauwens, R. and Boeynaems, J. M. (2005). The role of epithelial P2Y2 and P2Y4 receptors in the regulation of intestinal chloride secretion. *Br J Pharmacol* **146,** 364-9.

Ghanem, E., Robaye, B., Leal, T., Leipziger, J., Van Driessche, W., Beauwens, R. and Boeynaems, J. M. (2005). The role of epithelial P2Y2 and P2Y4 receptors in the regulation of intestinal chloride secretion. *Br. J. Pharmacol.* **146,** 364-369.

Giannattasio, G., Ohta, S., Boyce, J. R., Xing, W., Balestrieri, B. and Boyce, J. A. (2011). The purinergic G protein-coupled receptor 6 inhibits effector T cell activation in allergic pulmonary inflammation. *J. Immunol.* **187,** 1486-1495.

Giepmans, B. N. and van Ijzendoorn, S. C. (2009). Epithelial cell-cell junctions and plasma membrane domains. *Biochim. Biophys. Acta* **1788,** 820-831.

Ginsburg-Shmuel, T., Haas, M., Schumann, M., Reiser, G., Kalid, O., Stern, N. and Fischer, B. (2010). 5-OMe-UDP is a potent and selective P2Y(6)-receptor agonist. *J. Med. Chem.* **53,** 1673-1685.

Girones, N., Alverez, E., Seth, A., Lin, I. M., Latour, D. A. and Davis, R. J. (1991). Mutational analysis of the cytoplasmic tail of the human transferrin receptor. identification of a sub-domain that is required for rapid endocytosis. *J. Biol. Chem.* **266,** 19006-19012.

Goody, R. S., Eckstein, F. and Schirmer, R. H. (1972). The enzymatic synthesis of thiophosphate analogs of nucleotides. *Biochim. Biophys. Acta* **276,** 155-161.

Greig, A. V., Linge, C., Terenghi, G., McGrouther, D. A. and Burnstock, G. (2003). Purinergic receptors are part of a functional signaling system for proliferation and differentiation of human epidermal keratinocytes. *J. Invest. Dermatol.* **120,** 1007-1015.

Griffin, B. A., Adams, S. R. and Tsien, R. Y. (1998). Specific covalent labeling of recombinant protein molecules inside live cells. *Science* **281,** 269-272.

Gronemeyer, T., Chidley, C., Juillerat, A., Heinis, C. and Johnsson, K. (2006). Directed evolution of O6-alkylguanine-DNA alkyltransferase for applications in protein labeling. *Protein Eng. Des. Sel.* **19,** 309-316.

Guan, X. M., Kobilka, T. S. and Kobilka, B. K. (1992). Enhancement of membrane insertion and function in a type IIIb membrane protein following introduction of a cleavable signal peptide. *J Biol Chem* **267,** 21995-8.

Guarnieri, F. G., Arterburn, L. M., Penno, M. B., Cha, Y. and August, J. T. (1993). The motif tyr-X-X-hydrophobic residue mediates lysosomal membrane targeting of lysosome-associated membrane protein 1. *J. Biol. Chem.* **268,** 1941-1946.

Haardt, M., Benharouga, M., Lechardeur, D., Kartner, N. and Lukacs, G. L. (1999). C-terminal truncations destabilize the cystic fibrosis transmembrane conductance regulator without impairing its biogenesis. A novel class of mutation. *J. Biol. Chem.* **274,** 21873-21877.

Hechler, B., Leon, C., Vial, C., Vigne, P., Frelin, C., Cazenave, J. P. and Gachet, C. (1998). The P2Y1 receptor is necessary for adenosine 5'-diphosphate-induced platelet aggregation. *Blood* **92,** 152-159.

Herold, C. L., Li, Q., Schachter, J. B., Harden, T. K. and Nicholas, R. A. (1997). Lack of nucleotide-promoted second messenger signaling responses in 1321N1 cells expressing the proposed P2Y receptor, p2y7. *Biochem. Biophys. Res. Commun.* **235,** 717-721.

Herold, C. L., Qi, A. D., Harden, T. K. and Nicholas, R. A. (2004). Agonist versus antagonist action of ATP at the P2Y4 receptor is determined by the second extracellular loop. *J. Biol. Chem.* **279,** 11456-11464.

Hildebrandt, J. D. (1997). Role of subunit diversity in signaling by heterotrimeric G proteins. *Biochem. Pharmacol.* **54,** 325-339.

Ho, S. N., Hunt, H. D., Horton, R. M., Pullen, J. K. and Pease, L. R. (1989). Site-directed mutagenesis by overlap extension using the polymerase chain reaction. *Gene* **77,** 51-9.

Hodson, C. A., Ambrogi, I. G., Scott, R. O., Mohler, P. J. and Milgram, S. L. (2006). Polarized apical sorting of guanylyl cyclase C is specified by a cytosolic signal. *Traffic* **7,** 456-64.

Hoebertz, A., Mahendran, S., Burnstock, G. and Arnett, T. R. (2002). ATP and UTP at low concentrations strongly inhibit bone formation by osteoblasts: A novel role for the P2Y2 receptor in bone remodeling. *J. Cell. Biochem.* **86,** 413-419.

Hoebertz, A., Meghji, S., Burnstock, G. and Arnett, T. R. (2001). Extracellular ADP is a powerful osteolytic agent: Evidence for signaling through the P2Y(1) receptor on bone cells. *FASEB J.* **15,** 1139-1148.

Hollopeter, G., Jantzen, H. M., Vincent, D., Li, G., England, L., Ramakrishnan, V., Yang, R. B., Nurden, P., Nurden, A., Julius, D. et al. (2001). Identification of the platelet ADP receptor targeted by antithrombotic drugs. *Nature* **409,** 202-207.

Horckmans, M., Robaye, B., Leon-Gomicronmez, E., Lantz, N., Unger, P., Dol-Gleizes, F., Clouet, S., Cammarata, D., Schaeffer, P., Savi, P. et al. (2012). P2Y(4) nucleotide receptor: A novel actor in post-natal cardiac development. *Angiogenesis* **15,** 349-360.

Hosoya, K., Ueda, H., Kim, K. J. and Lee, V. H. (1999). Nucleotide stimulation of cl(-) secretion in the pigmented rabbit conjunctiva. *J. Pharmacol. Exp. Ther.* **291,** 53-59.

Hua, W., Sheff, D., Toomre, D. and Mellman, I. (2006). Vectorial insertion of apical and basolateral membrane proteins in polarized epithelial cells revealed by quantitative 3D live cell imaging. *J. Cell Biol.* **172,** 1035-1044.

Huang, K. and El-Husseini, A. (2005). Modulation of neuronal protein trafficking and function by palmitoylation. *Curr Opin Neurobiol* **15,** 527-35.

Humphrey, J. S., Peters, P. J., Yuan, L. C. and Bonifacino, J. S. (1993). Localization of TGN38 to the trans-golgi network: Involvement of a cytoplasmic tyrosine-containing sequence. *J. Cell Biol.* **120,** 1123-1135.

Hunziker, W. and Fumey, C. (1994). A di-leucine motif mediates endocytosis and basolateral sorting of macrophage IgG fc receptors in MDCK cells. *EMBO J* **13,** 2963-9.

Hunziker, W., Harter, C., Matter, K. and Mellman, I. (1991). Basolateral sorting in MDCK cells requires a distinct cytoplasmic domain determinant. *Cell* **66,** 907-20.

Hur, D. G., Lee, J. H., Oh, S. H., Kim, Y. H., Lee, J. H., Shin, D. H., Chang, S. O. and Kim, C. S. (2007). KCNQ1/KCNE1 K+ channel and P2Y4 receptor are co-expressed from the time of birth in the apical membrane of rat strial marginal cells. *Acta Otolaryngol. Suppl.* **(558),** 30-35.

Hwang, T. H., Schwiebert, E. M. and Guggino, W. B. (1996). Apical and basolateral ATP stimulates tracheal epithelial chloride secretion via multiple purinergic receptors. *Am. J. Physiol.* **270,** C1611-23.

Insel, P. A., Firestein, B. L., Xing, M., Post, S. R., Jacobson, J. P., Balboa, M. A. and Hughes, R. J. (1996). P2-purinoceptors utilize multiple signalling pathways in MDCK-D1 cells. *J. Auton. Pharmacol.* **16,** 311-313.

Iverson, H. A., Fox, D.,3rd, Nadler, L. S., Klevit, R. E. and Nathanson, N. M. (2005). Identification and structural determination of the M(3) muscarinic acetylcholine receptor basolateral sorting signal. *J. Biol. Chem.* **280,** 24568-24575.

Jacquet, S., Malaval, C., Martinez, L. O., Sak, K., Rolland, C., Perez, C., Nauze, M., Champagne, E., Terce, F., Gachet, C. et al. (2005). The nucleotide receptor P2Y13 is a key regulator of hepatic high-density lipoprotein (HDL) endocytosis. *Cell Mol. Life Sci.* **62,** 2508-2515.

Janssens, R., Boeynaems, J. M., Godart, M. and Communi, D. (1997). Cloning of a human heptahelical receptor closely related to the P2Y5 receptor. *Biochem Biophys Res Commun* **236,** 106-12.

Janvier, K., Kato, Y., Boehm, M., Rose, J. R., Martina, J. A., Kim, B. Y., Venkatesan, S. and Bonifacino, J. S. (2003). Recognition of dileucine-based sorting signals from HIV-1 nef and LIMP-II by the AP-1 gamma-sigma1 and AP-3 delta-sigma3 hemicomplexes. *J. Cell Biol.* **163,** 1281-1290.

Jin, J., Dasari, V. R., Sistare, F. D. and Kunapuli, S. P. (1998). Distribution of P2Y receptor subtypes on haematopoietic cells. *Br. J. Pharmacol.* **123,** 789-794.

Jolimay, N., Franck, L., Langlois, X., Hamon, M. and Darmon, M. (2000). Dominant role of the cytosolic C-terminal domain of the rat 5-HT1B receptor in axonal-apical targeting. *J Neurosci* **20,** 9111-8.

Joseph, S. M., Buchakjian, M. R. and Dubyak, G. R. (2003). Colocalization of ATP release sites and ecto-ATPase activity at the extracellular surface of human astrocytes. *J. Biol. Chem.* **278,** 23331-23342.

Juillerat, A., Gronemeyer, T., Keppler, A., Gendreizig, S., Pick, H., Vogel, H. and Johnsson, K. (2003). Directed evolution of O6-alkylguanine-DNA alkyltransferase for efficient labeling of fusion proteins with small molecules in vivo. *Chem. Biol.* **10,** 313-317.

Keefer, J. R. and Limbird, L. E. (1993). The alpha 2A-adrenergic receptor is targeted directly to the basolateral membrane domain of madin-darby canine kidney cells independent of coupling to pertussis toxin-sensitive GTP-binding proteins. *J Biol Chem* **268,** 11340-7.

Keitel, V., Nies, A. T., Brom, M., Hummel-Eisenbeiss, J., Spring, H. and Keppler, D. (2003). A common dubin-johnson syndrome mutation impairs protein maturation and transport activity of MRP2 (ABCC2). *Am J Physiol Gastrointest Liver Physiol* **284,** G165-74.

Kennedy, C., Qi, A. D., Herold, C. L., Harden, T. K. and Nicholas, R. A. (2000). ATP, an agonist at the rat P2Y(4) receptor, is an antagonist at the human P2Y(4) receptor. *Mol. Pharmacol.* **57,** 926-931.

Keppler, A., Gendreizig, S., Gronemeyer, T., Pick, H., Vogel, H. and Johnsson, K. (2003). A general method for the covalent labeling of fusion proteins with small molecules in vivo. *Nat. Biotechnol.* **21,** 86-89.

Kim, B., Jeong, H. K., Kim, J. H., Lee, S. Y., Jou, I. and Joe, E. H. (2011). Uridine 5'-diphosphate induces chemokine expression in microglia and astrocytes through activation of the P2Y6 receptor. *J. Immunol.* **186,** 3701-3709.

Kim, C. H., Kim, S. S., Choi, J. Y., Shin, J. H., Kim, J. Y., Namkung, W., Lee, J. G., Lee, M. G. and Yoon, J. H. (2004). Membrane-specific expression of functional purinergic receptors in normal human nasal epithelial cells. *Am. J. Physiol. Lung Cell. Mol. Physiol.* **287,** L835-42.

Kim, H. S., Ohno, M., Xu, B., Kim, H. O., Choi, Y., Ji, X. D., Maddileti, S., Marquez, V. E., Harden, T. K. and Jacobson, K. A. (2003). 2-substitution of adenine nucleotide analogues containing a bicyclo[3.1.0]hexane ring system locked in a northern conformation: Enhanced potency as P2Y1 receptor antagonists. *J. Med. Chem.* **46,** 4974-4987.

Kim, S. G., Gao, Z. G., Soltysiak, K. A., Chang, T. S., Brodie, C. and Jacobson, K. A. (2003). P2Y6 nucleotide receptor activates PKC to protect 1321N1 astrocytoma cells against tumor necrosis factor-induced apoptosis. *Cell. Mol. Neurobiol.* **23,** 401-418.

Kim, S. G., Soltysiak, K. A., Gao, Z. G., Chang, T. S., Chung, E. and Jacobson, K. A. (2003). Tumor necrosis factor alpha-induced apoptosis in astrocytes is prevented by the activation of P2Y6, but not P2Y4 nucleotide receptors. *Biochem. Pharmacol.* **65,** 923-931.

Kim, Y. C., Lee, J. S., Sak, K., Marteau, F., Mamedova, L., Boeynaems, J. M. and Jacobson, K. A. (2005). Synthesis of pyridoxal phosphate derivatives with antagonist activity at the P2Y13 receptor. *Biochem. Pharmacol.* **70,** 266-274.

Kleizen, B., Braakman, I. and de Jonge, H. R. (2000). Regulated trafficking of the CFTR chloride channel. *Eur J Cell Biol* **79,** 544-56.

Klemm, R. W., Ejsing, C. S., Surma, M. A., Kaiser, H. J., Gerl, M. J., Sampaio, J. L., de Robillard, Q., Ferguson, C., Proszynski, T. J., Shevchenko, A. et al. (2009). Segregation of sphingolipids and sterols during formation of secretory vesicles at the trans-golgi network. *J. Cell Biol.* **185,** 601-612.

Kook, S. H., Cho, J. S., Morrison, A., Wiener, E., Lee, S. B., Scadden, D. and Lee, B. C. (2013). The purinergic P2Y14 receptor axis is a molecular determinant for organism survival under in utero radiation toxicity. *Cell. Death Dis.* **4,** e703.

Kottgen, M., Loffler, T., Jacobi, C., Nitschke, R., Pavenstadt, H., Schreiber, R., Frische, S., Nielsen, S. and Leipziger, J. (2003). P2Y6 receptor mediates colonic NaCl secretion via differential activation of cAMP-mediated transport. *J. Clin. Invest.* **111,** 371-379.

Kozak, M. (1984). Point mutations close to the AUG initiator codon affect the efficiency of translation of rat preproinsulin in vivo. *Nature* **308,** 241-246.

Kruse, R., Save, S. and Persson, K. (2012). Adenosine triphosphate induced P2Y2 receptor activation induces proinflammatory cytokine release in uroepithelial cells. *J. Urol.* **188,** 2419-2425.

Kunzelmann, K. and Mall, M. (2002). Electrolyte transport in the mammalian colon: Mechanisms and implications for disease. *Physiol Rev* **82,** 245-89.

Lazarowski, E. R. (2012). Vesicular and conductive mechanisms of nucleotide release. *Purinergic Signal* **8,** 359-73.

Lazarowski, E. R., Boucher, R. C. and Harden, T. K. (2003). Mechanisms of release of nucleotides and integration of their action as P2X- and P2Y-receptor activating molecules. *Mol Pharmacol* **64,** 785-95.

Lazarowski, E. R., Rochelle, L. G., O'Neal, W. K., Ribeiro, C. M., Grubb, B. R., Zhang, V., Harden, T. K. and Boucher, R. C. (2001). Cloning and functional characterization of two murine uridine nucleotide receptors reveal a potential target for correcting ion transport deficiency in cystic fibrosis gallbladder. *J. Pharmacol. Exp. Ther.* **297,** 43-49.

Lazarowski, E. R., Shea, D. A., Boucher, R. C. and Harden, T. K. (2003). Release of cellular UDP-glucose as a potential extracellular signaling molecule. *Mol. Pharmacol.* **63,** 1190-1197.

Lazarowski, E. R., Watt, W. C., Stutts, M. J., Boucher, R. C. and Harden, T. K. (1995). Pharmacological selectivity of the cloned human P2U-purinoceptor: Potent activation by diadenosine tetraphosphate. *Br. J. Pharmacol.* **116,** 1619-1627.

Lee, J. H., Heo, J. H., Chang, S. O., Kim, C. S. and Oh, S. H. (2006). **Reactive blue 2, an antagonist of rat P2Y4, increases K+ secretion in rat cochlea strial marginal cells.**. *Hear Res.* **Sep;219(1-2),** 66-66-73.

Lee, B. C., Cheng, T., Adams, G. B., Attar, E. C., Miura, N., Lee, S. B., Saito, Y., Olszak, I., Dombkowski, D., Olson, D. P. et al. (2003). P2Y-like receptor, GPR105 (P2Y14), identifies and mediates chemotaxis of bone-marrow hematopoietic stem cells. *Genes Dev.* **17,** 1592-1604.

Lee, S. Y., Palmer, M. L., Maniak, P. J., Jang, S. H., Ryu, P. D. and O'Grady, S. M. (2007). P2Y receptor regulation of sodium transport in human mammary epithelial cells. *Am. J. Physiol. Cell. Physiol.* **293,** C1472-80.

Leon-Otegui, M., Gomez-Villafuertes, R., Diaz-Hernandez, J. I., Diaz-Hernandez, M., Miras-Portugal, M. T. and Gualix, J. (2011). Opposite effects of P2X7 and P2Y2 nucleotide receptors on alpha-secretase-dependent APP processing in neuro-2a cells. *FEBS Lett.* **585,** 2255-2262.

Letourneur, F. and Klausner, R. D. (1992). A novel di-leucine motif and a tyrosine-based motif independently mediate lysosomal targeting and endocytosis of CD3 chains. *Cell* **69,** 1143-1157.

Li, Q., Olesky, M., Palmer, R. K., Harden, T. K. and Nicholas, R. A. (1998). Evidence that the p2y3 receptor is the avian homologue of the mammalian P2Y6 receptor. *Mol. Pharmacol.* **54,** 541-546.

Linder, M. E. and Deschenes, R. J. (2007). Palmitoylation: Policing protein stability and traffic. *Nat Rev Mol Cell Biol* **8,** 74-84.

Lingwood, D. and Simons, K. (2010). Lipid rafts as a membrane-organizing principle. *Science* **327,** 46-50.

Lisanti, M. P., Caras, I. W., Davitz, M. A. and Rodriguez-Boulan, E. (1989). A glycophospholipid membrane anchor acts as an apical targeting signal in polarized epithelial cells. *J Cell Biol* **109,** 2145-56.

Lohse, M. J., Benovic, J. L., Codina, J., Caron, M. G. and Lefkowitz, R. J. (1990). Beta-arrestin: A protein that regulates beta-adrenergic receptor function. *Science* **248,** 1547-50.

Los, G. V., Encell, L. P., McDougall, M. G., Hartzell, D. D., Karassina, N., Zimprich, C., Wood, M. G., Learish, R., Ohana, R. F., Urh, M. et al. (2008). HaloTag: A novel protein labeling technology for cell imaging and protein analysis. *ACS Chem. Biol.* **3,** 373-382.

Luton, F., Hexham, M. J., Zhang, M. and Mostov, K. E. (2009). Identification of a cytoplasmic signal for apical transcytosis. *Traffic* **10,** 1128-1142.

Mallabiabarrena, A., Fresno, M. and Alarcon, B. (1992). An endoplasmic reticulum retention signal in the CD3 epsilon chain of the T-cell receptor. *Nature* **357,** 593-596.

Malmsjo, M., Adner, M., Harden, T. K., Pendergast, W., Edvinsson, L. and Erlinge, D. (2000). The stable pyrimidines UDPbetaS and UTPgammaS discriminate between the P2 receptors that mediate vascular contraction and relaxation of the rat mesenteric artery. *Br. J. Pharmacol.* **131,** 51-56.

Mamedova, L. K., Joshi, B. V., Gao, Z. G., von Kugelgen, I. and Jacobson, K. A. (2004). Diisothiocyanate derivatives as potent, insurmountable antagonists of P2Y6 nucleotide receptors. *Biochem. Pharmacol.* **67,** 1763-1770.

Mamedova, L. K., Wang, R., Besada, P., Liang, B. T. and Jacobson, K. A. (2008). Attenuation of apoptosis in vitro and ischemia/reperfusion injury in vivo in mouse skeletal muscle by P2Y6 receptor activation. *Pharmacol. Res.* **58,** 232-239.

Marcus, D. C. and Scofield, M. A. (2001). Apical P2Y4 purinergic receptor controls K+ secretion by vestibular dark cell epithelium. *Am J Physiol Cell Physiol* **281,** C282-9.

Marmorstein, A. D., Csaky, K. G., Baffi, J., Lam, L., Rahaal, F. and Rodriguez-Boulan, E. (2000). Saturation of, and competition for entry into, the apical secretory pathway. *Proc. Natl. Acad. Sci. U. S. A.* **97,** 3248-3253.

Marr, N., Bichet, D. G., Hoefs, S., Savelkoul, P. J., Konings, I. B., De Mattia, F., Graat, M. P., Arthus, M. F., Lonergan, M., Fujiwara, T. M. et al. (2002). Cell-biologic and functional analyses of five new aquaporin-2 missense mutations that cause recessive nephrogenic diabetes insipidus. *J Am Soc Nephrol* **13,** 2267-77.

Marr, N., Bichet, D. G., Lonergan, M., Arthus, M. F., Jeck, N., Seyberth, H. W., Rosenthal, W., van Os, C. H., Oksche, A. and Deen, P. M. (2002).

Heteroligomerization of an aquaporin-2 mutant with wild-type aquaporin-2 and their misrouting to late endosomes/lysosomes explains dominant nephrogenic diabetes insipidus. *Hum. Mol. Genet.* **11,** 779-789.

Marteau, F., Le Poul, E., Communi, D., Communi, D., Labouret, C., Savi, P., Boeynaems, J. M. and Gonzalez, N. S. (2003). Pharmacological characterization of the human P2Y13 receptor. *Mol. Pharmacol.* **64,** 104-112.

Maruoka, H., Jayasekara, M. P., Barrett, M. O., Franklin, D. A., de Castro, S., Kim, N., Costanzi, S., Harden, T. K. and Jacobson, K. A. (2011). Pyrimidine nucleotides with 4-alkyloxyimino and terminal tetraphosphate delta-ester modifications as selective agonists of the P2Y(4) receptor. *J. Med. Chem.* **54,** 4018-4033.

Matos, J. E., Robaye, B., Boeynaems, J. M., Beauwens, R. and Leipziger, J. (2005). K+ secretion activated by luminal P2Y2 and P2Y4 receptors in mouse colon. *J Physiol* **564,** 269-79.

Matter, K., Hunziker, W. and Mellman, I. (1992). Basolateral sorting of LDL receptor in MDCK cells: The cytoplasmic domain contains two tyrosine-dependent targeting determinants. *Cell* **71,** 741-753.

Matter, K., Yamamoto, E. M. and Mellman, I. (1994). Structural requirements and sequence motifs for polarized sorting and endocytosis of LDL and fc receptors in MDCK cells. *J Cell Biol* **126,** 991-1004.

McGarrigle, D. and Huang, X. Y. (2007). GPCRs signaling directly through src-family kinases. *Sci. STKE* **2007,** pe35.

McMillan, M. R., Burnstock, G. and Haworth, S. G. (1999). Vasodilatation of intrapulmonary arteries to P2-receptor nucleotides in normal and pulmonary hypertensive newborn piglets. *Br. J. Pharmacol.* **128,** 543-548.

McNamara, N., Khong, A., McKemy, D., Caterina, M., Boyer, J., Julius, D. and Basbaum, C. (2001). ATP transduces signals from ASGM1, a glycolipid that functions as a bacterial receptor. *Proc Natl Acad Sci U S A* **98,** 9086-91.

Meis, S., Hamacher, A., Hongwiset, D., Marzian, C., Wiese, M., Eckstein, N., Royer, H. D., Communi, D., Boeynaems, J. M., Hausmann, R. et al. (2010). NF546 [4,4'-(carbonylbis(imino-3,1-phenylene-carbonylimino-3,1-(4-methyl-phenylene)-car bonylimino))-bis(1,3-xylene-alpha,alpha'-diphosphonic acid) tetrasodium salt] is a non-nucleotide P2Y11 agonist and stimulates release of interleukin-8 from human monocyte-derived dendritic cells. *J. Pharmacol. Exp. Ther.* **332,** 238-247.

Meshki, J., Tuluc, F., Bredetean, O., Ding, Z. and Kunapuli, S. P. (2004). Molecular mechanism of nucleotide-induced primary granule release in human neutrophils: Role for the P2Y2 receptor. *Am. J. Physiol. Cell. Physiol.* **286,** C264-71.

Moore, D. J., Chambers, J. K., Wahlin, J. P., Tan, K. B., Moore, G. B., Jenkins, O., Emson, P. C. and Murdock, P. R. (2001). Expression pattern of human P2Y receptor

subtypes: A quantitative reverse transcription-polymerase chain reaction study. *Biochim Biophys Acta* **1521,** 107-19.

Moore, D. J., Murdock, P. R., Watson, J. M., Faull, R. L., Waldvogel, H. J., Szekeres, P. G., Wilson, S., Freeman, K. B. and Emson, P. C. (2003). GPR105, a novel gi/o-coupled UDP-glucose receptor expressed on brain glia and peripheral immune cells, is regulated by immunologic challenge: Possible role in neuroimmune function. *Brain Res. Mol. Brain Res.* **118,** 10-23.

Moreschi, I., Bruzzone, S., Bodrato, N., Usai, C., Guida, L., Nicholas, R. A., Kassack, M. U., Zocchi, E. and De Flora, A. (2008). NAADP+ is an agonist of the human P2Y11 purinergic receptor. *Cell Calcium* **43,** 344-355.

Moreschi, I., Bruzzone, S., Nicholas, R. A., Fruscione, F., Sturla, L., Benvenuto, F., Usai, C., Meis, S., Kassack, M. U., Zocchi, E. et al. (2006). Extracellular NAD+ is an agonist of the human P2Y11 purinergic receptor in human granulocytes. *J. Biol. Chem.* **281,** 31419-31429.

Moro, S., Guo, D., Camaioni, E., Boyer, J. L., Harden, T. K. and Jacobson, K. A. (1998). Human P2Y1 receptor: Molecular modeling and site-directed mutagenesis as tools to identify agonist and antagonist recognition sites. *J. Med. Chem.* **41,** 1456-1466.

Muller, T., Bayer, H., Myrtek, D., Ferrari, D., Sorichter, S., Ziegenhagen, M. W., Zissel, G., Virchow, J. C.,Jr, Luttmann, W., Norgauer, J. et al. (2005). The P2Y14 receptor of airway epithelial cells: Coupling to intracellular Ca2+ and IL-8 secretion. *Am. J. Respir. Cell Mol. Biol.* **33,** 601-609.

Muscella, A., Elia, M. G., Greco, S., Storelli, C. and Marsigliante, S. (2003). Activation of P2Y2 receptor induces c-FOS protein through a pathway involving mitogen-activated protein kinases and phosphoinositide 3-kinases in HeLa cells. *J. Cell. Physiol.* **195,** 234-240.

Nadler, L. S., Kumar, G. and Nathanson, N. M. (2001). Identification of a basolateral sorting signal for the M3 muscarinic acetylcholine receptor in madin-darby canine kidney cells. *J. Biol. Chem.* **276,** 10539-10547.

Nagao, S., Kugita, M., Yoshihara, D. and Yamaguchi, T. (2012). Animal models for human polycystic kidney disease. *Exp. Anim.* **61,** 477-488.

Nguyen, T., Erb, L., Weisman, G. A., Marchese, A., Heng, H. H., Garrad, R. C., George, S. R., Turner, J. T. and O'Dowd, B. F. (1995). Cloning, expression, and chromosomal localization of the human uridine nucleotide receptor gene. *J. Biol. Chem.* **270,** 30845-30848.

Nguyen, T. D., Meichle, S., Kim, U. S., Wong, T. and Moody, M. W. (2001). P2Y(11), a purinergic receptor acting via cAMP, mediates secretion by pancreatic duct epithelial cells. *Am. J. Physiol. Gastrointest. Liver Physiol.* **280,** G795-804.

Nicholas, R. A., Lazarowski, E. R., Watt, W. C., Li, Q., Boyer, J. and Harden, T. K. (1996). Pharmacological and second messenger signalling selectivities of cloned P2Y receptors. *J. Auton. Pharmacol.* **16,** 319-323.

Norgard, N. B. (2009). Cangrelor: A novel P2Y12 receptor antagonist. *Expert Opin. Investig. Drugs* **18,** 1219-1230.

Odorizzi, G. and Trowbridge, I. S. (1997). Structural requirements for basolateral sorting of the human transferrin receptor in the biosynthetic and endocytic pathways of madin-darby canine kidney cells. *J. Cell Biol.* **137,** 1255-1264.

Ohno, H., Aguilar, R. C., Yeh, D., Taura, D., Saito, T. and Bonifacino, J. S. (1998). The medium subunits of adaptor complexes recognize distinct but overlapping sets of tyrosine-based sorting signals. *J. Biol. Chem.* **273,** 25915-25921.

Ohno, H., Stewart, J., Fournier, M. C., Bosshart, H., Rhee, I., Miyatake, S., Saito, T., Gallusser, A., Kirchhausen, T. and Bonifacino, J. S. (1995). Interaction of tyrosine-based sorting signals with clathrin-associated proteins. *Science* **269,** 1872-5.

Ohno, H., Tomemori, T., Nakatsu, F., Okazaki, Y., Aguilar, R. C., Foelsch, H., Mellman, I., Saito, T., Shirasawa, T. and Bonifacino, J. S. (1999). Mu1B, a novel adaptor medium chain expressed in polarized epithelial cells. *FEBS Lett.* **449,** 215-220.

Ohsawa, K., Irino, Y., Nakamura, Y., Akazawa, C., Inoue, K. and Kohsaka, S. (2007). Involvement of P2X4 and P2Y12 receptors in ATP-induced microglial chemotaxis. *Glia* **55,** 604-616.

Oksche, A., Schulein, R., Rutz, C., Liebenhoff, U., Dickson, J., Muller, H., Birnbaumer, M. and Rosenthal, W. (1996). Vasopressin V2 receptor mutants that cause X-linked nephrogenic diabetes insipidus: Analysis of expression, processing, and function. *Mol. Pharmacol.* **50,** 820-828.

Orriss, I. R., Wang, N., Burnstock, G., Arnett, T. R., Gartland, A., Robaye, B. and Boeynaems, J. M. (2011). The P2Y(6) receptor stimulates bone resorption by osteoclasts. *Endocrinology* **152,** 3706-3716.

Paladino, S., Pocard, T., Catino, M. A. and Zurzolo, C. (2006). GPI-anchored proteins are directly targeted to the apical surface in fully polarized MDCK cells. *J. Cell Biol.* **172,** 1023-1034.

Paladino, S., Sarnataro, D., Pillich, R., Tivodar, S., Nitsch, L. and Zurzolo, C. (2004). Protein oligomerization modulates raft partitioning and apical sorting of GPI-anchored proteins. *J Cell Biol* **167,** 699-709.

Palmer, R. K., Boyer, J. L., Schachter, J. B., Nicholas, R. A. and Harden, T. K. (1998). Agonist action of adenosine triphosphates at the human P2Y1 receptor. *Mol. Pharmacol.* **54,** 1118-1123.

Park, H. S. and Hourani, S. M. (1999). Differential effects of adenine nucleotide analogues on shape change and aggregation induced by adnosine 5-diphosphate (ADP) in human platelets. *Br. J. Pharmacol.* **127,** 1359-1366.

Parr, C. E., Sullivan, D. M., Paradiso, A. M., Lazarowski, E. R., Burch, L. H., Olsen, J. C., Erb, L., Weisman, G. A., Boucher, R. C. and Turner, J. T. (1994). Cloning and expression of a human P2U nucleotide receptor, a target for cystic fibrosis pharmacotherapy. *Proc. Natl. Acad. Sci. U. S. A.* **91,** 3275-3279.

Pendergast, W., Yerxa, B. R., Douglass, J. G.,3rd, Shaver, S. R., Dougherty, R. W., Redick, C. C., Sims, I. F. and Rideout, J. L. (2001). Synthesis and P2Y receptor activity of a series of uridine dinucleoside 5'-polyphosphates. *Bioorg. Med. Chem. Lett.* **11,** 157-160.

Pintor, J., Peral, A., Hoyle, C. H., Redick, C., Douglass, J., Sims, I. and Yerxa, B. (2002). Effects of diadenosine polyphosphates on tear secretion in new zealand white rabbits. *J. Pharmacol. Exp. Ther.* **300,** 291-297.

Polishchuk, R., Di Pentima, A. and Lippincott-Schwartz, J. (2004). Delivery of raft-associated, GPI-anchored proteins to the apical surface of polarized MDCK cells by a transcytotic pathway. *Nat Cell Biol* **6,** 297-307.

Pond, L., Kuhn, L. A., Teyton, L., Schutze, M. P., Tainer, J. A., Jackson, M. R. and Peterson, P. A. (1995). A role for acidic residues in di-leucine motif-based targeting to the endocytic pathway. *J. Biol. Chem.* **270,** 19989-19997.

Post, S. R., Jacobson, J. P. and Insel, P. A. (1996). P2 purinergic receptor agonists enhance cAMP production in madin-darby canine kidney epithelial cells via an autocrine/paracrine mechanism. *J. Biol. Chem.* **271,** 2029-2032.

Post, S. R., Rump, L. C., Zambon, A., Hughes, R. J., Buda, M. D., Jacobson, J. P., Kao, C. C. and Insel, P. A. (1998). ATP activates cAMP production via multiple purinergic receptors in MDCK-D1 epithelial cells. blockade of an autocrine/paracrine pathway to define receptor preference of an agonist. *J. Biol. Chem.* **273,** 23093-23097.

Potter, B. A., Ihrke, G., Bruns, J. R., Weixel, K. M. and Weisz, O. A. (2004). Specific N-glycans direct apical delivery of transmembrane, but not soluble or glycosylphosphatidylinositol-anchored forms of endolyn in madin-darby canine kidney cells. *Mol. Biol. Cell* **15,** 1407-1416.

Prill, V., Lehmann, L., von Figura, K. and Peters, C. (1993). The cytoplasmic tail of lysosomal acid phosphatase contains overlapping but distinct signals for basolateral sorting and rapid internalization in polarized MDCK cells. *EMBO J.* **12,** 2181-2193.

Puig, B., Altmeppen, H. C., Thurm, D., Geissen, M., Conrad, C., Braulke, T. and Glatzel, M. (2011). N-glycans and glycosylphosphatidylinositol-anchor act on polarized sorting of mouse PrP(C) in madin-darby canine kidney cells. *PLoS One* **6,** e24624.

Qi, A. D., Harden, T. K. and Nicholas, R. A. (2004). GPR80/99, proposed to be the P2Y(15) receptor activated by adenosine and AMP, is not a P2Y receptor. *Purinergic Signal* **1,** 67-74.

Qi, A. D., Kennedy, C., Harden, T. K. and Nicholas, R. A. (2001). Differential coupling of the human P2Y(11) receptor to phospholipase C and adenylyl cyclase. *Br. J. Pharmacol.* **132,** 318-326.

Qi, A. D., Wolff, S. C. and Nicholas, R. A. (2005). The apical targeting signal of the P2Y2 receptor is located in its first extracellular loop. *J Biol Chem* **280,** 29169-75.

Qi, A. D., Zambon, A. C., Insel, P. A. and Nicholas, R. A. (2001). An arginine/glutamine difference at the juxtaposition of transmembrane domain 6 and the third extracellular loop contributes to the markedly different nucleotide selectivities of human and canine P2Y11 receptors. *Mol. Pharmacol.* **60,** 1375-1382.

Rajagopal, M., Kathpalia, P. P., Thomas, S. V. and Pao, A. C. (2011). Activation of P2Y1 and P2Y2 receptors induces chloride secretion via calcium-activated chloride channels in kidney inner medullary collecting duct cells. *Am. J. Physiol. Renal Physiol.* **301,** F544-53.

Ralevic, V. and Burnstock, G. (1998). Receptors for purines and pyrimidines. *Pharmacol. Rev.* **50,** 413-492.

Robaye, B., Ghanem, E., Wilkin, F., Fokan, D., Van Driessche, W., Schurmans, S., Boeynaems, J. M. and Beauwens, R. (2003). Loss of nucleotide regulation of epithelial chloride transport in the jejunum of P2Y4-null mice. *Mol Pharmacol* **63,** 777-83.

Rodriguez-Boulan, E., Musch, A. and Le Bivic, A. (2004). Epithelial trafficking: New routes to familiar places. *Curr Opin Cell Biol* **16,** 436-42.

Rotin, D., Kanelis, V. and Schild, L. (2001). Trafficking and cell surface stability of ENaC. *Am J Physiol Renal Physiol* **281,** F391-9.

Sakaki, H., Tsukimoto, M., Harada, H., Moriyama, Y. and Kojima, S. (2013). Autocrine regulation of macrophage activation via exocytosis of ATP and activation of P2Y11 receptor. *PLoS One* **8,** e59778.

Sarnataro, D., Paladino, S., Campana, V., Grassi, J., Nitsch, L. and Zurzolo, C. (2002). PrPC is sorted to the basolateral membrane of epithelial cells independently of its association with rafts. *Traffic* **3,** 810-821.

Sasaki, Y., Hoshi, M., Akazawa, C., Nakamura, Y., Tsuzuki, H., Inoue, K. and Kohsaka, S. (2003). Selective expression of gi/o-coupled ATP receptor P2Y12 in microglia in rat brain. *Glia* **44,** 242-250.

Saunders, C., Keefer, J. R., Bonner, C. A. and Limbird, L. E. (1998). Targeting of G protein-coupled receptors to the basolateral surface of polarized renal epithelial cells involves multiple, non-contiguous structural signals. *J. Biol. Chem.* **273,** 24196-24206.

Schaerer, E., Verrey, F., Racine, L., Tallichet, C., Reinhardt, M. and Kraehenbuhl, J. P. (1990). Polarized transport of the polymeric immunoglobulin receptor in transfected rabbit mammary epithelial cells. *J. Cell Biol.* **110,** 987-998.

Schafer, R., Hartig, R., Sedehizade, F., Welte, T. and Reiser, G. (2006). Adenine nucleotides inhibit proliferation of the human lung adenocarcinoma cell line LXF-289 by activation of nuclear factor kappaB1 and mitogen-activated protein kinase pathways. *FEBS J.* **273,** 3756-3767.

Schafer, R., Sedehizade, F., Welte, T. and Reiser, G. (2003). ATP- and UTP-activated P2Y receptors differently regulate proliferation of human lung epithelial tumor cells. *Am. J. Physiol. Lung Cell. Mol. Physiol.* **285,** L376-85.

Scheiffele, P., Peranen, J. and Simons, K. (1995). N-glycans as apical sorting signals in epithelial cells. *Nature* **378,** 96-8.

Schneider, C. A., Rasband, W. S. and Eliceiri, K. W. (2012). NIH image to ImageJ: 25 years of image analysis. *Nat. Methods* **9,** 671-675.

Schnurr, M., Toy, T., Stoitzner, P., Cameron, P., Shin, A., Beecroft, T., Davis, I. D., Cebon, J. and Maraskovsky, E. (2003). ATP gradients inhibit the migratory capacity of specific human dendritic cell types: Implications for P2Y11 receptor signaling. *Blood* **102,** 613-620.

Schreiber, R. and Kunzelmann, K. (2005). Purinergic P2Y6 receptors induce Ca2+ and CFTR dependent cl- secretion in mouse trachea. *Cell. Physiol. Biochem.* **16,** 99-108.

Schuchardt, M., Prufer, J., Prufer, N., Wiedon, A., Huang, T., Chebli, M., Jankowski, V., Jankowski, J., Schafer-Korting, M., Zidek, W. et al. (2011). The endothelium-derived contracting factor uridine adenosine tetraphosphate induces P2Y(2)-mediated pro-inflammatory signaling by monocyte chemoattractant protein-1 formation. *J. Mol. Med. (Berl)* **89,** 799-810.

Schuck, S., Honsho, M., Ekroos, K., Shevchenko, A. and Simons, K. (2003). Resistance of cell membranes to different detergents. *Proc. Natl. Acad. Sci. U. S. A.* **100,** 5795-5800.

Schuck, S. and Simons, K. (2004). Polarized sorting in epithelial cells: Raft clustering and the biogenesis of the apical membrane. *J Cell Sci* **117,** 5955-64.

Schumacher, D., Strilic, B., Sivaraj, K. K., Wettschureck, N. and Offermanns, S. (2013). Platelet-derived nucleotides promote tumor-cell transendothelial migration and metastasis via P2Y2 receptor. *Cancer. Cell.* **24,** 130-137.

Seror, C., Melki, M. T., Subra, F., Raza, S. Q., Bras, M., Saidi, H., Nardacci, R., Voisin, L., Paoletti, A., Law, F. et al. (2011). Extracellular ATP acts on P2Y2 purinergic receptors to facilitate HIV-1 infection. *J. Exp. Med.* **208,** 1823-1834.

Sesma, J. I., Kreda, S. M., Steinckwich-Besancon, N., Dang, H., Garcia-Mata, R., Harden, T. K. and Lazarowski, E. R. (2012). The UDP-sugar-sensing P2Y(14) receptor promotes rho-mediated signaling and chemotaxis in human neutrophils. *Am. J. Physiol. Cell. Physiol.* **303,** C490-8.

Seye, C. I., Yu, N., Jain, R., Kong, Q., Minor, T., Newton, J., Erb, L., Gonzalez, F. A. and Weisman, G. A. (2003). The P2Y2 nucleotide receptor mediates UTP-induced vascular cell adhesion molecule-1 expression in coronary artery endothelial cells. *J. Biol. Chem.* **278,** 24960-24965.

Sharma, M., Pampinella, F., Nemes, C., Benharouga, M., So, J., Du, K., Bache, K. G., Papsin, B., Zerangue, N., Stenmark, H. et al. (2004). Misfolding diverts CFTR from recycling to degradation: Quality control at early endosomes. *J. Cell Biol.* **164,** 923-933.

Shirasaki, H., Kanaizumi, E., Seki, N., Kikuchi, M. and Himi, T. (2013). Expression and localization of purinergic P2Y(12) receptor in human nasal mucosa. *Allergol. Int.* **62,** 239-244.

Simon, J., Vigne, P., Eklund, K. M., Michel, A. D., Carruthers, A. M., Humphrey, P. P., Frelin, C. and Barnard, E. A. (2001). Activity of adenosine diphosphates and triphosphates on a P2Y(T) -type receptor in brain capillary endothelial cells. *Br. J. Pharmacol.* **132,** 173-182.

Su, X., Floyd, D. H., Hughes, A., Xiang, J., Schneider, J. G., Uluckan, O., Heller, E., Deng, H., Zou, W., Craft, C. S. et al. (2012). The ADP receptor P2RY12 regulates osteoclast function and pathologic bone remodeling. *J. Clin. Invest.* **122,** 3579-3592.

Subramanian, V. S., Marchant, J. S., Boulware, M. J. and Said, H. M. (2004). A C-terminal region dictates the apical plasma membrane targeting of the human sodium-dependent vitamin C transporter-1 in polarized epithelia. *J Biol Chem* **279,** 27719-28.

Sullivan, E., Tucker, E. M. and Dale, I. L. (1999). Measurement of [Ca2+] using the fluorometric imaging plate reader (FLIPR). *Methods Mol. Biol.* **114,** 125-133.

Sun, A. Q., Balasubramaniyan, N., Liu, C. J., Shahid, M. and Suchy, F. J. (2004). Association of the 16-kDa subunit c of vacuolar proton pump with the ileal na+-dependent bile acid transporter: Protein-protein interaction and intracellular trafficking. *J Biol Chem* **279,** 16295-300.

Sun, A. Q., Salkar, R., Sachchidanand, Xu, S., Zeng, L., Zhou, M. M. and Suchy, F. J. (2003). A 14-amino acid sequence with a beta-turn structure is required for apical membrane sorting of the rat ileal bile acid transporter. *J Biol Chem* **278,** 4000-9.

Tai, A. W., Chuang, J. Z. and Sung, C. H. (2001). Cytoplasmic dynein regulation by subunit heterogeneity and its role in apical transport. *J Cell Biol* **153,** 1499-509.

Takasaki, J., Kamohara, M., Saito, T., Matsumoto, M., Matsumoto, S., Ohishi, T., Soga, T., Matsushime, H. and Furuichi, K. (2001). Molecular cloning of the platelet P2T(AC) ADP receptor: Pharmacological comparison with another ADP receptor, the P2Y(1) receptor. *Mol. Pharmacol.* **60,** 432-439.

Takeda, T., Yamazaki, H. and Farquhar, M. G. (2003). Identification of an apical sorting determinant in the cytoplasmic tail of megalin. *Am J Physiol Cell Physiol* **284,** C1105-13.

Thomas, D. C., Brewer, C. B. and Roth, M. G. (1993). Vesicular stomatitis virus glycoprotein contains a dominant cytoplasmic basolateral sorting signal critically dependent upon a tyrosine. *J. Biol. Chem.* **268,** 3313-3320.

Thomas, D. C. and Roth, M. G. (1994). The basolateral targeting signal in the cytoplasmic domain of glycoprotein G from vesicular stomatitis virus resembles a variety of intracellular targeting motifs related by primary sequence but having diverse targeting activities. *J. Biol. Chem.* **269,** 15732-15739.

Torres, B., Zambon, A. C. and Insel, P. A. (2002). P2Y11 receptors activate adenylyl cyclase and contribute to nucleotide-promoted cAMP formation in MDCK-D(1) cells. A mechanism for nucleotide-mediated autocrine-paracrine regulation. *J. Biol. Chem.* **277,** 7761-7765.

Tozaki-Saitoh, H., Tsuda, M., Miyata, H., Ueda, K., Kohsaka, S. and Inoue, K. (2008). P2Y12 receptors in spinal microglia are required for neuropathic pain after peripheral nerve injury. *J. Neurosci.* **28,** 4949-4956.

Tran Van Nhieu, G., Clair, C., Bruzzone, R., Mesnil, M., Sansonetti, P. and Combettes, L. (2003). Connexin-dependent inter-cellular communication increases invasion and dissemination of shigella in epithelial cells. *Nat Cell Biol* **5,** 720-6.

Ullmann, H., Meis, S., Hongwiset, D., Marzian, C., Wiese, M., Nickel, P., Communi, D., Boeynaems, J. M., Wolf, C., Hausmann, R. et al. (2005). Synthesis and structure-activity relationships of suramin-derived P2Y11 receptor antagonists with nanomolar potency. *J. Med. Chem.* **48,** 7040-7048.

Urban, J., Parczyk, K., Leutz, A., Kayne, M. and Kondor-Koch, C. (1987). Constitutive apical secretion of an 80-kD sulfated glycoprotein complex in the polarized epithelial madin-darby canine kidney cell line. *J. Cell Biol.* **105,** 2735-2743.

Vagin, O., Kraut, J. A. and Sachs, G. (2009). Role of N-glycosylation in trafficking of apical membrane proteins in epithelia. *Am. J. Physiol. Renal Physiol.* **296,** F459-69.

VAN Giezen, J. J., Nilsson, L., Berntsson, P., Wissing, B. M., Giordanetto, F., Tomlinson, W. and Greasley, P. J. (2009). Ticagrelor binds to human P2Y(12) independently from ADP but antagonizes ADP-induced receptor signaling and platelet aggregation. *J. Thromb. Haemost.* **7,** 1556-1565.

van Meer, G. and Simons, K. (1988). Lipid polarity and sorting in epithelial cells. *J. Cell. Biochem.* **36,** 51-58.

Vassilatis, D. K., Hohmann, J. G., Zeng, H., Li, F., Ranchalis, J. E., Mortrud, M. T., Brown, A., Rodriguez, S. S., Weller, J. R., Wright, A. C. et al. (2003). The G protein-coupled receptor repertoires of human and mouse. *Proc. Natl. Acad. Sci. U. S. A.* **100,** 4903-4908.

von Kugelgen, I. and Wetter, A. (2000). Molecular pharmacology of P2Y-receptors. *Naunyn Schmiedebergs Arch. Pharmacol.* **362,** 310-323.

Waldo, G. L. and Harden, T. K. (2004). Agonist binding and gq-stimulating activities of the purified human P2Y1 receptor. *Mol. Pharmacol.* **65,** 426-436.

Wang, L., Kolachala, V., Walia, B., Balasubramanian, S., Hall, R. A., Merlin, D. and Sitaraman, S. V. (2004). Agonist-induced polarized trafficking and surface expression of the adenosine 2b receptor in intestinal epithelial cells: Role of SNARE proteins. *Am. J. Physiol. Gastrointest. Liver Physiol.* **287,** G1100-7.

Wang, N., Rumney, R. M., Yang, L., Robaye, B., Boeynaems, J. M., Skerry, T. M. and Gartland, A. (2013). The P2Y(1)(3) receptor regulates extracellular ATP metabolism and the osteogenic response to mechanical loading. *J. Bone Miner. Res.* **28,** 1446-1456.

Warny, M., Aboudola, S., Robson, S. C., Sevigny, J., Communi, D., Soltoff, S. P. and Kelly, C. P. (2001). P2Y(6) nucleotide receptor mediates monocyte interleukin-8 production in response to UDP or lipopolysaccharide. *J. Biol. Chem.* **276,** 26051-26056.

Weisman, G. A., Ajit, D., Garrad, R., Peterson, T. S., Woods, L. T., Thebeau, C., Camden, J. M. and Erb, L. (2012). Neuroprotective roles of the P2Y(2) receptor. *Purinergic Signal.* **8,** 559-578.

Weisz, O. A. and Rodriguez-Boulan, E. (2009). Apical trafficking in epithelial cells: Signals, clusters and motors. *J. Cell. Sci.* **122,** 4253-4266.

Weyler, S., Baqi, Y., Hillmann, P., Kaulich, M., Hunder, A. M., Muller, I. A. and Muller, C. E. (2008). Combinatorial synthesis of anilinoanthraquinone derivatives and evaluation as non-nucleotide-derived P2Y2 receptor antagonists. *Bioorg. Med. Chem. Lett.* **18,** 223-227.

White, P. J., Webb, T. E. and Boarder, M. R. (2003). Characterization of a Ca2+ response to both UTP and ATP at human P2Y11 receptors: Evidence for agonist-specific signaling. *Mol. Pharmacol.* **63,** 1356-1363.

Wilkin, F., Duhant, X., Bruyns, C., Suarez-Huerta, N., Boeynaems, J. M. and Robaye, B. (2001). The P2Y11 receptor mediates the ATP-induced maturation of human monocyte-derived dendritic cells. *J. Immunol.* **166,** 7172-7177.

Wilson, J. M., Fasel, N. and Kraehenbuhl, J. P. (1990). Polarity of endogenous and exogenous glycosyl-phosphatidylinositol-anchored membrane proteins in madin-darby canine kidney cells. *J Cell Sci* **96 (Pt 1),** 143-9.

Wilson, P. D. (2011). Apico-basal polarity in polycystic kidney disease epithelia. *Biochim. Biophys. Acta* **1812,** 1239-1248.

Wirkner, K., Schweigel, J., Gerevich, Z., Franke, H., Allgaier, C., Barsoumian, E. L., Draheim, H. and Illes, P. (2004). Adenine nucleotides inhibit recombinant N-type

calcium channels via G protein-coupled mechanisms in HEK 293 cells; involvement of the P2Y13 receptor-type. *Br. J. Pharmacol.* **141,** 141-151.

Wolff, S. C., Qi, A. D., Harden, T. K. and Nicholas, R. A. (2005). Polarized expression of human P2Y receptors in epithelial cells from kidney, lung, and colon. *Am. J. Physiol. Cell. Physiol.* **288,** C624-32.

Wolff, S. C., Qi, A. D., Harden, T. K. and Nicholas, R. A. (2005). Polarized expression of human P2Y receptors in epithelial cells from kidney, lung, and colon. *Am J Physiol Cell Physiol* **288,** C624-32.

Wolff, S. C., Qi, A. D., Harden, T. K. and Nicholas, R. A. (2010). Charged residues in the C-terminus of the P2Y1 receptor constitute a basolateral-sorting signal. *J Cell Sci* **123,** 2512-20.

Wong, A. M., Chow, A. W., Au, S. C., Wong, C. C. and Ko, W. H. (2009). Apical versus basolateral P2Y(6) receptor-mediated cl(-) secretion in immortalized bronchial epithelia. *Am. J. Respir. Cell Mol. Biol.* **40,** 733-745.

Wong, S. H. and Hong, W. (1993). The SXYQRL sequence in the cytoplasmic domain of TGN38 plays a major role in trans-golgi network localization. *J. Biol. Chem.* **268,** 22853-22862.

Wozniak, M. and Limbird, L. E. (1996). The three alpha 2-adrenergic receptor subtypes achieve basolateral localization in madin-darby canine kidney II cells via different targeting mechanisms. *J Biol Chem* **271,** 5017-24.

Xiao, Z., Yang, M., Lv, Q., Wang, W., Deng, M., Liu, X., He, Q., Chen, X., Chen, M., Fang, L. et al. (2011). P2Y11 impairs cell proliferation by induction of cell cycle arrest and sensitizes endothelial cells to cisplatin-induced cell death. *J. Cell. Biochem.* **112,** 2257-2265.

Yano, S., Tsukimoto, M., Harada, H. and Kojima, S. (2012). Involvement of P2Y13 receptor in suppression of neuronal differentiation. *Neurosci. Lett.* **518,** 5-9.

Yeaman, C., Le Gall, A. H., Baldwin, A. N., Monlauzeur, L., Le Bivic, A. and Rodriguez-Boulan, E. (1997). The O-glycosylated stalk domain is required for apical sorting of neurotrophin receptors in polarized MDCK cells. *J Cell Biol* **139,** 929-40.

Yerxa, B. R., Sabater, J. R., Davis, C. W., Stutts, M. J., Lang-Furr, M., Picher, M., Jones, A. C., Cowlen, M., Dougherty, R., Boyer, J. et al. (2002). Pharmacology of INS37217 [P(1)-(uridine 5')-P(4)- (2'-deoxycytidine 5')tetraphosphate, tetrasodium salt], a next-generation P2Y(2) receptor agonist for the treatment of cystic fibrosis. *J. Pharmacol. Exp. Ther.* **302,** 871-880.

Yu, W. and Hill, W. G. (2013). Lack of specificity shown by P2Y receptor antibodies. *Naunyn Schmiedebergs Arch. Pharmacol.*

Zhang, F. L., Luo, L., Gustafson, E., Lachowicz, J., Smith, M., Qiao, X., Liu, Y. H., Chen, G., Pramanik, B., Laz, T. M. et al. (2001). ADP is the cognate ligand for the orphan G protein-coupled receptor SP1999. *J. Biol. Chem.* **276,** 8608-8615.

Zhang, F. L., Luo, L., Gustafson, E., Palmer, K., Qiao, X., Fan, X., Yang, S., Laz, T. M., Bayne, M. and Monsma, F.,Jr. (2002). P2Y(13): Identification and characterization of a novel galphai-coupled ADP receptor from human and mouse. *J. Pharmacol. Exp. Ther.* **301,** 705-713.

Zurzolo, C., Lisanti, M. P., Caras, I. W., Nitsch, L. and Rodriguez-Boulan, E. (1993). Glycosylphosphatidylinositol-anchored proteins are preferentially targeted to the basolateral surface in fischer rat thyroid epithelial cells. *J. Cell Biol.* **121,** 1031-1039.